Blood flow in biomimetics microchanels

Mehdi Inglebert

THÈSE

Pour obtenir le grade de

DOCTEUR DE L'UNIVERSITE GRENOBLE ALPES

Spécialité Physique pour les sciences du vivant

Arrêté ministériel : 25 mai 2016

Présentée par

Mehdi INGLEBERT

Thèse dirigée par **Lionel BUREAU, Chargé de recherche CNRS, LiPhy**, et
codirigée par **Chaouqi MISBAH, Directeur de recherche CNRS, LiPhy**

préparée au sein du **LiPhy**
dans **l'École Doctorale de physique**

Écoulements sanguins en microcanaux biomimétiques : étude de la fonction endothéliale

Thèse soutenue publiquement le **19 Février 2020**,
devant le jury composé de :

Madame, Debora, ANGELONI
Associate Professor, Scuola Superiore Sant'Anna Pisa, Rapporteur
Monsieur, Julien, HUSSON
Maître de conférences, Ladhyx Paris, Rapporteur
Madame, Jeanette, MAIER
Professor, Dep of Biomedical and Clinical Sciences Milano, Membre
Monsieur, Abdul, BARAKAT
Directeur de recherche Ladhyx Paris, Membre
Monsieur, Antoine, DELON
Professeur, LiPhy Grenoble, Membre, Président du jury

Chapter I: Introduction

Chapter II: A biomimetic microfluidic device: how to build endothelialized micro-channels

Chapter I - Introduction

As an introduction to this work we describe the human vasculature and its functions from the macroscopic level to the cellular level. Most of the figures and information presented in the first section of this chapter are taken from Sherwood L. *Human Physiology: From Cells to Systems* (1). We then describe the vascular endothelium and its functions, provide some examples of state-of-the-art in vitro studies of endothelial cells, and finally summarize the objectives of the present thesis.

I. The blood circulatory system

The circulatory system is the key actor for body homeostasis. Working as a transport platform, the circulatory system carries essential working supplies to organs, tissues and cells as well as it carries out wastes and heat. The circulatory system is composed of 3 parts:

(i) the heart, a hollow muscular organ acting as a pump that imparts the necessary pressure gradient for blood flow

(ii) the blood, carrying nutrients, oxygen and hormones to tissues, as well as their activity wastes such as CO_2.

(iii) the blood vessels, i.e. passageways through which blood flows from the heart to the tissues and organs and then back to the heart.

The circulatory system is divided in two loops (Fig. 1): one starting from the heart and going to the pulmonary system, where oxygen can be resupplied and carbon dioxide released, after which the heart pumps back the re-oxygenated blood to carry it out in the second loop, the systemic circulation. The heart being placed in the thoracic cavity, the systemic circulation forms two loops, one in the upper part of the body and one in the lower, allowing blood to flow through every single organ of the body and meet their need in O_2, nutrient delivery, waste removal, and hormonal signaling. Therefore,

blood transport contributes to homeostasis by serving as a pathway for the needs of the body.

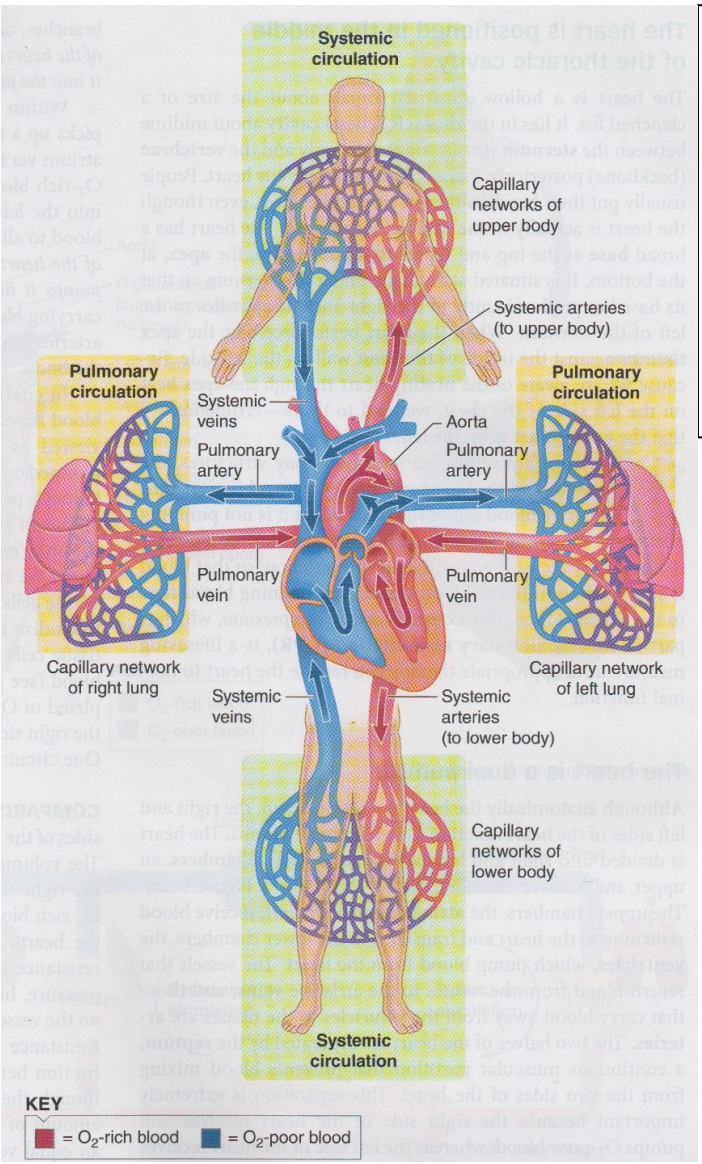

Fig 1: Basic organization of the cardiovascular system

The vascular loops of the circulatory system: the pulmonary circulation for reoxygenation of blood and systemic circulation for supplying organs.

The vascular tree is composed of three parts of distinct roles: the arteries, the veins and the microvasculature. As every fluid, blood needs a pressure gradient to flow. The heart applies pressure that allows blood to flow through the circulatory system, but as the pressure drops by frictional forces, and while the heart is relaxing and refilling, the pressure has to be maintained

by highly elastic arteries recoiling from dilation during systole (Fig. 2). The tight regulation of diameter and stiffness of these arteries defines the amount of blood supplied to a particular organ and can vary depending on the needs and activity of this organ at a certain time. Once the blood reaches the organ, it enters the microvascular network. The microvessels allow exchanges from blood to tissues. Indeed, owing to their thin walls, capillaries are permeable to oxygen and nutrient exiting the blood circulation and carbon dioxide and waste entering it. Then blood has to be pumped back through the venous system. Veins are highly distensible vessel, which start at the exit of every organ and end in the heart and serve as a blood reservoir.

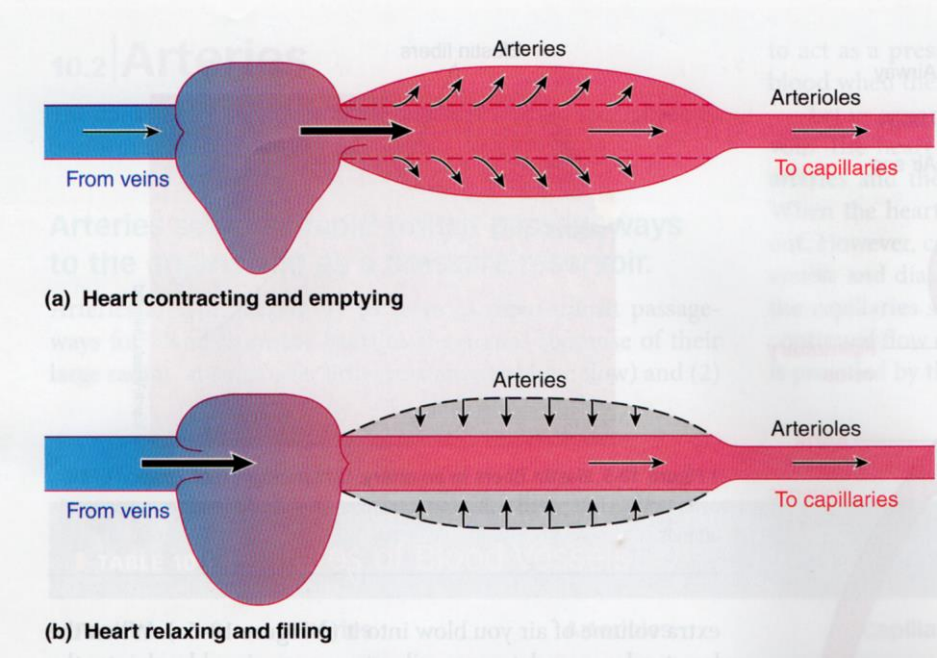

Fig 2: Arteries and pressure reservoir

Schematic representation of the mechanism of pressure reservoir in arteries, (a) arteries expending while heart is pumping and (b) recoiling while heart refills, leading to continuous flow into the arterial tree.

A. Arteries

Arteries are vessels that transport oxygenated blood from the heart to tissues and organs (at the exception of the pulmonary artery that transports carbon dioxide rich blood to the lung and pulmonary vein that transports oxygenated blood back to the heart). There are several hundred arteries in the body, they have thick, highly elastic walls and are of large radii to limit resistance to blood flow. Arteries are made of five layers (Fig. 3): from the lumen to the external part, as every blood vessel, a layer of endothelial cells covers the inner surface, this layer of endothelial cells is surrounded by elastin fibers, then a layer of smooth muscle cells that allows contraction of the vessel to maintain pressure, another layer of elastin fibers and finally a layer of connective tissues composed mostly of collagen.

In addition to transporting blood from the heart to organs and tissues, arteries act as pressure reservoir (Fig. 2). The elasticity of arteries allows maintaining blood flow while the heart is relaxing to refill. Indeed, when the heart is pumping blood, a greater volume is injected into arteries that leads to their dilation. While the heart temporarily stops pumping to refill, the stretched arteries passively recoil, and maintain pressure for the excess of blood to flow through the vascular tree. This pressure is known as the blood pressure, as measured with a sphygmomanometer and stethoscope, and is an average of the pressure while the heart is pumping blood in arteries and the pressure of the recoiling of arteries when heart is relaxing. The mean

arterial pressure is the driving force for blood to flow through the arterial tree.

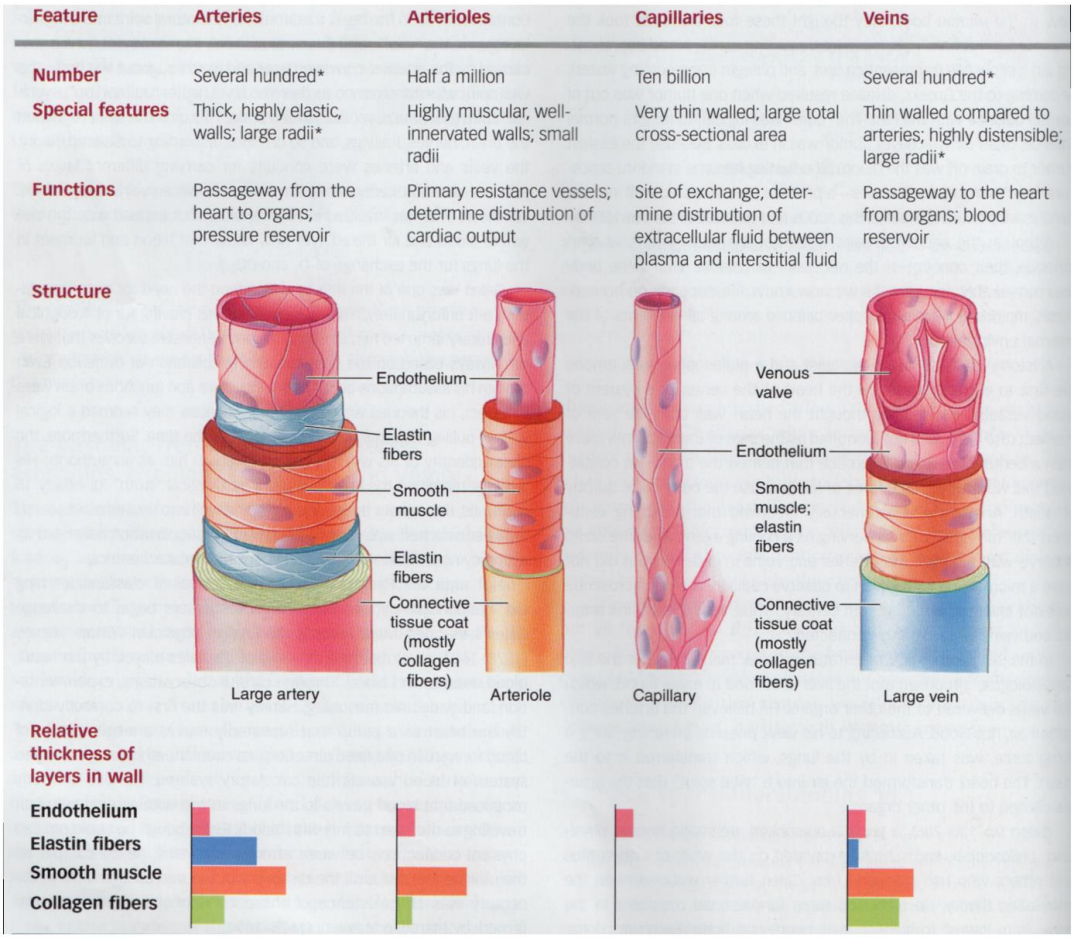

Fig 3: Vessels structure and function

Summary table of the structure of each type of vessels, their features, function and layers composition.

B. Arterioles

As blood input is not needed in the same amount during different activities, some regulation is required. After flowing through arteries, blood enters arterioles, which are the major resistance vessels. They are present in half

a million in the human body. This resistance is eliminating the pulsatile behavior of blood for its entrance into the microcirculation but also redistributing blood in relevant amount regarding organ needs. These different distributions are enabled by vasocontraction and vasodilation of the arterioles. Indeed, arterioles possess highly muscular and well-innervated walls and are of small radii. They are made of: a layer of endothelial cells lining the inner surface of the vessel, a smooth muscle layer and a surrounding connective tissue coat of collagen. The smooth muscle cells run circularly around the vessel, allowing contraction or dilation by sensing chemical or mechanical changes. Vasoconstriction refers to contraction of the vessel and is triggered by either (i) an increase in myogenic activity, oxygen, endothelin, sympathetic stimulation by vasopressin, angiotensin II or cold; or (ii) a decrease in carbon dioxide and other metabolites. This leads to contraction of the smooth muscle cells by depolarization of the membrane potential thanks to ion channels, resulting in a reduction of vessels circumference (and radius), increasing its resistance and decreasing blood flow in that vessel. In the opposite, vasodilation refers to enlargement of the vessel circumference and is triggered by: (i) a decrease of myogenic activity, oxygen or sympathetic stimulation by histamine release or heat; or (ii) an increase in nitric oxide, carbon dioxide and other metabolites. To allow either contraction or dilation, smooth muscle cells are maintained in a constant semi-contracted state known as vascular tone. Ca^{2+} ion channels located at the cell membrane maintain a resting potential to trigger this partial contraction and are regulated by neuronal or hormonal signaling. A constant release of norepinephrine by sympathetic nerves further enhances vascular tone.

There are many factors that can influence contraction of arteriolar smooth muscle and modify resistance to flow. Some can bypass ion channels and act directly on second messenger. These factors are distributed into two categories: local (intrinsic) factor controls, for regulation of cardiac output, and extrinsic factor controls, which are important for blood pressure

adjustment. They can be of chemical or mechanical nature, as listed and described in the following (Fig. 4).

1. Local chemical controls

Local metabolism: an increased consumption of oxygen and nutriment and a raise in waste and carbon dioxide concentration in an active organ such as a skeletal muscle, leads to vasodilation. This vasodilation leads to an increase in blood uptake in the organ to match its needs; this is called “Active Hyperemia”. In the opposite case when blood oxygen concentration increases, in resting or relaxing muscles for instance, arterioles constrict to reduce blood flow.

Endothelial derived vasoactive paracrines: Driven and secreted by endothelial cells lying on the inner surface of arterioles, these vasoactive paracrines are released in response to chemical or mechanical sensing of the endothelium. The most studied paracrine released by endothelial cells is nitric oxide. It acts locally for arterioles vasodilation by relaxing smooth muscle cells. It does so by increasing cyclic GMP, which leads to reduced phosphorylation of myosin. Among others, Endothelin is a vasoconstriction paracrine.

Reactive hyperemia: Usually appears when an occlusion prevents blood to flow through an organ. This leads to consumption of oxygen and to a rise in carbon dioxide but without any change in the tissue activity. As arterioles dilate, when the occlusion is removed the blood flow is higher in the transiently deprived tissue and recovery can be achieved rapidly**.**

Histamine release in pathological condition: Histamine is stored in connective tissues or certain white blood cells. When an organ is injured or during inflammation, Histamine triggers vasodilation and is responsible for the redness and swelling of the inflamed/injured regions.

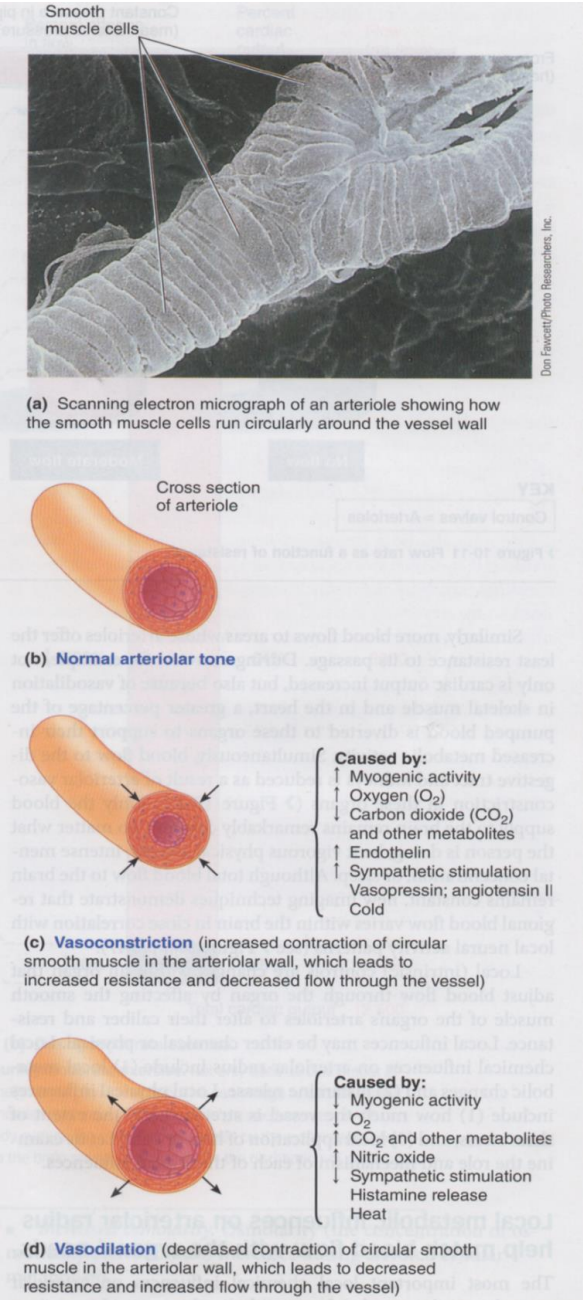

Fig 4: Strucures and function of arteries

(a) Electron micrograph of an arteriole and its layer of smooth muscle cells, (b) schematic representation of an arteriole and (c,d) vasodilation/constriction of arterioles under the influence of local, physical or extrinsic factors.

2. Physical local controls

Myogenic response: Arterioles are able to adapt vascular pressure by either contracting when the pressure passively stretches their walls, as well as vasodilating when the volume passing through is low. This response is driven by muscle cells sensing the stretch.

Nitric oxide production by shear stress sensing: Shear stress is applied on the surface of endothelial cells by blood flow friction. Endothelial cells release nitric oxide when shear stress rises, leading to an increase in arteriolar radii**.**

Local heat or cold: Applying heat or cold, which respectively results in vasodilation or vasoconstriction, is commonly exploited clinically. Vasodilation by heat can promote increased blood flow in an area, vasoconstriction by cold can reduce histamine-induced swelling.

3. Extrinsic neural and hormonal controls

Arterioles are all innervated, except from brain vessels. Sympathetic activity modulates vascular tone. Basically, high sympathetic activity leads to vasoconstriction while low sympathetic activity leads to vasodilation.

Total peripheral resistance maintains mean arterial pressure: By maintaining a higher pressure upward arterioles, the sympathetic activity allows blood to be efficiently distributed to all tissues and organs. Indeed, by globally applying resistance over the whole arteriolar system, the sympathetic constrictor is then overridden by local adjustment that allows providing adequate flow to organ in need.

Norepinephrin and epinephrin influence on smooth muscle cells: except for brain arterioles, all smooth muscle cells of arterioles possess α_1-

adrenergic receptors. Indeed, blood flow needs to be constant in the brain, in order to maintain oxygen supply irrespective of what happens in the rest of the body. Cerebral vessels are then almost entirely controlled by local factors. Vasoconstriction takes place when norepinephrin is released at the end of sympathetic nerves and activates α_1 receptors on smooth muscle cells. Epinephrin also plays a role in vasodilation. Secreted by endocrine glands after stimulation by the adrenal medulla in the brain, Epinephrine binds to β_1 receptors that are present only in skeletal muscles and heart arterioles.

Water balance regulation by vasopressin and angiotensin II: Vasopressin maintains fluid balance by acting on the amount of water that the kidneys retain during urine formation. Angiotensin works on salt concentration regulation. The angiotensin-aldosterone system promotes water retention by osmotic pressure effect of salt concentration. Maintaining water balance in turns regulates plasma volume and blood pressure.

Local control over sympathetic control: skeletal and cardiac muscles have the most efficient local control to override sympathetic control. Driven by metabolic cues, consumption of oxygen and nutrient always dictates the vascular tone.

C. Capillaries

Capillaries are the site for exchanges between blood and cells in tissues. They are present in between 10 to 40 billion in the body and have a radius of 30 to 7 microns. Red blood cells have to squeeze into the smaller vessels and flow into single file. Maximizing the surface of exchange, capillaries leave no cell farther than about 100 µm. As capillaries use no carrier for transport, exchanges are made by diffusion following Fick's law. They are formed of a single layer of endothelial cells supported by a thin basement membrane without any other layer of connective tissue or cell (Fig. 3).

Because of the extensive branching in the capillaries, blood flow is slower than anywhere else. This low speed results in a greater time for exchange of nutrient and metabolic products between blood and tissue cells. The cross sectional area of all the capillaries is greater than any other type of vessel. Even though they have smaller radii than arterioles, they induce less resistance to blood flow, again because of the extensive branching. Arterioles contribute more to peripheral resistance, as their radius is controlled whereas capillaries' is not.

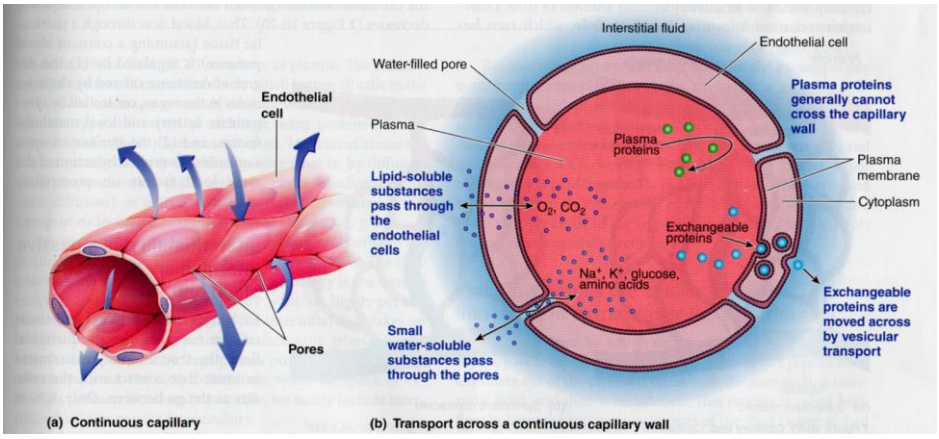

Fig 5: capillary structure and exchange

(a) Schematic representation of a capillary and, (b) cross section view including the different type of transport happening across the endothelial cell layer.

1. Transport through capillaries pores

Transport through capillaries is defined as permeability to water and molecules. To perform this transport, water and molecules need to pass through the vascular barrier formed by endothelial cells (Fig. 5). These cells are connected by junctions that are more or less permeable, depending on the tissue they are located in. Lipid-soluble molecules like oxygen and carbon dioxide can diffuse through the plasma membrane of endothelial cells without the need of passing through cell junctions.

Endothelial cells' permeability allows us to classify capillaries according to their "leakiness" (Fig. 6):

- The continuous, or nonsinusoidal nonfenestrated, capillaries are the less leaky. They can be found for instance in the brain and participate to the blood brain barrier. They possess tight junctions that allow no transcapillary passage of molecules.
- The nonsinusoidal fenestrated capillaries, in which endothelial cells possess pores in their membrane, which permits the passage of small water-soluble molecules such as ions or glucose. They are mostly present in smooth muscles or lung tissues. The presence or not of an endothelial surface layer (or glycocalyx) over these pores differs in diaphragmed or not diaphragmed fenestrated capillaries.
- The discontinuous, or sinusoidal non fenestrated or fenestrated, capillaries, where clefts are present in between cells. Of course sinusoidal fenestrated capillaries are the most leaky vessels in the body. They are mostly present in the liver or the spline.

Except for discontinuous capillaries, all types of capillaries are supported by a basement membrane so that the blood is never in direct contact with the surrounding tissue.

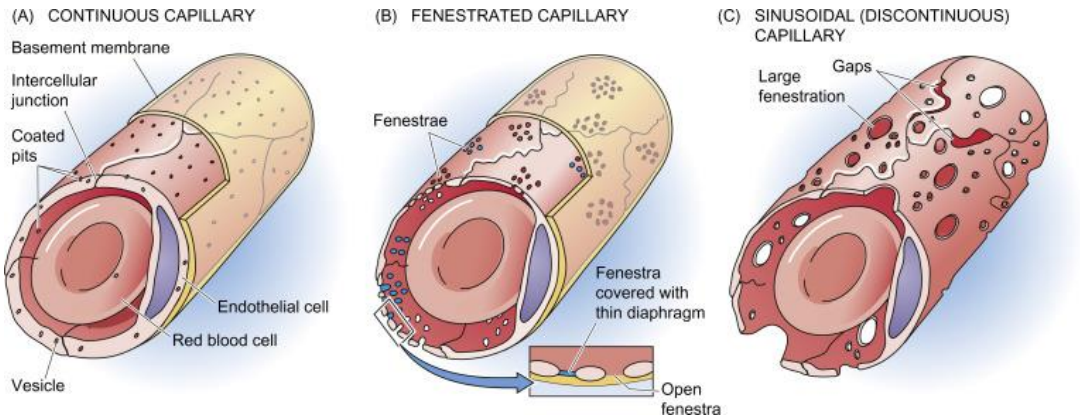

Fig 6: The different structure of capillaries defining their permability

The three types of capillaries, from A to C the less permeable to the most.

2. Precapillary sphincter

Blood intake can differ from one capillary bed to another. At rest, a capillary bed might not need blood to flow continuously through its vessels. Precapillary sphincters act to regulate blood flow in capillary beds (Fig. 7). Coming from arterioles and going to the capillary bed, blood passes through another type of vessel called metarteriole. These metarterioles possess a ring of smooth muscle around the entrance to a capillary. Precapillary sphincters are not innervated but have a high degree of myogenic tone and are sensitive to local metabolic changes. By contraction, they can regulate blood flow through the capillary bed of a tissue. For instance, in a skeletal muscle at rest, only 10% of the precapillary sphincters are open. When the activity increases in that muscle, sphincters open and more blood flows through the muscle. When sphincters are closed, blood flows from the arterioles through the metarterioles which join the thoroughfare channel (the vein equivalent of metarterioles without smooth muscle cells), and goes to venules to continue its way back to the heart.

Thus, blood flow through a particular tissue (assuming constant blood pressure) is regulated by: first, the degree of resistance offered by arterioles in the organ, controlled by sympathetic activity and local metabolic factors and, second, by the number of open capillaries, controlled by action of the same local factors on precapillary sphincters.

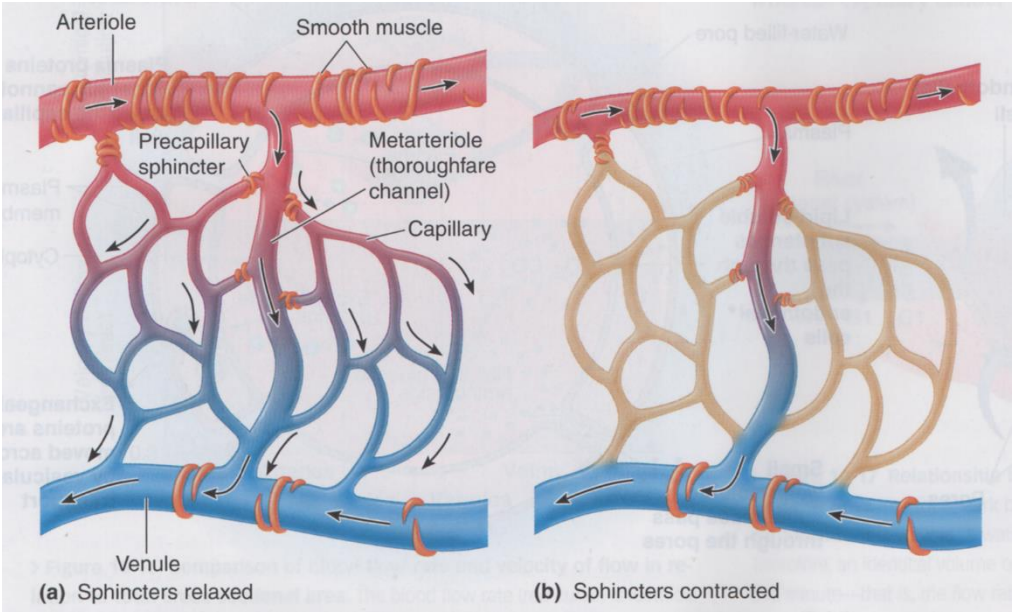

Fig 7: schematic representation of a macrovascular bed in active or resting condition

Precapillary sphincters are ring of smooth muscle cells located at branching between arterioles and microvessels, acting as a switch to turn on or off blood circulation in a capillary network. (a) Relaxed sphincter in an active tissue, smooth muscle cells are relaxed and let blood flow through the microvessels. (b) Contracted sphincter, smooth muscle cells are contracting, blocking the entrance of blood into capillaries, blood is flowing from arterials to metarterioles then thoroughfare canal and venules.

D. Veins and venules

The venous system completes the circulatory system. After gas and nutrient exchange in capillaries, blood enters the thoroughfare channel, then venules, and finally veins to go back to the heart.

Venules have the ability to chemically communicate with nearby arterioles in order to control blood input and output within an organ and have little tone and resistance.

Veins offer low resistance thanks to their large radii. In addition to be a passageway to the heart, they also act as a blood reservoir. Their walls are thinner and contain considerably less elastin and almost only collagen, conferring less recoil but still enough capacity of stretching in order to store some excess volume of blood. Indeed, at rest, vein contain 60% of the total volume of blood thanks to their passive distensibility.

The term cardiac return refers to the amount of blood entering the atria (ie the amount of blood circulating out of the vein). Cardiac contraction induces pressure on the whole circulation and influences venous storage: the less is pumped out of the heart and circulating, the more is stored in veins, and vice versa. Then, venous returns can be influenced by other factors such as (i) sympathetic stimulation, inducing venous smooth muscle contraction, (ii) venous vasoconstriction, leading to increased venous flow, (iii) the effect of venous valve preventing blood to flow backward because of gravity and hydrostatic pressure, (iv) the respiratory activity and the different gas pressure between chest vein and lower vein, and (v) the effect of cardiac suction.

E. The vascular endothelium

The vascular endothelium is formed by a single layer of endothelial cells, present on the inner surface of blood vessels. It is now no longer considered as a tissue but as a whole organ. Indeed, alterations of endothelial cells lead to a broad spectrum of human diseases. Endothelial cells are the only actor present all over the vascular tree from the heart to all kind of vessels and are directly involved in peripheral vascular diseases, strokes, heart diseases, diabetes, insulin resistance, chronic kidney failure, tumor growth, metastasis, venous thrombosis and severe viral infectious diseases (2). The vascular endothelium is therefore responsible for the maintenance of blood homeostasis and more broadly participates to human health.

Vascular endothelial cells serve their role in two ways: they act as a chemical and mechanical sensor, for instance to regulate blood pressure, but also as effectors to recruit immune cells in case of infection in nearby tissues. All these abilities are grouped under the name of vascular function, and will be described in the next section.

II. Endothelial function

The term "endothelial function" refers to all the mechanisms that imply an action by or on the endothelial cells. As we already mentioned before, endothelial cells are a central actor for the regulation of blood homeostasis, vascular health, immune system and general health. In this introduction chapter, we will focus on three aspects of the endothelial function : its passive action on flow structuration, its role in transport of water and molecules through the microvascular wall and finally its ability to sense mechanical forces and its response to it.

Vascular endothelial cells form a semi-selective barrier, and are highly sensitive to mechanical cues thanks to their cytoskeleton, adhesion molecules and polysaccharide coat on their luminal surface. Indeed, endothelial cells are constantly exposed to hydrodynamic shear stresses generated by blood flow. This dragging force influences endothelial cells' behavior, but reciprocally, endothelial cells also drive the flow in the vascular network, regulating vascular tone, structuring liquid and cellular flow in vessels and allowing passage of solute and water from the lumen to the surrounding tissues. In this way, endothelial cells are the link between tissues and the supply network that the vascular system is. Under chemical influence, they respond to organ and tissue needs by increased blood flow or wall permeability for water and molecules. This mutual influence is the key for endothelial function. The tight regulation of endothelial function is mandatory to maintain many biological functions. Usually referred to as endothelial dysfunction, perturbations in the paracrine sensing or

mechanosensing lead to vascular diseases or malfunction of tissues. Many biochemical and phenotypical modifications are associated with a perturbation in the endothelial function. The most studied marker of endothelial function is nitric oxide: when mechanosensing is altered, endothelial cells are no longer capable of sensing an increase in shear stress, resulting in the absence of vasodilation, an increased flow resistance and a lower perfusion of tissues. In region with turbulent streams, like at bifurcations or in aneurism, endothelial cells display an abnormal endothelial surface layer. Such an altered polysaccharide layer on the luminal surface of endothelial cells leads to the recruitment of lymphocyte in a region where inflammation or infection is absent, this is the starting point of the formation of an atherosclerotic plate. In physiological condition, endothelial cells submitted to constant shear stress display a particular cytoskeleton phenotype: long stress fibers cross the cells, are oriented parallel to the flow direction and are anchored at cell-cell junctions, which display a particular pattern of adherent plate at the cell periphery and possess tight junctions. This phenotype leads to a proper balance between low and high permeability and can be modulated depending on the tissue needs. Thereby endothelial dysfunction can be observed on morphological changes in endothelial cells, biochemical changes on the surface or in the endothelial paracrine function and finally on blood flow structure. An overview of endothelial function is summarized in figure 8.

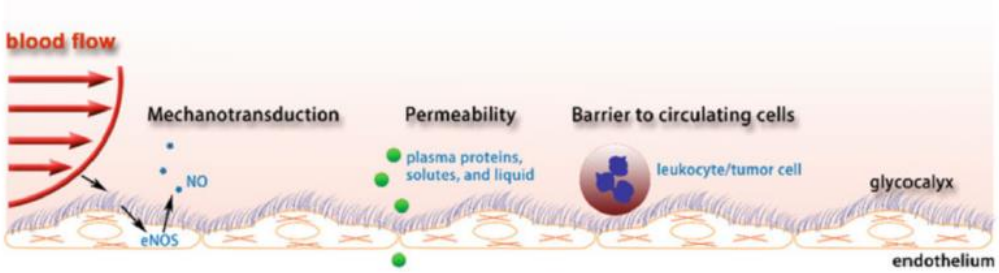

Fig 8: Schematic representation of the endothelial function. Mechanosensors allow endothelial cells to sense blood flow and respond accordingly. The endothelium is the platform for permeability of solvent and solute contained in blood, and form a selective barrier for circulating cells.

A. Mechanosensing and transduction of endothelial cells

Mechanosensing regroups all the functions allowing the endothelium to probe mechanical forces in the environment. Mechanotransduction is the biochemical response to mechanosensing.

Endothelial cell are submitted to three types of forces arising from blood flowing in vessel: pressure, shear and circumferential stretch. Pressure is the force per unit area exerted normal to the wall of blood vessels. The blood pressure ranges from almost zero to ~120 mmHg for a healthy adult human under resting conditions, and comes from the heart pumping blood into the vascular network. Circumferential stretch also comes from blood pressure and corresponds to the mechanical response of blood vessel. It depends on the structure of the vessel, the type of tissue layer surrounding the vessel and its internal counteracting force due to smooth muscle cells. When the heart pumps a greater amount than what blood vessels can contain, they stretch to increase their radius and allow more blood to pass. The last force and the one we will be particularly focusing on is shear stress. Shear stress is the result of the friction of blood on vessel walls, just as any liquid flowing

close to a surface. This dragging force is applied at the luminal surface of endothelial cells.

Endothelial cells have then developed ways to probe these forces and respond accordingly to them. Indeed, they possess many tools to sense these forces and co-actors that translate this mechanical signal into a biochemical response. Sensing these forces results in proper response to regulate vascular tone, permeability and barrier functions, but it also shapes the endothelium. It is now clearly agreed that the mechanical environment influences the ultrastructure of endothelial cells.

1. The endothelial surface layer or glycocalyx: a probe for shear stress

The endothelial surface layer or glycocalyx is a dense layer of elastic polymers attached to the cells' membrane. The ability of the glycocalyx to sense shear stress relies on its composition, which is summarized in figure 9. The glycocalyx composition has been deeply studied in the past 10 years (3–5). The polyanionic components range from glycoproteins anchored in the membrane supporting acidic polysaccharide chains ended by sialic acids to proteoglycans like heparan sulfate including syndecan and glypican core proteins with long glycoaminoglycans side chains. These negatively charged chains bind proteins from plasma, growth factor and cations (6). Heparan sulfate is the more represented glycosaminoglycan on the cell

surface (50-90%), along with chondroitin sulfate and hyaluronic acid they cover the surface of the cells (7).

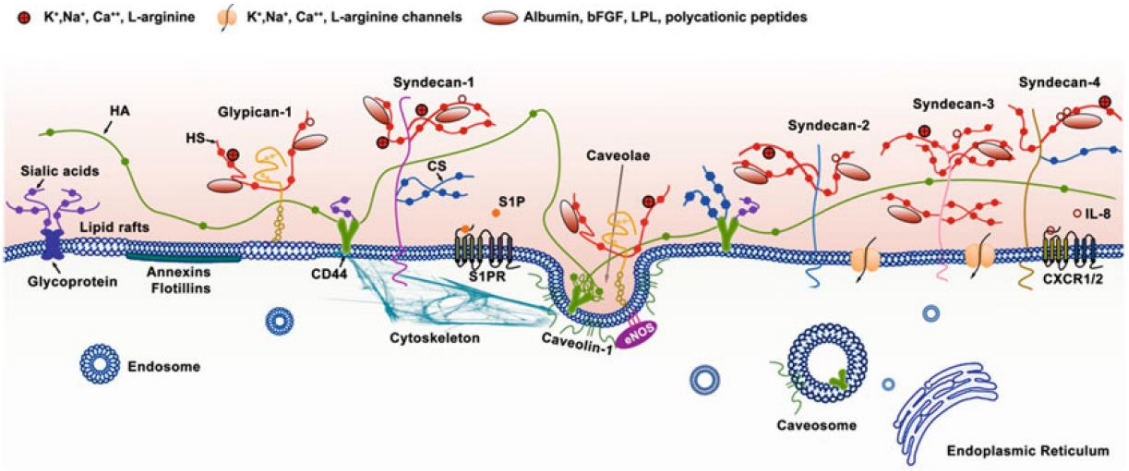

Fig 9: Structural components of the glycocalyx. Sialic acid bound to the membrane via glycoprotein. Long chain of non-sulfated glycosaminoglycan hyaluronic acid bound to its receptor CD44 located in the membrane but also in caveolin-1 enriched region. CD44 binds on it cytoplasmic side the actin cytoskeleton. Heparan sulfate syndecan-1 also bound to the actin cytoskeleton through its cytoplasmic end. Heparan sulfate glycpan-1 is present in lipids raft and caveloin-1 enriched region where it plays a role in eNOS activation.

The first observations of the glycocalyx were done by electron microscopy. These observations concluded on a thickness of 20-100 nm (8,9) but these results were biased by the technique used for fixation and labeling. Indeed, conventional protocols for preparation of biological tissues for electron microscopy go through dehydration, resulting in a loss of interactions with plasma proteins and a collapse of the core protein of the endothelial surface layer. Later, either using Alcian blue GX8 stabilization or cryo-electron microscopy that avoid dehydration, a glycocalyx thickness of 0.2µm to 11µm was measured (10,11). Finally, more recent techniques of fluorescence microscopy were also used to quantify the glycocalyx thickness, either indirectly, using labeled dextran in order to estimate a near-wall exclusion

layer, or directly using specific markers of the glycocalyx such as antibodies or wheat germ agglutinin enabling the identification of the glycocalyx components (12–14). These different observations are displayed in figure 10.

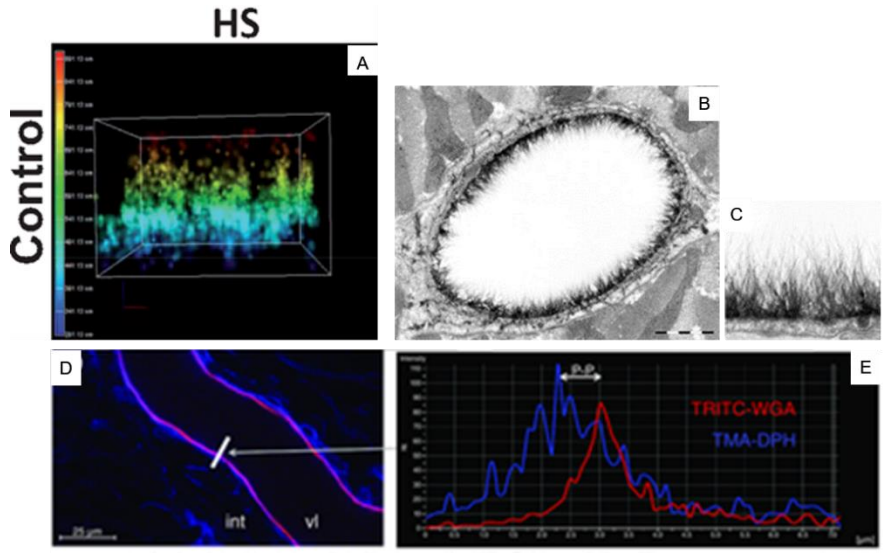

Fig 10: imaging the glycocalyx. (A) 3D representation after STORM (stochastic optical reconstruction microscopy) imaging of heparan sulfate on the surface of an endothelial cell (color code for height from plasma membrane). (B-C) transmission electron microscopy of an alcian blue GX8 labeled rat myocardiac capillary. (D-C) Fluorescent microscopy of a rat mesenteric microvessel perfused with WGA for glycocalyx staining and TMA for membrane staining and measurement of the thickness with fluorescence intensity plot of the white bar in (D).

Endothelial cells need to be submitted to shear stress to synthetize and display a proper glycocalyx (15,16). As its presence is induced by shear stress, and as suggested by its location in direct contact with blood stream, the endothelial surface layer has been supposed to be the principal actor for shear sensing. Several attempts on non-specific degradation of the glycocalyx members have led to the conclusion that it is needed for flow sensing.

Flow sensing has multiple consequences regarding endothelial cells response. Indeed one of the first, but at this time not related to the glycocalyx, observed effect of shear stress on endothelial cells was cell alignment and organization of the actin cytoskeleton (17,18). Later works focusing on the specific degradation of members of the glycocalyx have shown that the heparan sulfate family was necessary for the establishment of the elongated phenotype with the presence of long stress fibers of actin crossing the cell and oriented parallel to the flow direction (19). Several members of the heparan family are present at the cell surface, but expression knockdown experiments have shown that sydecan-1 was responsible for F-actin alignment in endothelial cells (20).

In addition to endothelial cell adaption to shear stress, mechanotransduction of shear results in nitric oxide production. There is actually a threshold concerning nitric oxide production. It has been shown that under a certain level of shear stress (4 dyn/cm²) eNOS activity (enzyme for nitric oxide synthesis) is inhibited while for shear stress above 15 dyn/cm² the eNOS activity is increased (21). Enzymatic degradation of the glycocalyx and particularly of heparan members shows a loss of nitric oxide production in response to shear stress increase (22). More precisely, knockdown of Glypican-1 transcription blocks eNOS activation (19), as confirmed by AFM experiments where mechanical stimulation of Glypican-1 on the surface of endothelial cell with Glypican-1 antibodies coated beads resulted in activation of eNOS (23).

2. Endothelial cell adaptation to shear stress

As mentioned earlier, endothelial cells undergo important morphological changes when submitted to shear stress. This is known from in vitro experiments, in which endothelial cells initially cultured in the absence of shear are subsequently submitted to flow. In vivo, however, endothelial cells are submitted to shear from early angiogenesis. The morphological changes

include cell shape (18), actin (17) and microtubules cytoskeleton remodeling (24) and focal adhesion relocation (19).

Cell shape change is driven by actin fibers polymerization (25). Formation of actin fibers goes through nucleation of thin parallel bundles at the cell boundaries. This leads to the formation of membrane protrusion called filopodia. Coordination of the formation of these actin bundles with remodeling of the cell-matrix interactions allows the elongation of the cell body.

Before exposition to shear stress, when cells are cultured in static condition, the actin cytoskeleton is composed of three main structures: (i) the cortical actin web (ACW) attached to the endothelial surface layer beneath the luminal plasma membrane via syndecan-1 intra-cellular domain; (ii) the dense peripheral actin band (DAPB) that transmits forces to cell-cell junctions and also links to ACW; (iii) the actin stress fibers, anchored to the basal membrane on one side and to the DAPB or luminal membrane on the other side (26). The transduction of a mechanical signal can be presented

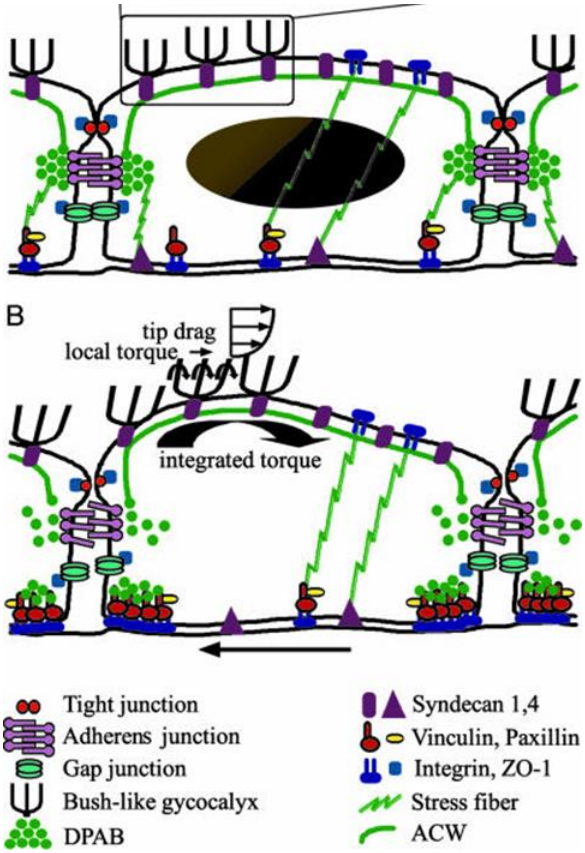

Fig 11: Model for initiation of early morphological changes in endothelial cells submitted to shear stress (adapted from (25)). Shear force is transmitted to the cytoskeleton and cell-cell junctions via the glycocalyx which in turns activate actin stress fibers polymerization and focal adhesion relocation.

briefly as follows: after exposure of endothelial cells to shear stress, the ACW transmits the force acting on the glycocalyx to cell-cell junctions and disrupts the DAPB. This initial mechanism of endothelial cell adaption to shear stress is schematized in Figure 11.

Cell-cell interactions play a role in endothelial remodeling too. Indeed, PECAM-1 is able to sense tension between cells (27). Transmitting this tension to VE-cadherin induces the activation of focal adhesions via phosphoinoisitides production.

The role of the endothelial surface layer in mechanosensing and mechanotransduction has been clearly demonstrated, but this is not its only function. Indeed, the glycocalyx interacts with flowing cells of the blood stream and participates to the endothelial barrier function. Some of its components serve as anchors for lymphocytes adhesion before extravasation (28), and in addition to the negatively charged glycosaminoglycans pushing away from the wall the negatively charged particles flowing in the stream, the elastic properties of the polysaccharide matrix induce forces that repel flowing cells, as we now briefly describe.

B. Influence on blood flow structure

Both in vitro and vivo studies have shown the influence of vessel wall on flow structure. One of the main characteristics of a cell suspension flowing in a cylindrical channel is the structuration of the particle flowing and the suspending liquid. Indeed there are many properties that influence the location and mutual interaction of the suspended particles in a stream. The blood composition varies depending on the location respective to the center of the vessel: platelets and white blood cells are marginated in the periphery of the vessel, close to the wall, and deformable red blood cells tend to flow at the center. There exists, in the vicinity of the vessel walls, a region that is fully depleted in red blood cell. This "cell free layer" is a region where red

blood cell or any deformable particles are excluded. Poiseuille revealed, in his pioneer work on blood circulation, the presence of the depleted region in vivo (29). A drawing from his observations is presented in figure 12. This layer, located close to the wall of the vessels, acts as a lubricant, reducing flow resistance. This exclusion from the boundary of the vessel relies on the following lift-generating phenomena.

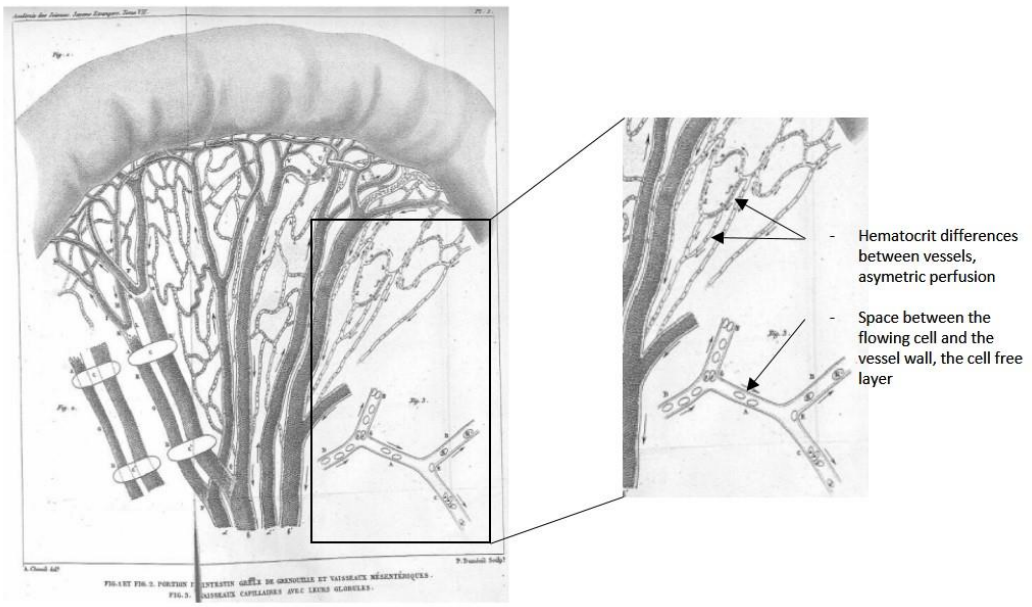

Fig 12 : Drawing from the book « Recherches sur les causes du mouvement du sang dans les vaisseaux capillaires » J.M. Poiseuille 1835. Drawing of the observation made on a part of the circulatory system of the frog small intestine. Representation of the asymmetric perfusion of red blood cells in the capillary network and the cell free layer.

A spherical deformable particle in shear elongates and looses its symmetry. From this loss of symmetry, when flowing close to a wall, the liquid trapped between the wall and the particle has to flow in a space that gets narrower creating a pressure in between the wall and the particle. Directly related to this pressure appears a force pushing the particle away from the wall (30). The steps of particle lifting are represented in figure13.

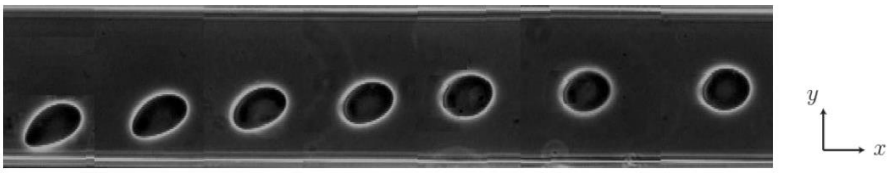

Fig 13: Timelapse image of a lipid vesicle in a 70 µm microfluidic channel. First the vesicle stretches and elongates under shear force. A pressure arise from the liquid flowing between the asymmetric vesicle and the wall, pushing the particle towards the center.

The second force that pushes a cell or particle away from the wall comes from the fact that not only the flowing objects are deformable or asymmetric but walls are covered by a deformable layer. Indeed, the endothelial surface layer or glycocalyx is a thin (100–1000 nm) and soft (elastic modulus of 10–100 Pa) layer of polysaccharides bound to the walls, which is directly submitted to flow and is sensitive to the flow pressure field. Just as well as a deformable particle breaks its symmetry under shear, submitted to shear a particle on top of an elastic wall creates a flow in between itself and the wall, the flow creates a pressure in the gap, and that pressure is able to deformed the soft wall, breaking the symmetry and leading to a pressure difference directly along the area of closeness. This pressure is related to a lift force (31–33), as illustrated in figure 14.

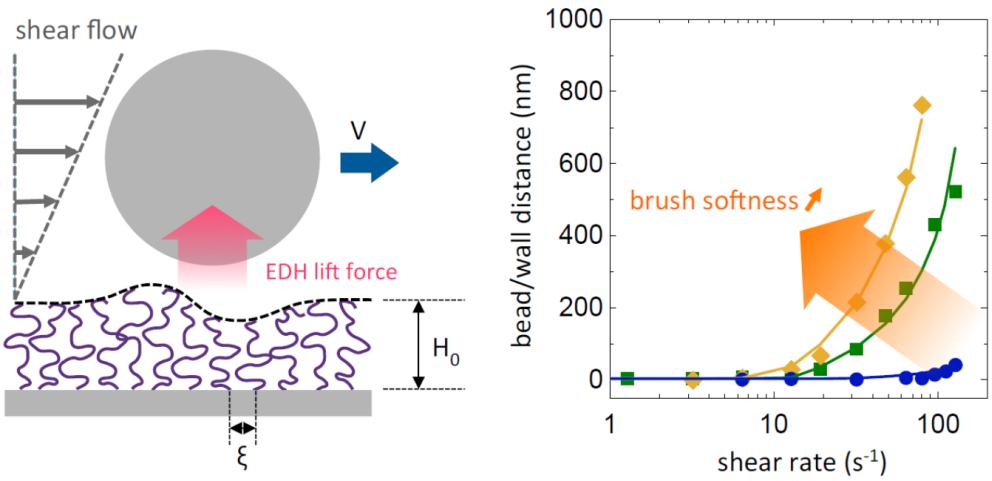

Fig 14: schematic representation of elastohydrodynamic lift force generation. Flowing of a rigid particle over a soft wall. The local flow is driven by a pressure gradient generated by the fluid entrainment in the gap and by the shear stresses exerted by the walls, producing a combined Poiseuille-Couette flow and a net upwards lift force. Adapted from (33).

In conclusion, endothelial cells participate passively and actively to flow structuration. Either thanks to the endothelial surface layer that induces a lift and generates a lubricant layer of plasma or by actively controlling vessels diameter and flow rate, modifying the concentration of circulating cells in the vessel. As mentioned earlier, the whole interest of controlling flow in vessels is to supply organs in agreement with their needs. The next chapter will focus on how endothelial cells adapt their permeability to transport metabolite needed for proper organ function.

C. Permeability

The vascular system is the pathway for nutrient and oxygen required for organ function and tissue survival. Transported by blood, the fuel for every cells of the body needs to exit the blood circulation and enter the extravascular space. As we have seen earlier in the ultrastructure of

capillaries, the level of permeability depends on the type of capillaries. Permeability relies on both trans-cellular transport and filtration through intercellular space. Trans-cellular transport concerns small lipid-soluble molecules such as gas, which diffuse through the membrane and cytoplasm of endothelial cells, and large molecules that need specific protein transporters or vesicular trafficking through the cell. On the other hand, water, ions and smaller molecules can pass through the endothelial barrier via intercellular gaps. This type of gap defines capillary type, and the size or type of gaps ensure different level of permeability. Regular spacing between two endothelial cells varies between 6 and 8 nm (34), and broadening or opening of this space leads to more permeability. The size of the gap between endothelial cells depends on the location of the endothelial cells (some organs possess higher permeability than others), the amount and type of cellular junctions and the patho-physological state of the endothelium. The regulation in expression and activation of the junction is critical to maintain a physiological level of permeability. Part of this regulation is comprised in the endothelial function. There are many factors that can influence a dis-regulation of the junctions, from genetic cues such as hereditary deficiency, sepsis or simply a modification of the physiologic state of the endothelium by reduction of shear stress.

1. Intercellular cell to cell junctions

In physiological condition, endothelial cells are constantly submitted to shear stress. Mechanosensing of shear stress maintains the intracellular signaling for junction stabilization. Endothelial cells are connected through a set of protein complexes forming the junctions: adherent junctions, tight junctions and gap junctions. Tight junctions are responsible for the sealing of the gap between cells. Adherent junctions provide the mechanical strength between neighboring cells. Gap junctions act as a filter or channel

for water, ions a small molecules (35). Their organization is presented in figure 15.

Adherent junctions are of fundamental importance in regulating endothelial cell barrier function. VE-Cadherin is the major protein in the complex involved in homophilic Ca^{2+} dependent binding. The extracellular domain is composed of five cadherin-like monomers that bind to the same complex on the adjacent cell. The cytoplasmic tail contains two functional parts, the juxtamembrane domain and the C-terminal domain which bind to β-catenin and plakoglobin to form the link with the actin cytoskeleton. VE-Cadherin deletion in transgenic mice is lethal due to immature vascular development. Perturbations in the binding of VE-cadherin between adjacent cells cause a great increase in vascular permeability. VE-Cadherin stabilization goes through its binding to GTPase RAP1, the CCM complex and beta-catenin which would stabilize its connection with actin cytoskeleton and maintain a proper barrier function. As well, VE-cadherin plays a role in apico-basal polarity, which is important for lymphocyte extravasation (36).

Tight junctions represent approximately 20% of total junction complexes present on endothelial cells. They have been identified as the points of direct contact of the membranes of adjacent cells by electron microscopy. Tight junctions are formed of claudins, occludin and junctional adhesion molecules. Their number differs along the vascular tree, being more present in arteries than in veins. Their role in vascular permeability is still poorly understood. Homotypic bonds with adjacent cells are formed by 2 extracellular loops of Occludin, while Claudins forms homotypic and heterotypic bonds. Both protein have their C-terminal intracellular ends interacting with ZO-1 and α-catenin to bind the actin cytoskeleton. Perturbation of the NH_2 terminal link leads to increased permeability. The level of expression of occludin is related to the endothelial barrier function. The central nervous system possesses the higher level of expression of occludin, which has a restrictive epitheloid-like barrier (37).

Gap junctions work with couples of Connexons formed by 6 Connexins subunits. Each adjacent cell possess two connexons in their gap junctions, which bind together. They form intercellular pores that allow signal transmission from cell to cell through second messenger such as Ca^{2+} and IP_3.

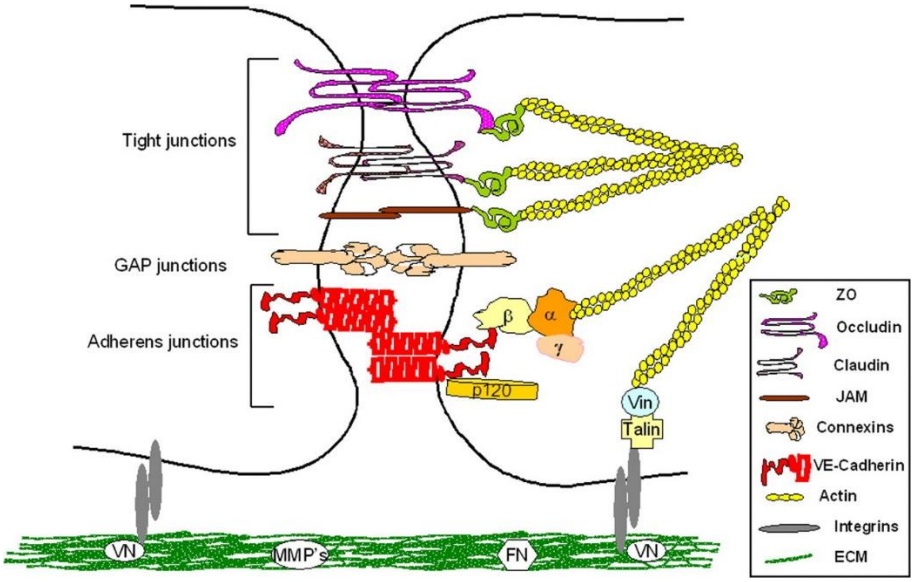

Fig 15: Schematic representation of the structural organization of endothelial cells and matrix interaction (from (35)). The set of typical endothelial cell junctions comprising tight junctions, gap junctions, adherent junctions and integrin receptors by which endothelial cells adhere to each other and to ECM to maintain barrier function and intercellular communications. Occludin, claudins, and JAMs are the backbones of tight junctions, whereas VE-cadherin is required for formation of adherent junctions. Connexins form gap junctions. While the extracellular domains of occludin, claudins, and VE-cadherin maintain cell-cell contact, intracellular domains provide junctional stability through their linkages with the actin cytoskeleton via catenins or ZO-1. Gap junctions allow the rapid exchange of information in the form of low-molecular-mass second messengers Ca^{2+} and IP_3 between contiguous cells. Integrin receptors link endothelial cells with ECM through matrix proteins which are fibronectin (FN) or vitronectin (VN). The cytosolic domains of integrins are linked with actin cytoskeleton through proteins talin and vinculin (Vin).

2. Endothelial cells to extra cellular matrix junction

Interaction of endothelial cells with their environment is critical for the maintenance of endothelial barrier function. Integrins are receptors for sub-endothelial extracellular matrix proteins. The locus of the interactions of integrins with the extra cellular matrix is commonly named "focal adhesion". Focal adhesions are highly regulated complexes for cell adhesion to ECM which defines cell shape, cell ability to migrate and monolayer integrity for the maintenance of barrier function.

The link between endothelial cells and the extra cellular matrix relies on the ability of integrins to connect the intracellular cytoskeleton to the protein fibers of the extracellular matrix. In endothelial cells, most of the integrins are found at the abluminal membrane. They form heterodimers of two subunits α and β integrins. Subunit compositions found in endothelial cells are $\alpha_1\beta_1$, $\alpha_2\beta_1$, $\alpha_3\beta_1$, $\alpha_5\beta_1$, $\alpha_6\beta_1$, $\alpha_v\beta_3$, $\alpha_v\beta_5$, and $\alpha_1\beta_5$. Each subunit is a type I transmembrane glycoprotein composed of a large ectodomain, and in most cases, a small cytoplasmic domain. The RGD (Arg-Gly-Asp) peptide of extra cellular matrix proteins fibronectin, fibrinogen, vitronectin and collagen is the ligand of the extracellular domain of integrin. Competition with synthetic RGD peptides leads to loss of endothelial cell anchorage to extra cellular matric, loss of monolayer integrity and increased vascular permeability (38).

The short cytoplasmic tails of integrins bind to the actin cytoskeleton through actin-binding proteins vinculin, α-actinin, paxillin, talin, zyxin, FAK, and VASP (39). Each of these partners interacts with other proteins, allowing this complex platform of adhesion to control actin polymerization and focal adhesion function (see Fig. 16).

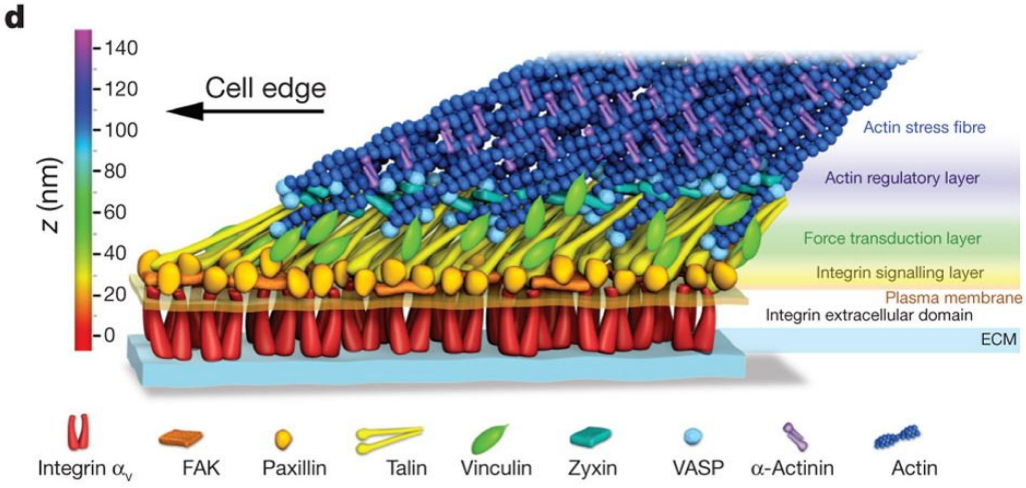

Fig 16: Model of focal adhesion molecular complexes in endothelial cells, integrin subunits bind to the actin cytoskeleton through a set of signaling proteins which play a role in activation/stabilization of the focal adhesion. Adapted from (37).

Here we have presented the multiple implications of junctions for vascular integrity and their role in vascular permeability. Junctions either work as a strict impermeable barrier, force transmitting complex or selective transporter. The regulation of these junctions is of major importance for solute, water and cells' permeability and transport but also for vascular cytoskeleton stability and adhesion to the extracellular matrix.

III. Biomimetic devices and scope of the thesis

Studying the endothelial function requires to take into account the endothelium as a whole organ, responsible for many functions, and which is not ubiquitously identical. From the type of vessel and the particular function associated, it is mandatory to place endothelial cells into a relevant physiological, biochemical, but also mechanical environment. Shear stress biomimetic devices have proven their efficiency to address questions regarding either mechanosensing of blood flow for endothelial cells integrity, the influence of pathological conditions on the endothelial function and

barrier function of the endothelium. In this work we will show how we developed an endothelialized microfluidic device that allows for the culture of confined human endothelial cells under constant shear conditions, its observation via confocal microscopy and the image analysis performed.

Works done on endothelial cells usually miss either structural or mechanical parameters. Most of the studies done on endothelial cells adaptation to shear stress involve shear chamber composed of a rotating plate placed over endothelial cells cultured on a glass slide. By rotating the top plate, the medium trapped in between generates a shear stress on top of the cells. These studies are totally relevant from the mechanical point of view but miss the common structure of vessels and even more micro vessels where cells are arranged and confined in micrometer-sized vessels. Endothelial cells cultured on soft surfaces like collagen gels tend to self-arrange in tubular structures (40,41), being relevant from the structural point of view but missing the influence of the shear stimulation. Combining the microfluidic technique and the use of soft hydrogel or microporous membrane, permeability to molecule and cells have been investigated (42–44). The use of both techniques allows probing endothelial cell barrier function in shear condition, but usually such experiments are performed in large channels of few hundred micrometers with a discontinuity in substrate stiffness and composition. Finally the use of confined microchannels are suitable for the study of interaction dynamics between circulating cells and wall cells (45). Indeed such devices allow perfusing healthy or pathologic blood cell suspension and study the adhesion of circulating cells on endothelial cells or endothelial cells' response. Some examples are presented in figure 17.

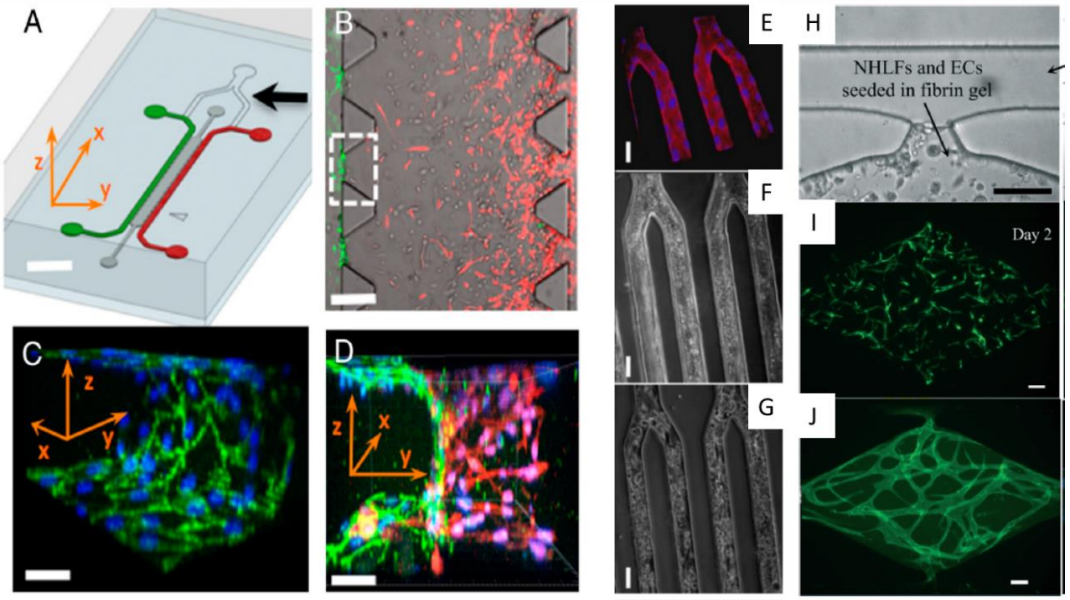

Fig 17: Examples of works done with endothelial cells. Left panel shows an extravasation experimental device, (A) schematic representation of the microfluidic device with, in green, the endothelialized channel, in grey the channel containing hydrogel and in red the channel with cancer cells. (B) Microscopy acquisition of cancer cells (red) migrating through the hydrogel to reach the endothelium (green). (C) 3D representation of the endothelialized channel with labeling of VE-Cadherin in green and nuclei in blue. (D) 3D representation of tumor cells (red) invading and extravasating the endothelium (from (41)). Central panel shows an endothelialized microfluidics device perfused with sickles red blood cells. (E) Bright field fluorescence microscopy acquisition of 30µm endothelialized channel. (F) Endothelialized 30 µm channel perfused with healthy blood suspension. (G) Endothelialized 30 µm channel perfused with sickle cell suspension with obstructive events, stop of suspension flow or strongly reduced speed of flow (from (43)). Right panel shows an acquisition of endothelial cell forming tubular structure in an hydrogel, (H) at Day 0, (I) Day 2 and (H) Day 12 with micro vessel formed in the gel (CD31 labeled in green)(from (39)).

In the present work, our first concern was to be able to submit endothelial cells to physiological shear stress. As the mechanical environment plays a key role in endothelial function, we have developed a device that allows us to precisely control the perfusion of culture medium at constant rate, mimicking blood microcirculation. Conventional microfluidic devices allow

multiplexing of the experiments in channels with micrometric controlled sections, and allow for easy microscopy observations.

By modifying the perfusion parameters we have tackled the impact of shear stress on the endothelial integrity. Indeed, most previous studies have focused on the adaption of endothelial cells to physiological shear stress. Here, we have addressed the question of the impact of a perturbation of physiological level of shear stress on the endothelial function. Controlling the composition of the perfusion fluid, we have used enzymatic degradation of the endothelial surface layer to observe the impact of loss of mechanosensing on the actin cytoskeleton as well as with an increase glucose concentration in the culture medium to mimic diabetes. Also, pretreatment of the microfluidics walls allowed us to assay endothelial permeability using fluorescent trackers diffusing through junctions of an intact or perturbed endothelium.

Chapter II - A biomimetic microfluidic device: how to build endothelialized micro-channels

We describe in this chapter the various methods employed in order to create our biomimetic microvessels, challenge them under different mechanical and chemical conditions, and image them to assess the response of endothelial cells.

The strength of our system comes from (i) the versatile choice of patterns and size of the micro fabricated channels, (ii) the tight control of composition of the flowing media, allowing perfusion of fluorescent molecules for observation and biochemical treatment for perturbation of the physiological state, and (iii) the ability for qualitative and quantitative observation with confocal microscopy.

Mainly inspired by the work of Myers *et al.* (45), the preparation of endothelialized microfluidics channel follows three steps: (i) preparation of PDMS (Polydimethylsiloxane) microfluidic devices, (ii) seeding of the endothelial cells within the microchannels, (iii) cell growth in situ and under flow. All these preparation steps were performed in the laboratory.

Building upon the work initiated by D. Tsvirkun at LIPhy (46), we have improved the protocols for fabrication and cell seeding, and explored the condition of the endothelial cells in order to obtain a well characterized system.

I. Pdms soft litography

Microchannel networks are fabricated using a standard soft lithography technique. A silicon wafer is first cleaned into an oxygen plasma for 5 min, then placed onto a hot plate at 130°C for dehydration. A permanent epoxy negative photosensitive resin (SU8 1060 from Gersteltec) is spin coated at a speed of 2600 rpm, yielding a layer of 30 µm thick on the silicon wafer. A pre-baking of 10 minutes at 65°C and 40 minutes at 95°C is then necessary in order to remove the solvent from the resin.

The design of the circuit is based on a reproduction of a portion of the circulatory system, from small arterioles to microvessels then venules. We have used a quartz-chromium photomask that displays a symmetric pattern of a starting and ending branch of 480 µm and four branching points where the width of the channel is divided or multiplied by two, with in the center 16 straights channels of 30 µm in width (Fig. 18). This mask is placed over the silicon wafer into a UV light exposer for 12 sec (~ 610 mJ/cm^2). The resin is finally baked at 65°C for 10 minutes and 95°C for 30 minutes and then the non-crosslinked resin is removed in a PGMEA bath (Propylene glycol methyl ether acetate) for 5 minutes, rinsed with isopropanol and dried with nitrogen. A last hard baking of 2 hours at 135°C is done in an oven to avoid cracking of the resin.

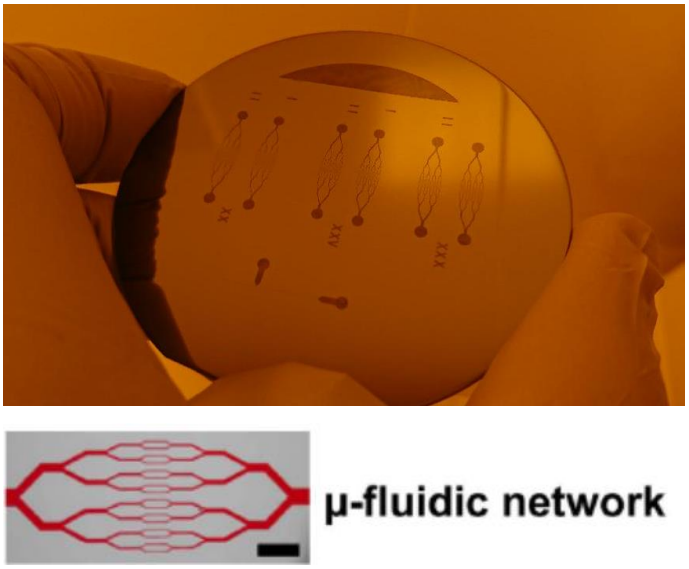

Fig 18: Picture of the 3 inches silicon wafer. Channels of 20-25-30 µm width from left to right after hard baking, fabricated with the technique explained above. Lower panel : picture of the microfluidic network filled with colored water.

We use such a silicon wafer as a positive mold for the preparation of the circuit. PDMS (Sylgard 184) is mixed in a plastic beaker with its curing agent (ratio 1/10 volume). The preparation is placed in a vacuum chamber to remove bubbles introduced during stirring. After complete removal of the air bubbles, the mixture of PDMS can be poured onto the wafer, usually in a petri dish of 9 cm in diameter. The PDMS is then cured by placing the Petri dish in an oven for two hours at 65°C.

The size of the channels (width and height) is measured by cutting a slice of the PDMS circuit. Observing this slice under the microscope allows us to estimate whether the microfabrication process was successfully done and check that we reached a 30µm square section for the smallest channels.

Once the PDMS is cured, we cut out the circuit with a scalpel. Inlet and outlet wells are punched at a size of 0.8 mm. In order to seal the fourth wall of the channel, a glass cover slip of 24/50 mm #0 (thickness -/+ 100µm) is placed with the circuit facing up in a plasma chamber. Oxygen plasma treatment creates radicals on both surfaces. After 30 sec of treatment, both

surfaces are put in contact, which results in permanent and irreversible bonding of the device. Oxygen plasma has a hydrophilic effect on surfaces, and this avoids air bubble trapping in the circuit in later injections.

All this steps of preparation are done in a clean room. This avoids dust contamination and reduces biological contamination too. Moreover, plasma cleaning can be considered as sterilizing. The microchip is stored in a sterile petri dish and is ready for coating and preparation for seeding.

II. Growth of an endothelium in a microfluidic device

As we use primary human endothelial cells, a coating with extracellular matrix is necessary for adhesion and migration on the walls of the channels. We have found a better cell adhesion during seeding if the human fibronectin solution (50µg/mL) is injected rapidly after plasma treatment. To avoid any detachment of PDMS debris from the punched well of entry, it is recommended to use a syringe pump for gentle injection of the fibronectin solution. The coating was usually done by leaving the fibronectin adsorb onto the channel surfaces overnight at 37°C in the cell culture incubator, but this time can be reduced to 2 or 3 hours without noticeable effect.

Before injection of the cell suspension in the microfluidic device, the circuit needs to be rinsed from the fibronectin solution with 1mL of PBS. From this step it is mandatory that all the media used in the seeding process are tempered and degassed in the CO_2 incubator at 37°C for at least 3 hours (usually done over-night).

A $1x10^7$ cells/mL suspension is prepared from HUVEC (human umbilical endothelial cells, Promocell GmbH, Germany) cultured in CO_2 incubator in endothelial cells growth medium supplemented by growth factor (SupplementMix, Promocell GmbH, Germany). Cells are detached from two 25cm² flasks with a 0.25 % solution of trypsin EDTA (Gibco). Competitive blocking of trypsin is done with cell culture medium and cells are centrifuged

at 2500 rpm for 5 min. The cell pellet is re-suspended in 200µL of culture medium and filtered through a nylon cell strainer with pores of 40µm.

Originally, the seeding was done by manual injection of the cell suspension with a 1mL syringe. This technique is easy to handle but faces many problems for cell attachment. Indeed, reaching a complete stop of medium flow to allow cell attachment is hardly possible because of residual hydrostatic pressure. Also, the circuit is highly sensitive to every movement in the tubing, generating medium flow in the channels. High flow gradient is also an issue. Manual injection does not allow for an accurate control of flow speed. Even if this technique permits to look at the channels under a microscope while performing the seeding by hand, we decided to use a computer-assisted seeding. The injection is performed with a pressure controller. The channels are observed through a video camera on the computer screen and an imposed pressure to the inlet reservoir drives the flow in the circuit. The OB-1 MK2 (Elveflow, France) pressure controller controlled by the ESI software allows 0.1mBar accuracy with almost no time delay. Imposing a positive pressure to the inlet reservoir allows competing hydrostatic pressure and completely stopping the cell suspension in the channels. This technique does not require any manual interaction with the circuit from the seeding operator.

Still, the seeding density reached in the channels was not sufficient. Mainly because of sedimentation, the seeding has to be done within minutes. If the seeding density was not sufficient after a few minutes of injection, the operator was forced to re-suspend the cells, generating risks for contamination and damage to cells. Fortunately, we found out that sedimentation could be useful for the seeding. Indeed, it appeared that cells in the tubing were sedimenting in the entry and exit wells of the microfluidic device while the flow was stopped. This sedimentation was locally greatly increasing the cell concentration (using high cell concentration over the whole system generates too much aggregates, resulting in clogging of the channels). Then, by applying short pressure impulsions, we were able to transfer these accumulated cells directly in the channels of interest. The

seeding protocol now consists of a few seconds of continuous injection filing the system with the suspension, stop of flow for several minutes (5/10 minutes), a short pulse of high flow speed for one or two second to move the sedimented cells to the channels. With this protocol, the density of cells in the channels of interest was greatly improved as shown in figure 19. This sequence can be repeated several times to reach the desired density. Finally, a step of washing is needed to remove the non-attached cells from the tubing and the channels.

Even if the duration of seeding was greatly diminished, a thermostated chamber was implemented on the microscope, allowing the seeding to be performed at 37°C instead of room temperature.

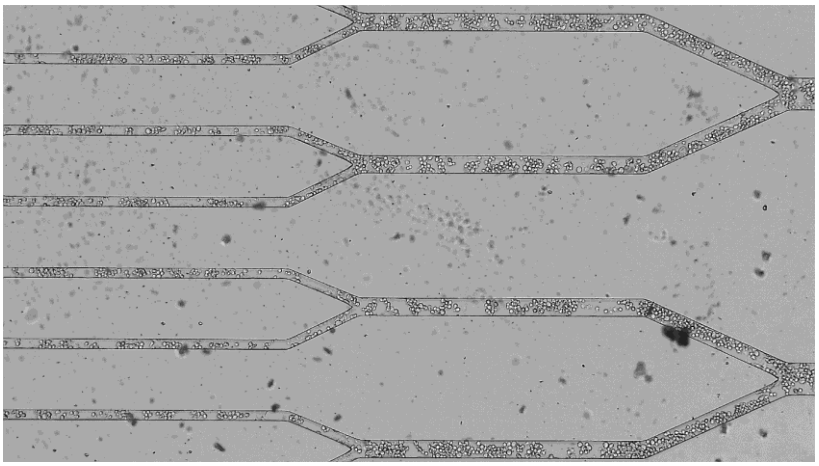

Fig 19: Picture of the microfluidic channels during the seeding, acquired with a video camera on a microscope. A set of 3 bifurcations is visible. From left to right, 30-60-120µm-wide channels. This picture was taken after one sequence of injection-sediment-pulse. Cells in suspension on their way for adhesion appear as bright sphere.

From this point, the outlet tubing was connected to a 1mL syringe placed on a syringe pump, and the inlet tubing immersed into a medium-filled reservoir consisting of a centrifuge tube of 15mL with a pierced cap sealed with paraffin (Fig. 20). The pumped was only turned on after 30-60 min, allowing cells to rest, adhere and recover from the seeding. For the first 24 hours, the imposed flow rate was set to 0.6 µL/min and for the next 3-5 days the continuous flow rate was set at 1 µL/min with a syringe of 5mL.

Such a flow condition corresponds to a shear stress at the wall, τ, which can be estimated from:

$$\tau = \frac{A}{P}\frac{R_h}{L}\,Q$$

with Q the flow rate, A, P and L respectively the cross-section area, perimeter and length of the channel, and R_h its hydraulic resistance. For a square section channel, the latter is given by:

$$R_h = \frac{12\eta L}{0.422b^4}$$

with η the viscosity of the liquid, and b the lateral size of the channel. Hence, we can compute the stress in one of the 16 central channels experiencing a flow rate of Q/16, taking η≈0.001 Pa.s and b≈27 µm (the initial 30 µm minus the thickness occupied by the cells (46)) : τ≈ 0.4 Pa with Q=1 µL/min. This is typical of the level of shear stress experienced by endothelial cells in post-capillary venules.

It is of major importance that the flow is maintained continuously during the culture in order for endothelial cells to adapt to shear stress. Even a few minutes of flow interruption (taking the inertia of the system for restarting the flow into account) have a dramatic effect on the integrity of the endothelium. It is strongly advised to let the system under flow during intermediate observation (these flow perturbations will be investigated and discussed in the next chapter). After 3-5 days of culture under constant shear stress, we obtain a fully confluent endothelium covering the four walls of the channels (see Fig. 20)

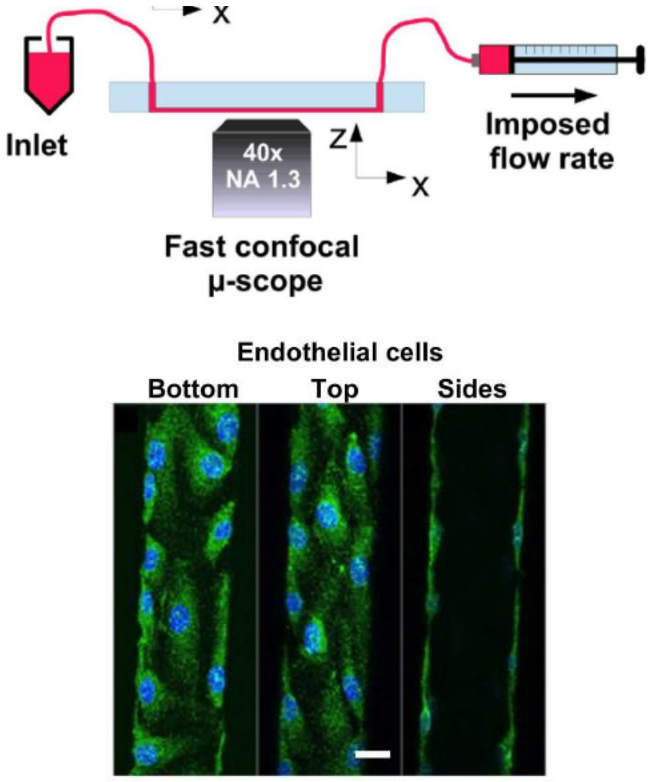

Fig 20: Top: Schematic representation of the microfluidic device with its inlet reservoir, tubing and syringe placed in the syringe pump for medium perfusion. Bottom: Confocal image of the four walls of the channels fully covered by endothelial cells, cell nuclei are labeled in blue and the cell cytoplasm in green.

III. Microscopy: treatment, staining, observation and data processing of living and fixed endothelial cells

Three types of pathological conditions were investigated during this work:

- perturbation of mecanosensing using specific enzymes to degrade the endothelial surface layer and modification of the strength of the mechanical forces applied on cells
- modification of the glucose concentration in the medium to mimic type I diabetes
- permeability assay by bradykinin-induced leakage of the endothelium

For each condition, morphological changes and vascular barrier function were monitored using fluorescence confocal microscopy on living or fixed cells.

A. Fluorescent labeling

In order to study endothelial cells response to various stimuli, we used fluorescent labeling of glycocalyx, actin cytoskeleton, fluorescent circulating proteins, cytoplasm, mitochondria and nuclei to look at phenotypic, barrier function and energy production modifications. The endothelial surface layer being composed of polysaccharide chains, the lectin Weat germ agglutinin is an easy-to-handle fluorescent probe that binds to the glycocalyx. WGA-alexa488 (5µg/mL, from Molecular Probes^{TM}) was perfused in the channels. This staining can be performed on fixed or living cells. Glycosaminoglycan immuno-staining were performed with mouse anti-heparan sulfate (F58-10E4, AMSBIO, USA) and alexa488/555/647 coupled donkey anti-mouse IgG (Invitrogen). Actin cytoskeleton labeling was performed using Phalloidin-TRITC (Sigma Aldrich) on fixed sample or Sir-Actin700 (50nM, Spirochrome) on living cells. To assay vascular leakage, we used a technique inspired by (47): the walls of the channels were coated with biotinylated fibronectin (Cytoskeleton Inc, USA) before seeding, rapidly after confluence was reached (to overcome the turnover of extracellular matrix protein by endothelial cells), labeled avidin-FITC (Molecular Probes^{TM}) was perfused in the channels. Vascular leakage of avidin was measured by fluorescent quantification on the wall of the channels. Cytoplasm was stained with CellTracker Red (Molecular Probes^{TM}). Mitochondria activity can be observed thanks to membrane potential modification. The JC-1 probes (Molecular Probes^{TM}) exhibit potential-dependent accumulation in mitochondria, indicated by a fluorescence emission shift from green (~525 nm) to red (~590 nm). Consequently, mitochondrial depolarization is indicated by a decrease in the red/ green fluorescence intensity ratio.

Finally, nuclei shape was observed by staining with Hoechst 33342 (Molecular Probes™). The dyes were used in accordance with manufacturer's specification. Staining were performed on living cells or after fixation with 4% paraformaldehyde in PBS for 30 min at 37 °C.

B. Microscopy

Confocal fluorescence microscopy was performed on an inverted microscope. XYZ image stacks were obtained in raster mode using a Zeiss LSM710 module and a 40x/NA1.3 oil-immersion objective, with a lateral size of 1024 × 200 pixels, a lateral resolution of 0.225 μm/pixel, and a Z-slice spacing of 0.46 μm.

C. Perturbation of mechanosensing

It has been often reported in the literature that enzymatic degradation of the glycocalyx impaired the endothelial function (4,26,48). As we intended to characterize the endothelial cells in our system, we decided, as a confirmation for fluorescent staining, to label the endothelial surface layer before and after digestion with neuraminidase. 150mUI/mL solution of Neuraminidase diluted in non-supplemented medium was perfused for 3 hours in circuit where cells have been cultured for 5 days under constant shear stress. The thickness of the endothelial layer was measured by fluorescent intensity plot of the signal at the luminal membrane of endothelial cells. The effective degradation of the endothelial surface layer was assayed by global fluorescent intensity between control and digested samples.

Vascular endothelial cells adaption to shear stress is a broadly investigated topic, but to the best of our knowledge nothing was done concerning the effect of reduction or absence of shear on endothelial cells cultured in

constant shear stress condition. We therefore performed reduced shear stress experiments (RSS): Starting from a healthy endothelium grown under constant shear stress as described above, shear was decreased by five-fold. The imposed flow rate was set from 1µL/min to 0.2µL/min for a duration of 1 hour or 6 hours. For observation of fixed sample, the perfusion of the fixing solution was done at 0.2µL/min without any interruption of flow.

D. High glucose concentration condition

Glucose concentration was modified by adding D-glucose (sigma) filtered solution to supplemented medium. Final concentration of the medium was 30mM and perfused in the microfluidics device for 24h.

E. Vascular permeability assay

To assay permeability on endothelial cells cultured under constant shear stress, cells were exposed for 15 min to a constant flow of one of the following media: (i) usual endothelial cells culture medium as a control, (ii) plasma from healthy volunteer—blood was withdrawn in Sodium Citrate tubes, plasma was separated from cells by centrifugation and diluted 1:1 with medium for ECs culturing, (iii) bradykinin (Sigma, USA) diluted in endothelial cells culture medium at a concentration of 25 µM. FITC-conjugated avidin was finally added to the perfusion solution (final concentration is 25 µg/ml for 5 min) before cells were fixed.

F. Data processing

The acquired image stacks were processed and analyzed using the Fiji open-source platform and its built-in plugins.

3-dimensional XYZ image stacks were treated as follows. A point spread function (PSF) of the microscope was generated numerically with Fiji, using the “Diffraction PSF 3D” plugin fed with the experimental characteristics of our imaging system (*i.e.* refraction index of immersion liquid, objective numerical aperture, lateral magnification and *z* slice spacing of the stack). We have further checked for the consistency of such a generated PSF by using it to deconvolve images of fluorescent latex beads of known diameter (500 nm) and ensuring that the bead size measured from the deconvolved images agreed with the expected one. PSF deconvolution was then performed on image stacks of the stained cells using the “Iterative deconvolve 3D” plugin, projection of deconvolved image stacks were then made, summing the intensity of each slices.

IV. Validation of the technique

Here we present a set of experiments and stainings that validates the technique for growing a healthy endothelium in a microfluidic device. Indeed, we decided to check for integrity of the endothelium, proper display of the endothelial surface layer, shear stress related actin cytoskeleton phenotype and proper barrier function. These experiments can be seen as a control of the physiological state of endothelial cell in our system and show how we believe endothelial cells should be considered for further investigation of pathological conditions.

As we have shown in figure 20, endothelial cells cultured in our microfluidic devices fully cover the walls of the channels. We decided to verify if the endothelial surface layer was properly synthetized after 3-5 days of cultured under constant shear stress. Do to so, we used two type of labeling: first the non-specific markers of the glycocalyx WGA in order to be able to measure the size of the polysaccharide brush, second a specific anti-body against

Heparan sulfate residues to show that in our condition the shear stress mechanosensor of endothelial cells is present at the luminal membrane.

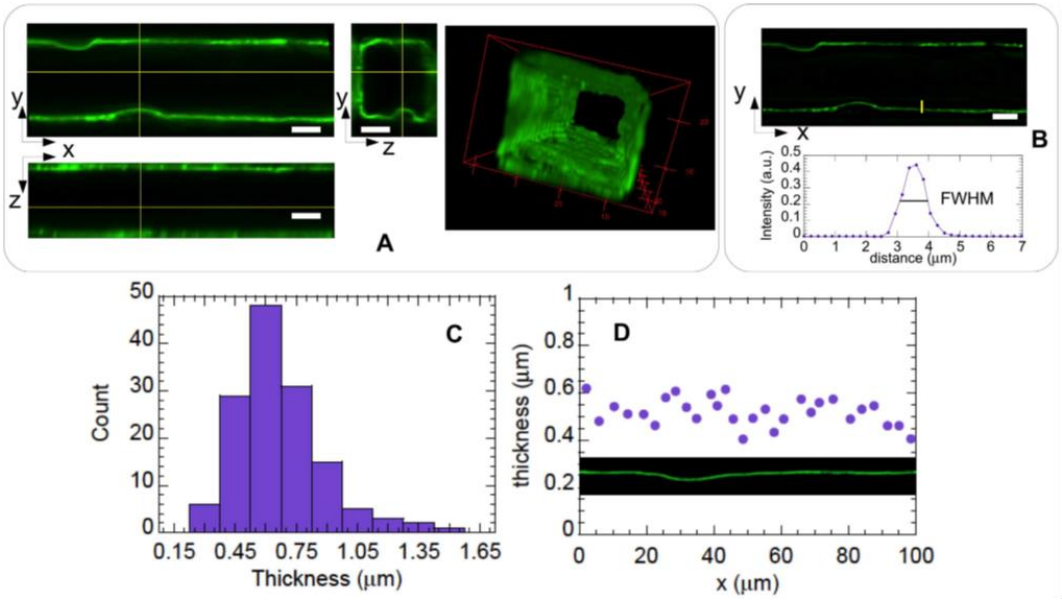

Fig 21: Fluorescent staining of living and fixed HUVEC glycocalyx after cultured for 3-5 days under constant shear stress, channels of 30x30 µm section are observed. (A) 3D acquisition on living endothelial cells labeled with WGA-alexa488, cross sectional view of the channel walls on left side of the panel and 3D reconstruction on the right side. (B) Fluorescence intensity profile of the WGA staining along the yellow line, the thickness of the brush is measure as the full width at half maximum on the plot. (C) Histogram of all the measurement done over the image in (D), the purple dot represent point of measure with their respective result in thickness at full width at half maximum, values on the Y axis.

Previous work done by Tsvirkun *et al.* (46) have shown that in our system the endothelial surface layer is properly expressed. As shown in fig. 21 A,B,D, the WGA staining displays a homogenous coverage of the cell luminal membrane. Measurements performed on the signal from labelled polysaccharide with WGA-alexa488 result in a 0.7 µm mean in thickness over the luminal membrane of the cell. This result is in good agreement with

previous measurements done in/ex vivo on vessel of comparable size (49,50). As shown in (C) the thickness of the ESL can reach values larger than 1µm, but as the representation in (D) shows, no pattern or trend was observe concerning differences in thickness depending on the location of measure, either over a nucleus or at cell border.

In order to go beyond these first results, we have performed the following complementary experiments.

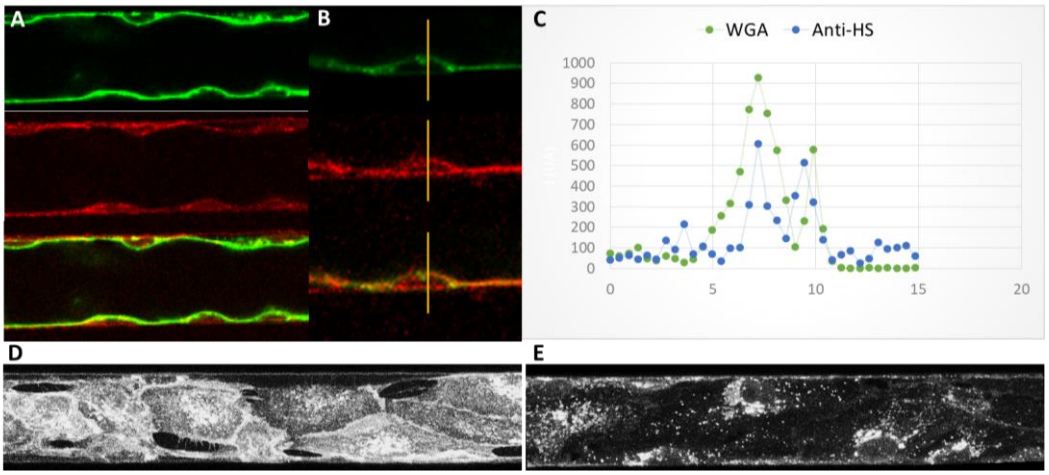

Figure 22 : Fluorescent staining of the endothelial surface layer of HUVEC cultured under constant shear stress for 3-5 days (A) Slice of a stack of images taken in a channel with HUVEC cultured for 3-5 days under constant shear stress, fixed and label with WGA-alexa488 and anti-HS coupled with 555-anti-mouse IgG. First image of the panel is the immunostaining, second is WGA and third is a merge of the two signals. (B) Fluorescence intensity profile of the yellow bar in (C). (D) Glycocalyx staining with WGA-Alexa488 of HUVEC cultured for 3-5 days under constant shear stress and fixed, (E) HUVEC treated with Neuraminidase (150 mUI/mL, 3 hours) after 3-5 days culture under constant, fixation was done after enzyme treatment

As we intended to confirm the WGA staining of the glycocalyx, we performed enzyme treatment. We used neuraminidase, which is known to degrade the ESL (51), and performed labeling of the glycocalyx after fixation. We observed a clear diminution of the WGA signal intensity after

enzymatic treatment (Fig 22 D) compared to control (Fig 22 E). WGA labeling on fixed samples revealed a strong intra-cellular staining. We believe that this signal comes from part of the ESL that is internalized during membrane trafficking. Overall, the strong decrease of the signal clearly demonstrates that after enzyme treatment the WGA is no longer able to fix on polysaccharide chains. This confirms both the use of WGA as a marker for the glycocalyx and the use of Neuraminidase for partial removal of the endothelial surface layer.

Next, in order to confirm that HUVEC were synthetizing also the proteoglycans responsible for mechanosensing of fluid shear stress, we performed immunochemistry labeling of heparan sulfate. The results displayed in fig 22 (A, B, and C) show that: (i) the heparan sulfate is present at the cell luminal side of the membrane but not as much homogenous as the WGA. It is also present at the basal side of the cells. (ii) The intensity profile plot clearly demonstrates that heparan sulfate is located at the same place than the WGA staining. The presence of signal at the basal membrane of the cells could be an artefact from the fixation as some WGA signal is present there too, but is not in living samples. There is also evidence in the literature that heparan sulfate is a mechanosensor that is not only responsible for fluid shear stress sensing of blood flow but also for interstitial flow (52); this could explain why we observed some signal at the basal membrane of HUVEC in our system. Both results from (E) and (F) confirm that heparan sulfate is properly expressed in HUVEC cultured in our system and that its location in the endothelial surface layer on the luminal side of the cells is confirmed. The presence of heparan sulfate in patch-like patterns is in good agreement with the work of Thi *et al.* (26), the staining was perform with the same antibody (F58 10E4) and the confirmation of antibody specificity with specific degradation of heparan sulfate by Heparinase III is done in the aforementioned work.

Along the same idea of characterization of HUVEC in our system, we performed two other phenotypic analysis: (i) the expression of the endothelial specific junctional protein VE-Cadherin and (ii), the presence of

stress fibers oriented parallel to the flow direction, which are responsible for cell shape and elongation. Fluorescent labeling of VE-cadherin was performed with mouse monoclonal antibody TEA 1.31. It reveals, as shown in fig 23, that endothelial cells cultured in our system for 3-5 days expressed specific markers of tight cell-cell junction, the staining is continuous along cell-cell border. Labeling F-Actin with Rhodamine coupled phalloidin shows in HUVEC cultured under constant shear stress for 3-5 days the presence of long and thick stress fibers. These actin fibers cross the cells from side to side, parallel to the flow direction, and seem to be anchored at the cell borders. The actin cytoskeleton phenotype will be described in more detail in the next chapter.

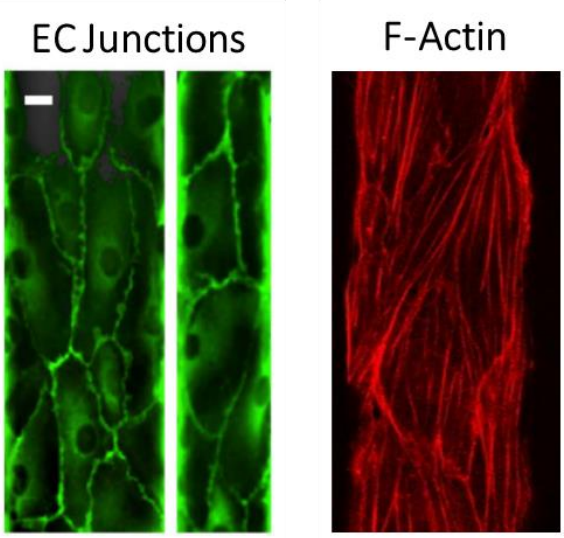

Fig 23: Fluorescent staining of VE-Cadherin and F-Actin of HUVEC cultured under constant shear stress in our microfluidic device. In Green VE-Cadherin in a 60/30µm channel on the left and 30/30µm on the right. In red F-Actin staining in a 60/30µm channel. (Scale bar: 12µm)

Chapter III: Effect shear stress reduction on endothelial cells

As stated earlier, most of the studies focusing on the effect of shear stress on endothelial cells have looked at the adaptation from static culture to shear condition. The shear stimulation is inherent in our system, as flow is needed for medium supply. Therefore the system is perfectly suitable for the study of the impact of a loss or a perturbation of shear forces. In this chapter, we describe and discuss how endothelial cells react to an enzymatic degradation of the glycocalyx, and how they adapt to a significant reduction of shear mechanical forces after a culture and exposition to physiological shear for several days. We compare our control condition (ie endothelial cells cultured under constant shear stress) to: Static 2D cultured HUVEC; HUVEC cultured for 3-5 days and exposed to a shear stress value reduced by fivefold compared to control and finally, HUVEC cultured under constant shear stress for 3-5 days and treated with 150 mUI/mL of neuraminidase for 3h.

I. Comparison between 2D static and shear adapted endothelial cells actin cytoskeleton

HUVEC cultured in 2D condition were seeded at approximately 75% confluence. Once confluence was reached, medium was changed and cells were kept for 24 hours. Fixation was performed as described in the material and methods chapter. Cells were stained for actin and nuclei. Cells display a cobblestone shaped monolayer with no particular orientation of the cell

body. Actin staining reveals primarily a marked peripheral band and an enrichment in cortical grooves. Few stress fibers are also present in various length and thickness. We can observe 3 types of fibers: most of them are ventral fibers crossing the cell body underneath the nuclei, or arc fibers following the curvature of the cell membrane, and few dorsal fibers crossing the cell perpendicular to its longest axis and (see fig 24).

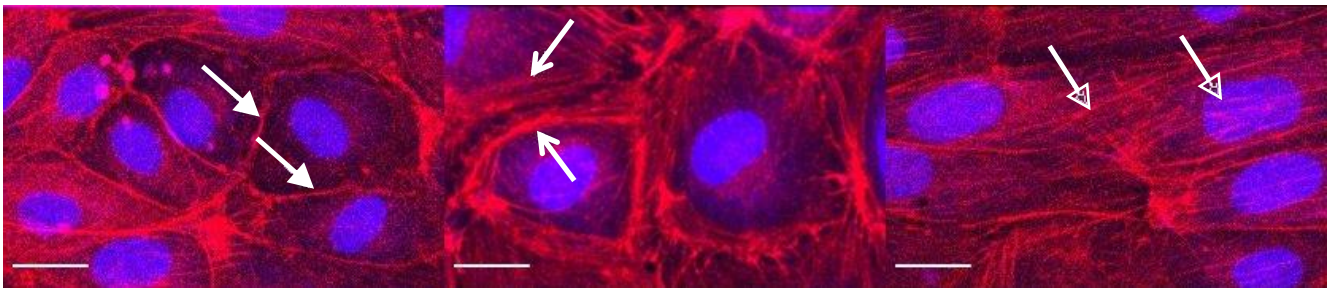

Figure 24: Static 2D culture of HUVEC. HUVEC display a cobblestone shape monolayer. F-actin labeling reveals dorsal stress fibers (empty arrow head), arc fibers (open arrow head) and enrichment at the cell cortex and presence of a dense peripheral actin band (filled arrow head). (scale bar = 20µm)

HUVEC cultured under constant shear stress of 0.4 Pa during 3 to 5 days after seeding inside the microfluidic network form a tight confluent monolayer, covering the 4 walls of the channels. As mentioned in chapter I part IV, cells display a ~700 nm endothelial surface layer fully covering the luminal membrane of the cells, with Heparan sulfate proteoglycan also present more punctually. Also, VE-Cadherin staining reveals a strong signal at cell-cell junction. After fixation and labeling of F-actin and nuclei, cells display long and thick stress fibers, oriented parallel to the flow direction (fig 25). The actin fibers are ventral fibers going underneath the nuclei (see fig 25 B) and are grouped in bundles, forming thick structures that split or join while they cross the cell length (fig 25 A). The poor signal at the cell membrane shows that actin is sparsely present in the cortex. The small amount of actin remaining at the cell membrane still allows us to observe

that the cell body is orientated in the same direction than the stress fibers, the longest axis is parallel to the flow direction (here from left to right on the images of fig 25). The stress fibers cross the cells from side to side underneath the nucleus and seem to be attached to cell-cell junctions as they continue end to end into the neighboring cell (arrow in fig 25 B).

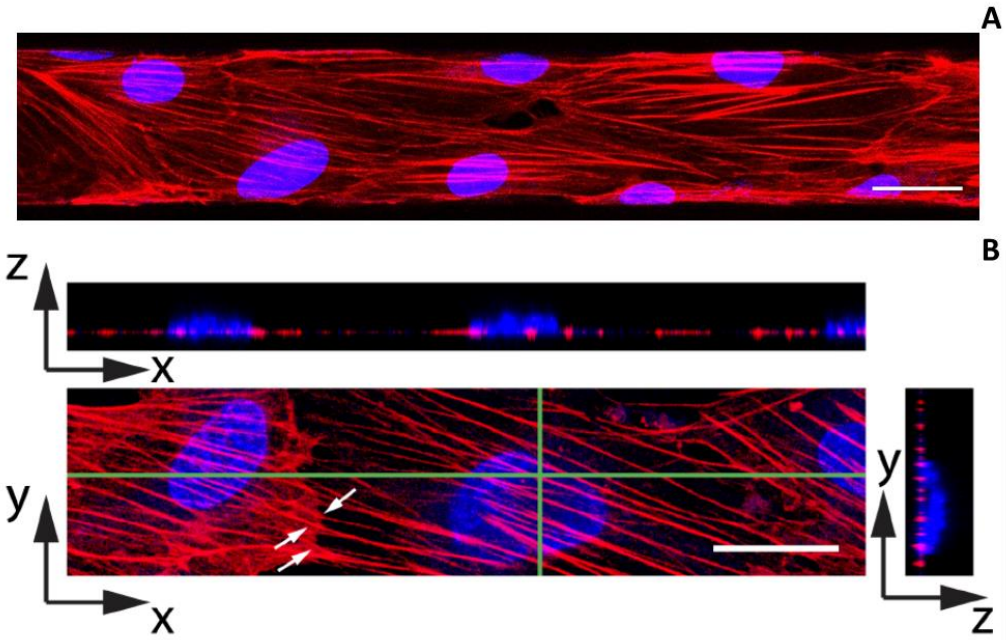

Figure 25: F-actin and nucleus staining of HUVEC cultured under constant shear stress of 0.4 Pa for 3 to 5 days in a channel of 30 µm square section. (A) Z-projection of an image stack of cell lining the bottom surface of the channel, showing the thick and oriented actin fibers displayed by HUVEC cultured under 0.4 Pa shears stress (flow direction from left to right. Scale bar 20 µm). (B) Image of adjacent cells (xy panel) showing actin fibers “crossing” the cells' boundary (white arrows). Stress fibers are located at the basal side of the cells, as seen on the two orthogonal images showing fiber cross-sections running below the nuclei (xz and yz panels taken along the directions indicated by green lines on the xy view. Scale bar 20 µm)

As we intended not only to qualitatively describe the actin cytoskeleton of HUVEC but also to quantify the orientation of the stress fibers, we used the features of the OrientationJ plugin written for ImageJ (53). This plugin computes the structure tensor from the intensity gradient of an image, and

attributes to each pixel in the image a pair of values, between 0 and 1, corresponding to the local values of the (normalized) energy, E, and coherency, C, of the structure tensor. Low values of E correspond to regions in the image where intensity is uniform, while large values indicate regions having one or multiple orientations. C is a measure of the local degree of anisotropy, with values closer to 1 corresponding to regions of stronger anisotropy.

For each experimental conditions, we compute E and C maps of the F-actin images (see fig 26 B and C) obtained in several channels (n=8 to 16), and build a final map where each pixel contains the value of $\sqrt{(EC)}$, which allows us identifying regions displaying both non-uniform and strongly elongated F-actin structures. Plotting the distribution of $\sqrt{(EC)}$ from such maps, for each condition, can thus be used as a proxy for the amount of oriented actin structures present on images.

From the computation of the structure tensor, OrientationJ also provides a map of the local orientation. The plugin associates an orientation to each pixel in the image, including in regions of low E and C where this quantity is not meaningful. Such an orientation map can then be filtered by thresholding on E and C values in order to retain only the orientation values of pixels that are actually part of anisotropic structures. Doing so using the built-in thresholding feature of OrientationJ, we observed that, with our type of images, the filtered orientation maps display a spatial resolution that is clearly lower than the initial image, with blurred features and inclusion of pixels that are actually outside of the fibers (see Fig. 26). We could not find a set of OrientationJ parameters that would allow us to increase further the resolution of the orientation map without losing part of the elongated structures that were visible in the original image. As an alternative to the built-in thresholding feature of the plugin, we find that the following procedure performs better in terms of final resolution: starting from the input image, we run orientationJ to obtain E, C and unfiltered orientation maps. We then threshold the E and C images (at the same levels used in the built-in function of the plugin) and binarize them. In parallel, we binarize the input

image using the local threshold Bernsen method implemented in ImageJ. We then multiply the binarized E, C and Bernsen image in order to create a binary mask that we use to filter the orientation map. A comparison of the built-in and custom-made thresholding is provided in Fig. 26.

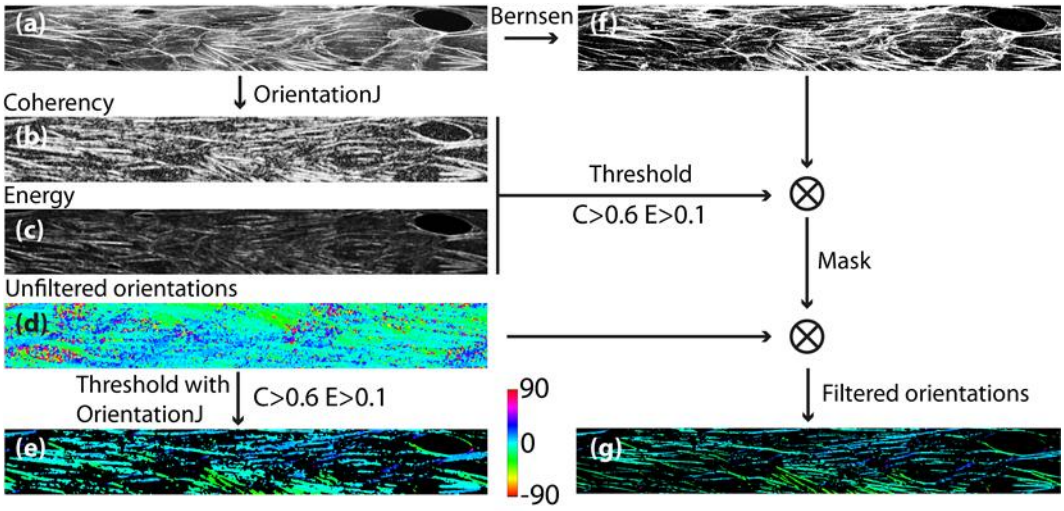

Figure 26: Flowchart of image analysis: starting from a F-actin image (a), the OrientationJ plugin outputs Coherency (b), Energy(c), and Orientation (d) maps. OrientationJ allows filtering the orientation map in order to retain only pixels involved in regions having coherency and energy values larger than a given threshold (E > 0,1 and C > 0,6 here) (e). As an alternative to the latter step, we apply a local thresholding scheme (Bernsen) to the initial image (f) and multiply this segmented image by the thresholded maps (b) and (c) in order to create a binary mask. We then use such a mask in order to discard irrelevant pixels from the raw orientation map (d), and obtain the orientation map (g), with better spatial resolution than (e). Colors on images (d), (e) and (g) code for the local angle, according to the lookup table displayed at the bottom of the figure.

We first describe quantitatively the phenotypic difference between HUVEC cultured under static 2D condition and 3D 0.4 Pa shear flow condition. The output of our image processing shows that:

(i) Comparing the distribution of √EC of static and flow conditions, we observe a greater population upon large values for shear-adapted cells (√EC > 0.2), consistent with the presence of anisotropic structures such as stress fibers, whereas the distribution of √EC is more peaked around smaller value for 2D condition (√EC max value around 0.08) (fig 27 A),

(ii) the angular distribution is sharply peaked around 0° (corresponding to the flow direction) for cells submitted to shear stress, indicating that the stress fibers orientation is along the flow direction, whereas 2D cultures show no particular preferred orientation of anisotropic structure, resulting in broad distribution of the angle histogram (fig 27 B).

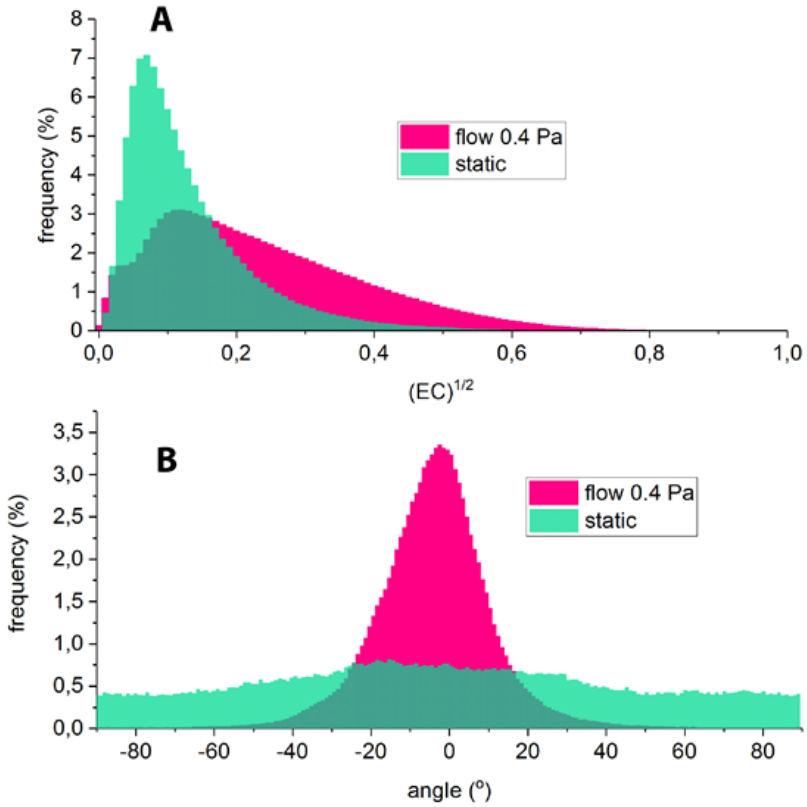

Figure 27: (A) Distribution of √EC for HUVEC cultured under 0.4 Pa in microfluidic channels (Magenta) and under static conditions (Green). (B) Angular distribution of actin filamentous structures observed under flow (Magenta) and static conditions (Green).

II. Impact of reduced shear stress on shear-adapted endothelial cells

Here we propose to consider shear-adapted endothelial cells as the control condition, and look at modifications of the physiological phenotype when shear stress is greatly diminished. To do so, we reduced by fivefold the flow rate of culture medium flowing in channels where cells have been cultured for 3 to 5 days under 0.4 Pa shear. After 1 or 6 hours of reduced shear stress, the medium reservoir was replaced by the fixation solution without flow interruption.

F-actin staining after 1 hour of shear reduction reveals a major disruption of the cytoskeleton compared to control condition (fig 28 B). Indeed, most of the stress fibers are disassembled or reoriented. The remaining structures are thinner and their path is less rectilinear. Stress fibers display a more "chaotic" pattern. This trend is maintained and amplified in cells exposed for 6 hours to reduced shear stress (fig 28 C). We also observe an important increase of background signal consistent with an elevation of the signal at the cell membrane. Region with really high uniform staining appears. Finally, this relocation of the signal to the cell border shows that cell shape and orientation is also more randomized compared to control.

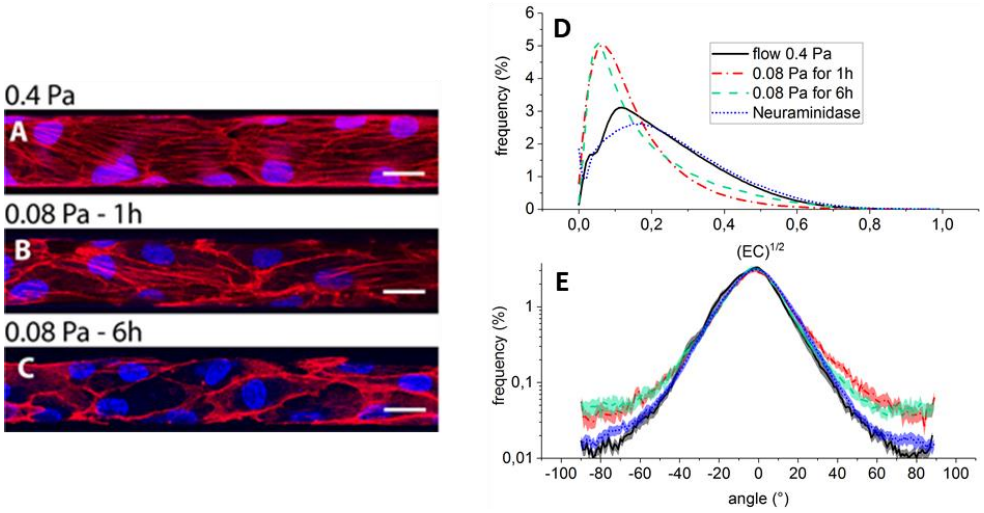

Figure 28: Reduced shear stress exposure after culture under constant shear stress of 0.4 Pa for 3 to 5 days. Overlay images of cells' nuclei (blue) and F-actin (red) under control condition at 0.4 Pa (A), 1h at 0.08 Pa (B) and 6h at 0.08 Pa (C). (D) √EC distribution for control condition (black), reduce shear stress 1h (Red), 6h (Green) and Neuraminidase treated samples (Blue). (E) Angular distribution histogram of anisotropic structure for control condition (black), reduce shear stress 1h (Red), 6h (Green) and Neuraminidase treated samples (Blue). Error bar correspond to +/- standard error.

In 3D observations of cells submitted to reduced shear stress we observe a slight increase in cell body thickness. To quantify this increase, we have measured the height of nuclei in both normal and low shear stress conditions. The results are shown in fig 29 A. In addition to this, we notice that upon long exposure to reduced shear stress (6 hours or more) cells were detaching from the substrate. Indeed, as show in fig 29 B, cells are no longer attached to the corner of the channel wall, while maintaining cell-cell contact.

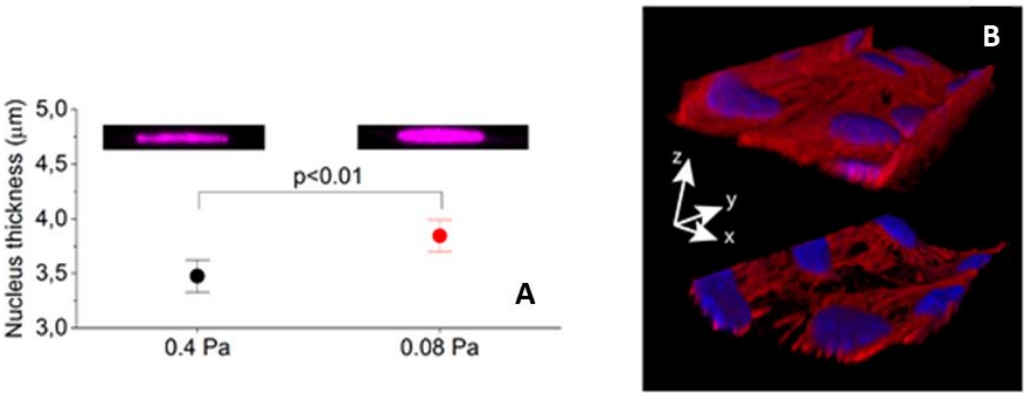

Figure 29: Panel (A): Vertical projections of nucleus under 0.4 Pa (left image) and 0.08 Pa (right image). Such images were taken over about 80 cells for each condition (0.4 Pa and 6h at 0.08 Pa) and used to measure the maximum thickness of the nuclei. The plot reports the mean of these measurements (error bars correspond to 99% confidence interval), which is seen to be ~ 0,3 µm larger ($p < 0,01$ in two-sample t-test) under low shear condition. (B) 3D reconstructions of the bottom part of a channel showing cells lying in the corners under 0.4 Pa (top image), while they tend to detach from corners and round up the effective lumen under 0.08 Pa (bottom image). The lateral channel size is 30 µm.

Quantitatively, the √EC distribution under reduced shear stress is more populated below 0.2 value, indicating, just as for purely static cultures, that the quantity of anisotropic structures is reduced compared to cells adapted at 0.4 Pa (fig 28D). Moreover, when looking at the distribution of angles in the images, the larger values between 40 and 90° are more represented for cells submitted to reduced shear stress during 1 or 6 hours. The loss of stress fibers is therefore accompanied by a disorientation of the actin cytoskeleton resulting in a broadening of the angular distribution (fig 29E). These results will be discussed in more detail in the chapter VI.

III. Impact of partial degradation of the endothelial surface glycocalyx by neuraminidase

When degrading the endothelial surface layer by neuraminidase, we observe a signal decrease of WGA-alexa488 staining (fig 30A, B and C), which indicates the actual removal of some components of the glycocalyx. However, we note that such a degradation does not affect the cytoskeleton organization when compared to the shear-adapted intact cells: as shown in Fig. 28D, the fraction of anisotropic structures (distribution of √EC values) and angular distribution are very similar to control (Fig 28E).

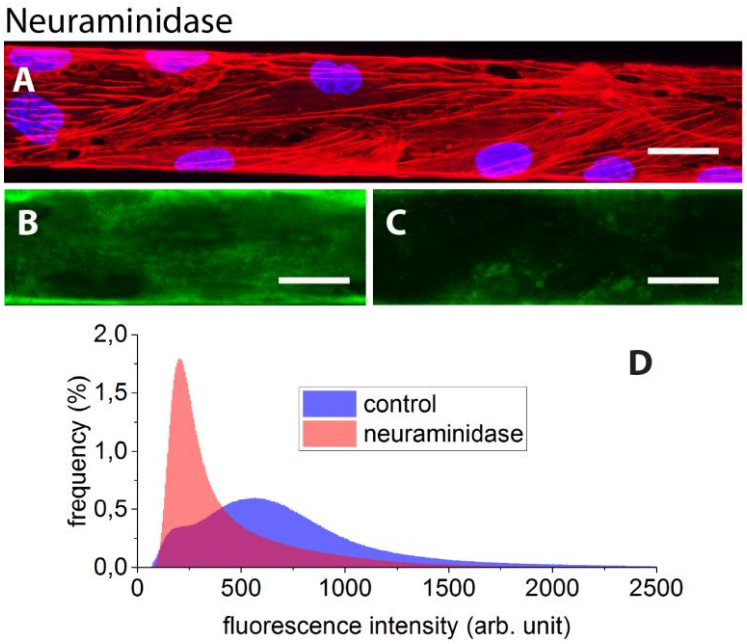

Figure 30 : Neuraminidase treated shear adapted endothelial cells. (A) F-actin cytoskeleton imaged after enzymatic degradation of the endothelial surface layer with Neuraminidase. Staining of the glycocalyx before (B) and after treatment with neuraminidase (C). (D) Intensity histogram of the alexa488-WGA staining before and after treatment with Neuraminidase.

This set of results, along with all the data presented in the following chapters, will be discussed in chapter VI.

Chapter IV: Impact of high glucose concentration on endothelial cells

The relation between diabetes and cardiovascular diseases has been established for decades. Diabetes concern 2 – 5 % of the population of most western countries (54,55). Hyperglycemia presents an increased cardiovascular risk and mortality such as atherosclerosis, obesity, hypertension, metabolic syndrome and heart failure. Some of the effects of hyperglycemia on endothelial cells are known, but not so much importance has been given to its effect on the F-actin cytoskeleton phenotype of endothelial cells. Indeed, most experiments are done on 2D static cultures, where shear stress is totally absent. Here we propose to look at the effect of an increased concentration of glucose in cell culture medium on the phenotype of HUVEC cultured in 2D static condition and in 3D under constant shear stress of 0. 4 Pa.

HUVEC cultured in 2D glass-bottom dishes were grown to confluence, then medium was changed and replaced by culture medium with a 30mM concentration of glucose. HUVEC exposed to high glucose concentration in 2D culture show a similar F-actin cytoskeleton compared to control condition (Fig 31 A and B). This is confirmed by the √EC distribution which shows that the relative amount of anisotropic structures remains unchanged between control and high glucose condition (Fig 31 C). In the same way the angular distribution of anisotropic structures remains similar in control and high glucose condition (Fig 31 D).

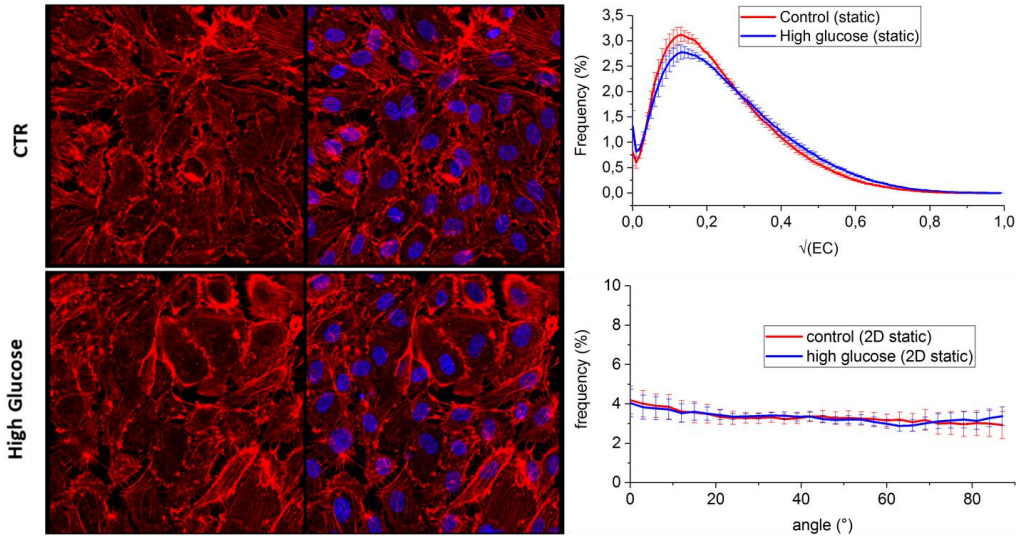

Figure 31: Exposition of 2D static culture of HUVEC to high glucose concentration. (A) control condition (B) 30 mM glucose concentration stain for nuclei (Blue) and F-Actin (Red). (C) √EC distribution of anisotropic structure in control (Red) and high glucose (Blue). (D) Angular distribution histogram of anisotropic structure in control condition (Red) and high glucose (Blue). Error bar correspond to +/- standard error.

After HUVEC were cultured under constant shear stress of 0.4 Pa during 3 to 5 days after seeding inside the microfluidic network, the medium reservoir was changed and replaced by medium with 30 mM of total glucose.

We observe that cell morphology is impaired by the exposition to high glucose concentration (Fig 32 C). Indeed the cell body is no longer elongated as in control condition, cells adopt a more squared shape. 3D stacks also show that cell thickness is bigger. Cells are less stretched and more relaxed. F-actin cytoskeleton is also clearly affected by the exposure to high concentration of glucose. Even if stress fibers appear to be present as numerous as in the control we observe shorter and thicker stress fibers compared to control and their organization is different. Stress fibers are less oriented parallel to the flow direction. It also appears that some of the stress fibers are no longer crossing the cell from side to side. On the other hand 3D stacks show that just as in control stress fiber appear to be ventral as

they go underneath the nuclei. Interestingly there is a strong relocation of actin at the cell membrane. Indeed microscopy observation shows the presence of an increase signal of F-actin at the cell cortex compare to control.

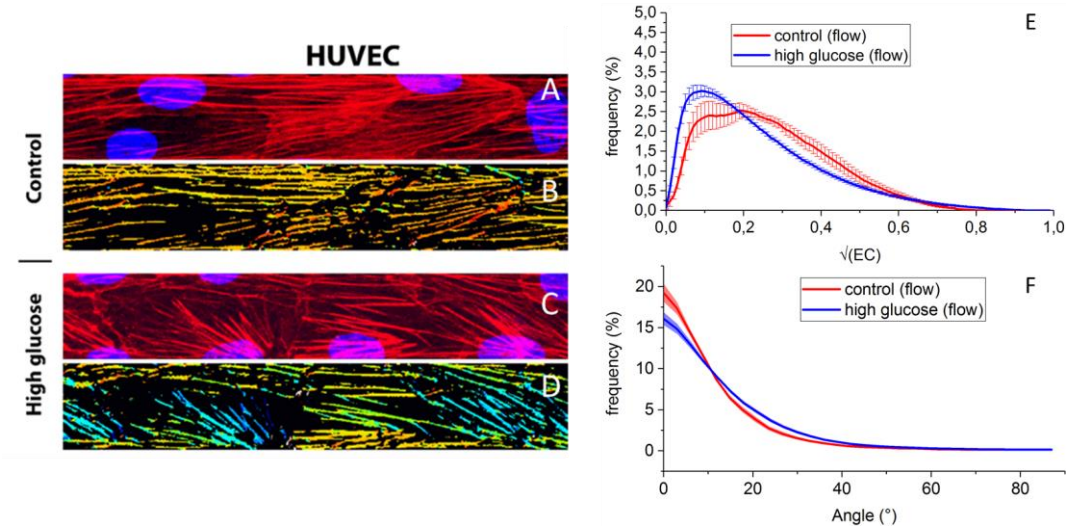

Figure 32 : Impact of 30mM glucose on endothelial cell Actin cytoskeleton. Overlay images of nuclei (blue) and F-actin (red) of endothelial cell culture in control condition and 30 mM glucose (e and g), Color map of actin structure orientation measured with imageJ orientation J in control and 30 mM glucose condition (f and h). Angular distribution of actin structure measured in control (red) and glucose condition (blue). Error bar correspond to +/- standard error.

In order to confirm and quantify the change in orientation of actin stress fiber we proceed to the same processing done on images of control HUVEC. The relative amount of anisotropic structures is slightly reduce in high glucose concentration (Fig 32 F). The curve corresponding to high glucose is peaked around 0.1 whereas the control curve is peaked around 0.2. Comparing the relative frequency of orientation of stress fibers (Fig 32 E), the processing shows that in high glucose condition a lower amount of fibers are oriented between 0 and 16° and that this amount increases after 16°, meaning that less fibers are oriented in the flow direction. The distribution of angle is broadened compare to control.

These results only allow us to observe the loss of orientation of Actin stress fibers when cells are exposed to high glucose concentration. The mechanism behind this orientation could be affected either by a perturbation of the mechanosensory machine of the cell or by a loss of the polarity establish during adaption to shears stress. These results will be discussed in more detail in chapter VI.

Chapter V: Assessment of endothelial barrier function for the study of paroxysmal permeability disorders

Vascular permeability disorders regroup some clinical conditions that can be lethal, such as in laryngeal edema caused by primary angioedema, or can be a systemic derangement such as in idiopathic systemic capillary syndrome, which can give rise to hypovolemic shock due to massive plasma and protein extravasation. Massive leaks of solute from blood vessel are caused by a dysfunction of the endothelium, and more precisely by a deregulation of the barrier function at cell-cell junctions. This barrier function is regulated by two types of protein complexes: (i) adherent junctions with VE-Cadherin as core protein (specifically in endothelial cell) , and (ii) tight junctions with claudin-5.

Among permeability disorders, there exist some cases where the dysfunction is periodic and degenerative phenotype, inflammation and vascular injury are absent. This group of clinical condition is named as Paroxysmal Permeability Disorders. The table in figure 33 regroups the features for inclusion and exclusion with currently identifiable clinical phenotypes.

Again, most techniques developed to assay permeability of endothelial cells under clinical conditions lack the mechanical environment which shear stress represents. We used our system, combined with the use of the high affinity couple Biotin/Avidin. Prior to seeding, the extracellular matrix coating was replaced by a Biotin conjugated fibronectin. Fully grown endothelium under constant shear stress were tested for permeability in different

conditions and then, before fixation, a solution of fluorescent Avidin was perfused for 5 min.

PAROXYSMAL PERMEABILITY DISORDERS

CRITERIA
Features for inclusion
- Recurrent self-limiting local or systemic interstitial edema
- For non-lethal episodes, complete healing max 1 week, mostly 1–3 days
Features for exclusion
- Any underlying clinical condition causing increase in endothelial permeability (infections, systemic inflammation, allergy, malignancy, injury, autoimmune disease etc.)
- Local signs of inflammation, ischemia-necrosis, tissue degeneration
CLINICAL PHENOTYPES
Primary Angioedema
- Idiopathic histaminergic angioedema
- Hereditary/acquired angioedema due to C1 inhibitor deficiency
- Hereditary angioedema with normal C1 inhibitor
- Idiopathic non-histaminergic angioedema
Idiopathic Systemic Capillary Leak Syndrome
Yet poorly defined forms of periodic edema
- Recurrent retroperitoneal edema
- Recurrent female periodic edema of unknown origin
- Recurrent edema in patients with hypereosinophilia (Gleich's syndrome)

Figure 33: Table for paroxysmal permeability disorders, features for inclusion/exclusion together with currently identifiable clinical phenotypes. Adapted from (32)

After HUVEC were cultured under constant shear stress of 0.4 Pa during 3 to 5 days after seeding inside the microfluidic channels, cells were stained for cytoplasm with CellTracker Red, and the integrity of the endothelium was checked. As show in Figure 34 A, the bottom, sides and top of the channels are fully covered by endothelial cells. After this step, cells were exposed to a constant flow of the following media: (i) usual endothelial cells culture medium as a control, (ii) plasma from healthy volunteers—blood was withdrawn in Sodium Citrate tubes, plasma was separated from cells by centrifugation and diluted 1:1 with medium for ECs culturing, (iii) bradykinin

diluted in endothelial cells culture medium at a concentration of 25µM. Exposure to these different media lasted for 15 minutes and was immediately followed by perfusion of fluorescent Avidin for 5 minutes before rising and fixation for microscopic observation.

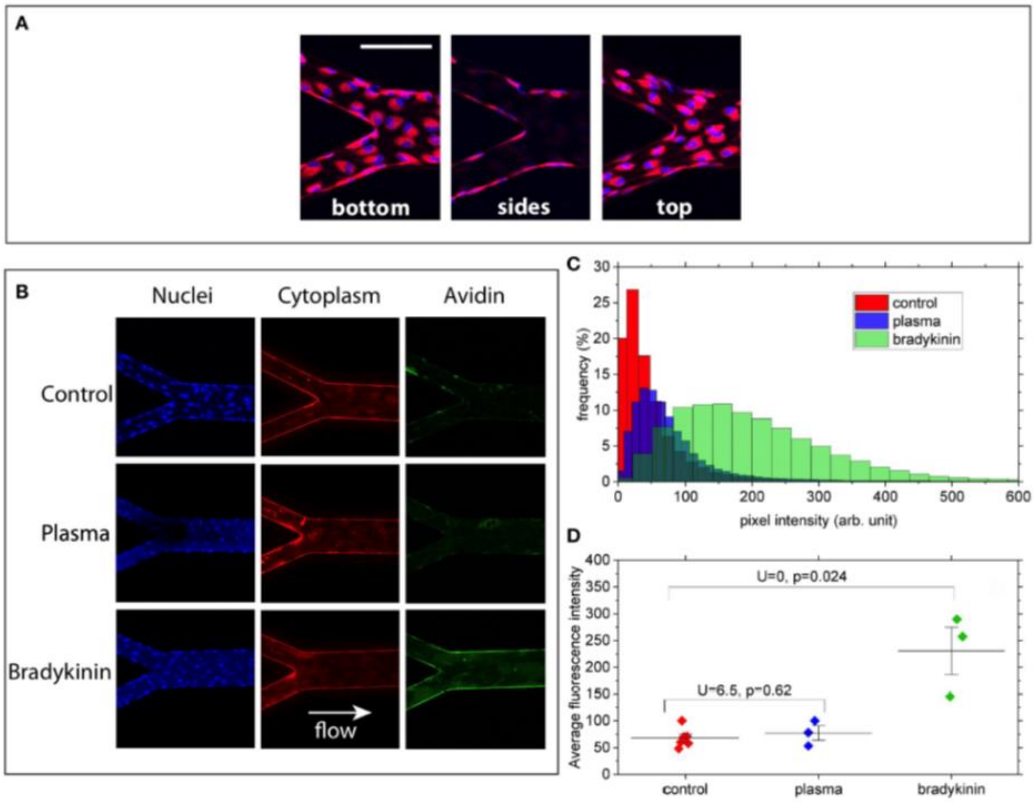

Figure 34: Bradykinin-induced permeability of endothelial cells. (A) merged images showing cell nuclei (blue) and cytoplasm (red) at the bottom, on the lateral walls and at the top of the channels (scale bar: 100µm). (B) Z-summed images obtained from 3D-stacks showing nuclei (blue), cytoplasm (red), and wall-bound Avidin (green) for the 3 conditions: control, 50%-plasma, and bradykinin. Image size is 425 × 425µm. Imaged regions correspond to a merging point between two 60 µm-wide channels and one 120 µm-wide. (C) FITC intensity histograms (relative frequency as a function of pixel intensity) computed for the 3 conditions from the images shown in (A). (D) Average fluorescence intensity values measured for the various conditions over 3–6 different bifurcation areas of the networks. U and *P*-values correspond to two-samples Mann–Whitney *U*-tests showing that, at the 5% threshold, Bradykinin and Control data are different whereas Plasma and Control are not.

For the purpose of this experiment, image acquisition parameters were different from what was described in the chapter materials and methods. In

order to quantitatively compare images of the channels perfused with different media, a particular care was taken for acquiring all of the image stacks with the same parameters: 3D stacks of 425 x 425 x 35 µm (0.140µm/pixel in X/Y and 1.5 µm/pixel in Z), acquired with a 20x objective, over the 30 µm to 60µm bifurcations. Stacks were transformed into 2D images by summing the intensity of each slice. Representative images of the 3 conditions are given in fig 34 B, and intensity histograms and mean values of intensity of the conjugated Avidin measured on area of the same size (49.000 µm²) are displayed in fig 34 C and D.

The principle of these experiments relies on the high affinity of Avidin for biotin. Avidin in the channels covered by a healthy endothelium should flow without being able to reach the underlying biotin. If the endothelial barrier function is altered, then avidin can pass through cellular junctions and bind to biotin. The fluorescence measured at the wall of the channels after rinsing of the avidin solution is therefore the consequence of a leak of the solution when living cells were perfused. Doing so we observe that (Fig 34 C):

(i) no major difference in histogram peak or width can be seen between the control and the 50%-plasma from healthy volunteer conditions,

(ii) in the circuit exposed to 25µM solution of bradykinin, the histogram is clearly shifted to larger intensity values compared to that obtained for the control.

This trend is confirmed by the mean value measured on 3-6 different channel bifurcations: in bradykinin-infused channels, the mean intensity is 230 -/+ 76 (intensity arbitrary unit), significantly higher compared to control and diluted plasma conditions, respectively measured at 68 -/+ 18 and 77-/+ 23 intensity units. Since the intensity value depends on the amount of Avidin that have passed the endothelial barrier and linked Biotin, this result can be considered as a sign of increased permeability after bradykinin perfusion.

In order to confirm this result, conjugated Avidin was perfused into channels which were coated with non-biotinylated fibronectin (native human Fibronectin). With no cell present in the channel and fibronectin freely accessible to conjugated Avidin, we measured an average fluorescence at the wall of the channel close to the detection noise of the equipment (15 +/- 8 arbitrary unit measured compared to a noise level of 10 +/- 4). This result shows that conjugated Avidin has a very low level of affinity for native fibronectin. With cell-coated channels, the level of intensity is similar to the one measured in control and plasma condition (38 +/- 6). This fluorescence being measured inside cell cytoplasm and not at the walls of the channel suggests that the major part of the signal detected in these negative control experiments corresponds to endothelial uptake of flowing conjugated Avidin.

Chapter VI: Conclusions, discussion and perspectives

Biomimetic devices aim at reproducing in vitro environmental conditions as close as possible as the one experienced by a biological system in vivo. In this work we aimed at developing a system reproducing the viscous friction experienced by endothelial cells in vivo, with a control of the biochemical composition of the fluid, in order to test endothelial cells' response to pathological conditions. The microfluidic system developed allows microscopic observation of endothelial cell morphological changes in response to these perturbations. In contrast to most of the studies focused on cell adaption to mechanical or biochemical stimulation, here we proposed a viewpoint where shear-adapted endothelial cells are considered as the control condition, and validated our technique by a set of experiments to describe the morphological profile of endothelial cells grown in these conditions. We showed that in our control condition, under constant physiological level of shear stress, Human Umbilical Vascular Endothelial Cells display the so-called atheroprotective phenotype. Observations of the endothelial surface layer by fluorescent staining of polysaccharide chain of the glycocalyx with alexa488 coupled WGA show a uniform signal on the cells' surface. The staining was verified by enzymatic degradation of the endothelial surface layer with neuraminidase. We observed a strong decrease of the fluorescent signal in treated samples. This labeling also allowed us to measure a mean thickness of 0.7 µm of the glycocalyx, this measurement being in good agreement with in vivo observations. In addition, as heparan sulfate residues are known to be essential for fluid shear stress mechanosensing by the glycocalyx, we decided to use antibody specific staining. This labeling revealed that heparan sulfate was present and located at the cell surface in the glycocalyx. Phalloidin-TRITC

stainings show long and thick F-actin stress fibers oriented parallel to the flow direction, crossing the cell from side to side and anchored at the cell border. Finally, specific antibody labeling of Ve-Cadherin revealed a strong signal along the cell borders, indicating that cells form proper tight junctions essential for vascular permeability. Taking together all these morphological observations, we can affirm that in our control condition, endothelial cells display the atheroprotective phenotype, which is a sign for a proper endothelial function.

In order to go beyond qualitative description of phenotypes, we have performed quantitative analysis of the F-actin cytoskeleton by using the imageJ built-in plugin OrientationJ. This plugin allowed us determining the orientation of anisotropic structures such as stress fibers, but also to quantify the fraction of these anisotropic structures present on images. Based on the comparison with 2D static cultures of HUVEC, we showed that the fraction of anisotropic structures was greater in shear-adapted cells. Moreover, 2D static endothelial cells show no particular orientation of these actin structures, whereas shear-adapted endothelial cells display a clear orientation of the fibers, with an angle corresponding to the flow direction. These results are in good agreement with already published data (56).

Effect of reduced shear stress

In vivo, endothelial cells are constantly submitted to shear stress, except during angiogenesis. This motivated us to perform experiments on flow reduction. We observe that, after 1 or 6 h of flow reduction (0.08 Pa instead of 0.4), shear-adapted endothelial cells display a modified F-actin cytoskeleton phenotype. Confocal image stacks show a clear reorganization of F-actin, fewer stress fibers that seem to randomly reorient in sample exposed for 1 hours to reduce shear stress, and in some case a complete loss of all the stress fibers for longer exposure to reduced shear stress. These observations are confirmed by the data analysis used. The fraction of anisotropic structures is lowered, and the angular distribution is

broadened. The concomitantly observed thickening of nuclei suggest a slight inflation of the cells' body. This is consistent with the decrease in stress fibers which we expect to be associated with a relaxation of the cells' internal stresses. We can therefore conclude that exposure to a reduced shear stress induces a loss of the oriented phenotype in shear-adapted endothelial cells. Taking together this set of experiments along with the trend for cells to detach from the walls at long exposure to low shear, strongly suggests that upon a five-fold decrease of the wall shear stress, HUVEC switch from an atheroprotective to an atheroprone and more motile phenotype (53)

To the best of our knowledge, only few studies have looked into the effect of a loss of shear stress or simulated ischemia, most of them focusing on the consequences on ROS (Reactive Oxygen species) production, and only one publication is related to the actin cytoskeleton in vivo (57–60). As mentioned in these studies, during ischemia, the endothelial cells' response can be influenced by the increased production of ROS, and later by the lack of dioxygen. Indeed, in flow chamber or microfluidic experiments, the amount of medium accessible to cells is reduced, and when flow is stopped the dioxygen concentration may decrease fast. In our experimental setup the internal volume of the network is 0.25 µL, which means that even with a shear stress of 0.08 Pa corresponding to a flow rate 0.2µL/min the entire volume of medium in the channels is renewed each minute. Therefore the remaining flow is sufficient for oxygen supply and the observation made are the result of a perturbation of the mechanosensory machinery and not a consequence of anoxia. Nevertheless, Po_2 could be assayed using optical probes such as described in (61) to verify oxygenation of the cells. The production of ROS could be also investigated in our conditions. Actually, in preliminary experiments performed during this thesis, we have used JC-1, a fluorescent probe sensitive to mitochondria membrane potential. The use of this probe required some adaptation of the protocols, since the observations under reduced shear stress had to been done with living cells. The data obtained are too preliminary to be conclusive and are not included

in this manuscript. However, such experiments could bring insight into the redox state of the cells by looking at the mitochondria organization and activity.

Along this line, it has been shown in (57-59) that ischemia-like flow reduction induces a redox stress. In parallel, it has been demonstrated in (62) that oxidative stress provoked by hydrogen peroxide treatment of endothelial cells favors the organization of actin under the form of stress fibers. Taken together these two studies would suggest that flow reduction should yield an increase of stress fibers which is opposite to what we observe.

However, as shown also in (62), hydrogen peroxide treatment under mild, low-dose, conditions do not perturb the actin organization. It is therefore likely that the redox stress induced by ischemia isn't sufficient to induce actin recruitment. Finally, as the adaptation of endothelial cells to shear stress goes through polarization of the cell for orientation of cytoskeleton component (63,64), it would be interesting to look at polarity markers such as microtubules, endoplasmic reticulum and PAR-3/aPKCλ before and after shear stress reduction.

The partial degradation of the ESL with neuraminidase yielding no discernible change in actin organization may seem puzzling in the first place, as the glycocalyx is directly involved in flow sensing of endothelial cells. However, neuraminidase specifically targets syalic acid in the ESL, while it is expected to leave intact glycosaminoglycans such as Heparan Sulfate (12). Our first hypothesis was that the glycocalyx was entirely dragged by shear forces and that removing a component as abundant as sialic acid would be sufficient to either collapse or diminish the displacement of other members of the ESL, thus blocking the mechnotransduction. In the end, the remaining part of glycocalyx seems sufficient for mechanical transduction and our observation is therefore qualitatively consistent with previous studies pointing at heparan sulfate as being one of the main player, connected to the cyctoskeleton through syndecans, in glycocalyx-mediated mechanotransduction.

Effect of high glucose concentration

Diabetes are associated with a number of macro and microvascular complications that are pathophysiologically linked with the development of endothelial dysfunction (65–67). In this work we investigated the impact of an increased concentration of glucose in the medium on HUVEC phenotype. After exposure to 30mM of glucose during 24 hours, cells were fixed and observed in fluorescent confocal microscopy. We first examined HUVEC cultured in 2D static condition, in presence of a normal glucose concentration and with a high concentration. In 2D condition, we have not observed any modification of the actin cytoskeleton. Indeed, measurements of the relative portion of anisotropic structures revealed no significant difference between high glucose concentration and control. The angular distribution remains unchanged as well. In contrast, exposition of shear-adapted endothelial cells to high glucose concentration leads to a clear change of phenotype. We observe a reorganization of actin stress fibers, mainly as a reorientation. Indeed, we show that √EC distributions were not significantly different, whereas comparing the angular distributions of anisotropic structures, we find a lower amount of flow oriented fibers under high glucose condition. The distribution of angle is broadened compared to control.

Although we lack a clear picture that could explain such an observation, we give below some hints concerning the impact of high glucose condition on endothelial function:

- Hyperglycemia is known to decrease NO production either because eNOS activity is perturb by redox stress generated by the over-consumption of glucose, or due to the presence of oxidized LDL in the plasma membrane, disturbing cholesterol in caveole.

- as shown in (68), oxidative stress induced by treatment with hydrogen peroxide results in a shedding of the endothelial surface layer and a diminution of the heparan sulfate on the surface of the cells after a few hours of treatment.
- The extensive glycation of proteins activates inflammatory genes such as NF-κB via RAGE receptor (54,55).
- Little is known on how endothelial cells orient their stress fibers in physiological condition. Some evidence show that planar cell polarity is driven by RhoA and PAR3-aPKC gradient which stabilizes microtubules downstream the flow direction in the cells (63,64). This polarity would drive the orientation of actin stress fibers.

Therefore, even if our results only allow us to observe the loss of orientation of actin stress fibers, we could imagine that, just as redox or glycated proteins perturb the endothelial function, the over consumption of glucose could impact the mechanism which orients the stress fibers. This could arise either by perturbing the mechanosensory machine of the cell or by inducing a loss of the polarity established during adaption to shears stress.

Irrespective of the detailed mechanism perturbing the actin orientation, it is noteworthy that this effect of high glucose concentration is visible only on cells submitted to shear stress. This point to the importance of placing endothelial cells into proper mechanical environment.

An assay of the endothelial permeability

Most techniques developed to assay permeability of endothelial cells under clinical condition lack the mechanical stimulus associated to shear stress. We have used our microfluidic system, combined with the use of the high affinity couple Biotin/Avidin, in order to assay the barrier function of HUVEC confined into perfused microchannels. Permeability was assayed in three different conditions: (i) control with medium, (ii) plasma from healthy volunteers and, (iii) Bradykinin infused channel. Doing so, we observe that no major difference in permeability can be seen between the control and the 50%-plasma from healthy volunteer conditions. In the circuit exposed to

25µM solution of bradykinin, the presence of fluorescent avidin linked to biotinylated fibronectin indicates a leak of the flowing solution through the endothelium. This experiment, performed using a well-known permeability factor, demonstrates that our system is suitable for the study of paroxysmal permeability disorders, and provides a first proof-of-concept. It thus open routes for personalized treatment. For instance, plasma withdrawn from patient during acute phase could be tested in controlled environment such as our systems, with the possibility of exploring the biological response of HUVEC to circulating factors. On the other hand, isolation of circulating endothelial cells or extracting patient endothelial cells from tissues could help in determining the cellular clues of paroxysmal permeability disorder.

Further technological steps

One limitation of our system is that endothelial cells are cultured onto surfaces of materials (PDMS and glass) which are mechanically much stiffer than tissues surrounding the endothelium in vivo. A more realistic implementation would be to culture cells into channels made in a soft substrate. Prompted by the constantly growing number of studies of HUVEC in soft microfluidic devices, we started to think about a way to introduce a collagen layer into our devices. Preliminary results are show in fig 35. The process of fabrication of such a collagen substrate relies on the activity of a photosensitive molecule, the ruthenium complex. While excited by a two photon laser beam, the ruthenium complex generates radicals allowing the crosslinking of collagen fibers. A solution of liquid collagen mixed with ruthenium complex was first injected into the microfluidic device. Using the reaction described above, combined with a 3D laser beam scanning system, we have been able to form half of a channel of collagen inside a microfluidic channel. This promising preliminary result raises many possibilities concerning the study of endothelial cells:

- To the best of our knowledge, observation of endothelial cell's actin cytoskeleton phenotype in confined soft microfluidic devices has not been reported. The same experiments of flow reduction could be performed in order to appreciate the behavior of endothelial cells in ischemic condition while cultured on soft substrates.
- Incorporating fluorescent beads inside the collagen gel would allow to perform traction force microscopy and bring insights into the mechanical behavior of endothelial cells submitted to physiologic level of shear stress or in pathological condition.
- Finally, permeability to circulating cells could be investigated. Indeed, with a proper stimulation of endothelial cells and the presence of chemoattractant molecules in the collagen gel, the extravasation process of circulating lymphocytes could be investigated.

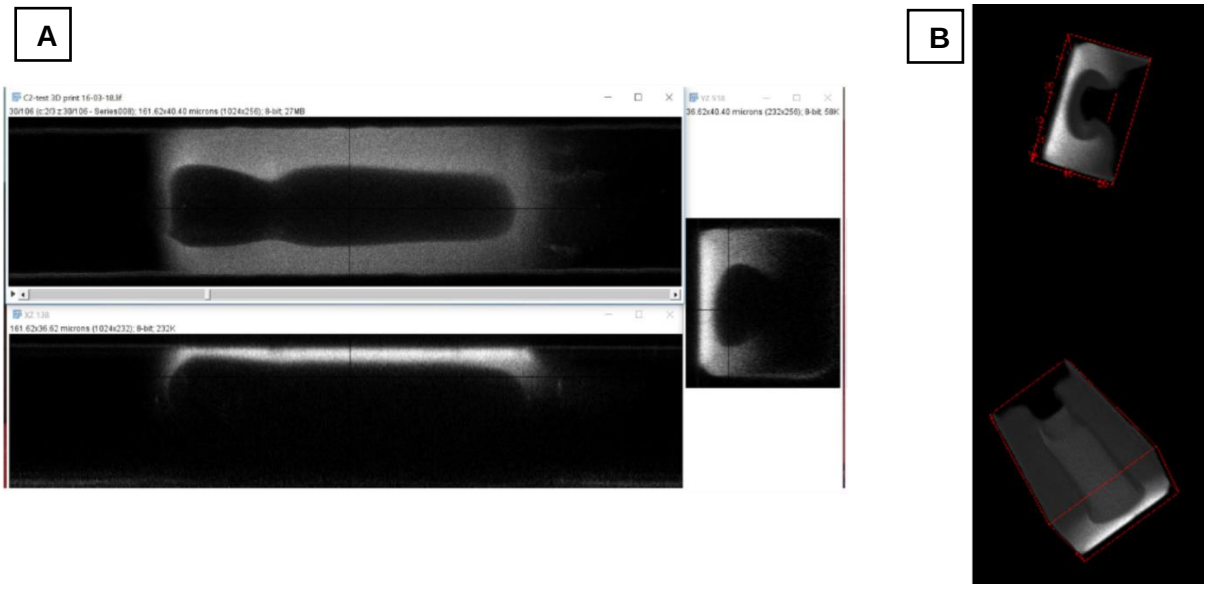

Figure 35: Microscopic observation of a crosslinked collagen gel into a 30µm square section of a microfluidic channel. The signal observed come from collagen autofluorescence. (A) Cross sectional view of the polymerized collagen channel. (B) 3D dimensional representation of the collagen gel channel observe in autofluorescence.

Finally, the development of these biomimetic devices was also part of the will to design a model experiment for the study of endothelial cells behavior in micro-, hyper- or altered-gravity. During long-term space flights, the human body loses its fluid balance. This results, for the blood circulation, in a decreased volume because of fluid repartition in tissues inducing a decreased shear stress, an increased oxidative stress because of space radiation and a perturbation of the mechanosensory machinery of the cell. Cell sensitivity to altered gravity conditions has been demonstrated experimentally, in particular in the case of endothelial cells: using ground-based hypo- or hyper-gravity simulation devices, it has been evidenced that cytoskeletal organization, cell proliferation, migration, nitric oxide production, or gene expression are affected by both reduced or increased gravitational loadings (69). However, a clear picture of the impact of altered gravity on endothelial cells is still to be reached. Indeed, comparison between studies is currently complicated by the fact that (i) endothelial cells from different blood vessel districts (macro or microvessels) have been used, and (ii) gravitational conditions vary between studies. Moreover, previous works have been performed using sub-confluent (less than a cell monolayer) 2D cultures, in the absence of shear flow. This is markedly different from the normal in vivo “working” conditions of endothelial cells, which are arranged into a 3D confluent monolayer continuously submitted to the hydrodynamic shear stress arising from blood flow. We therefore could, in order to stick closer to physiological situations, study the altered-gravity sensitivity of endothelial cells grown to confluence into microfluidic channels and stimulated by a shear flow. This work could be conducted either in hypergravity in large diameter centrifuge or as it is currently developed in sounding rocket to study the impact of zero-gravity on the endothelial phenotype.

Bibliography

1. Sherwood L. *Human Physiology: From Cells to Systems*. Cengage Learning (2015).

2. Rajendran P, Rengarajan T, Thangavel J, Nishigaki Y, Sakthisekaran D, Sethi G, Nishigaki I. The Vascular Endothelium and Human Diseases. *Int J Biol Sci* (2013) **9**:1057–1069. doi:10.7150/ijbs.7502

3. Tarbell JM, Cancel LM. The glycocalyx and its significance in human medicine. *Journal of Internal Medicine* (2016) **280**:97–113. doi:10.1111/joim.12465

4. Zeng Y, Ebong EE, Fu BM, Tarbell JM. The Structural Stability of the Endothelial Glycocalyx after Enzymatic Removal of Glycosaminoglycans. *PLoS One* (2012) **7**: doi:10.1371/journal.pone.0043168

5. Fu BM, Tarbell JM. Mechano-sensing and transduction by endothelial surface glycocalyx: composition, structure, and function. *Wiley Interdisciplinary Reviews: Systems Biology and Medicine* (2013) **5**:381–390. doi:10.1002/wsbm.1211

6. Zeng Y, Zhang XF, Fu BM, Tarbell JM. "The Role of Endothelial Surface Glycocalyx in Mechanosensing and Transduction," in *Molecular, Cellular, and Tissue Engineering of the Vascular System* Advances in Experimental Medicine and Biology., eds. B. M. Fu, N. T. Wright (Cham: Springer International Publishing), 1–27. doi:10.1007/978-3-319-96445-4_1

7. Sarrazin S, Lamanna WC, Esko JD. Heparan Sulfate Proteoglycans. *Cold Spring Harb Perspect Biol* (2011) **3**:a004952. doi:10.1101/cshperspect.a004952

8. Luft JH. Fine structures of capillary and endocapillary layer as revealed by ruthenium red. *Fed Proc* (1966) **25**:1773–1783.

9. Rostgaard J, Qvortrup K. Electron Microscopic Demonstrations of Filamentous Molecular Sieve Plugs in Capillary Fenestrae. *Microvascular Research* (1997) **53**:1–13. doi:10.1006/mvre.1996.1987

10. van den Berg Bernard M., Vink Hans, Spaan Jos A.E. The Endothelial Glycocalyx Protects Against Myocardial Edema. *Circulation Research* (2003) **92**:592–594. doi:10.1161/01.RES.0000065917.53950.75

11. Ebong Eno E., Macaluso Frank P., Spray David C., Tarbell John M. Imaging the Endothelial Glycocalyx In Vitro by Rapid Freezing/Freeze Substitution Transmission Electron Microscopy. *Arteriosclerosis, Thrombosis, and*

Vascular Biology (2011) **31**:1908–1915. doi:10.1161/ATVBAHA.111.225268

12. Betteridge KB, Arkill KP, Neal CR, Harper SJ, Foster RR, Satchell SC, Bates DO, Salmon AHJ. Sialic acids regulate microvessel permeability, revealed by novel in vivo studies of endothelial glycocalyx structure and function. *The Journal of Physiology* (2017) **595**:5015–5035. doi:10.1113/JP274167

13. Zullo JA, Fan J, Azar TT, Yen W, Zeng M, Chen J, Ratliff BB, Song J, Tarbell JM, Goligorsky MS, et al. Exocytosis of Endothelial Lysosome-Related Organelles Hair-Triggers a Patchy Loss of Glycocalyx at the Onset of Sepsis. *The American Journal of Pathology* (2016) **186**:248–258. doi:10.1016/j.ajpath.2015.10.001

14. Song JW, Zullo J, Lipphardt M, Dragovich M, Zhang FX, Fu B, Goligorsky MS. Endothelial glycocalyx—the battleground for complications of sepsis and kidney injury. *Nephrol Dial Transplant* (2018) **33**:203–211. doi:10.1093/ndt/gfx076

15. Zeng Y, Tarbell JM. The Adaptive Remodeling of Endothelial Glycocalyx in Response to Fluid Shear Stress. *PLOS ONE* (2014) **9**:e86249. doi:10.1371/journal.pone.0086249

16. Arisaka T, Mitsumata M, Kawasumi M, Tohjima T, Hirose S, Yoshida Y. Effects of Shear Stress on Glycosaminoglycan Synthesis in Vascular Endothelial Cellsa. *Annals of the New York Academy of Sciences* (1994) **748**:543–554. doi:10.1111/j.1749-6632.1994.tb17359.x

17. Franke R-P, Gräfe M, Schnittler H, Seiffge D, Mittermayer C, Drenckhahn D. Induction of human vascular endothelial stress fibres by fluid shear stress. *Nature* (1984) **307**:648–649. doi:10.1038/307648a0

18. Levesque MJ, Nerem RM. The Elongation and Orientation of Cultured Endothelial Cells in Response to Shear Stress. *J Biomech Eng* (1985) **107**:341–347. doi:10.1115/1.3138567

19. Thi MM, Tarbell JM, Weinbaum S, Spray DC. The role of the glycocalyx in reorganization of the actin cytoskeleton under fluid shear stress: A "bumper-car" model. *Proc Natl Acad Sci U S A* (2004) **101**:16483–16488. doi:10.1073/pnas.0407474101

20. Ebong EE, Lopez-Quintero SV, Rizzo V, Spray DC, Tarbell JM. Shear-induced endothelial NOS activation and remodeling via heparan sulfate, glypican-1, and syndecan-1. *Int Bio (Cam)* (2014) **6**:338–347. doi:10.1039/c3ib40199e

21. Zeng Y, Liu J. Role of glypican-1 in endothelial NOS activation under various steady shear stress magnitudes. *Experimental Cell Research* (2016) **348**:184–189. doi:10.1016/j.yexcr.2016.09.017

22. Yen W, Cai B, Yang J, Zhang L, Zeng M, Tarbell JM, Fu BM. Endothelial Surface Glycocalyx Can Regulate Flow-Induced Nitric Oxide Production in Microvessels In Vivo. *PLOS ONE* (2015) **10**:e0117133. doi:10.1371/journal.pone.0117133

23. Bartosch AMW, Mathews R, Tarbell JM. Endothelial Glycocalyx-Mediated Nitric Oxide Production in Response to Selective AFM Pulling. *Biophysical Journal* (2017) **113**:101–108. doi:10.1016/j.bpj.2017.05.033

24. Malek AM, Izumo S. Mechanism of endothelial cell shape change and cytoskeletal remodeling in response to fluid shear stress. *Journal of Cell Science* (1996) **109**:713–726.

25. Noria S, Xu F, McCue S, Jones M, Gotlieb AI, Langille BL. Assembly and Reorientation of Stress Fibers Drives Morphological Changes to Endothelial Cells Exposed to Shear Stress. *The American Journal of Pathology* (2004) **164**:1211–1223. doi:10.1016/S0002-9440(10)63209-9

26. Thi MM, Tarbell JM, Weinbaum S, Spray DC. The role of the glycocalyx in reorganization of the actin cytoskeleton under fluid shear stress: A "bumper-car" model. *Proc Natl Acad Sci U S A* (2004) **101**:16483–16488. doi:10.1073/pnas.0407474101

27. Conway DE, Breckenridge MT, Hinde E, Gratton E, Chen CS, Schwartz MA. Fluid shear stress on endothelial cells modulates mechanical tension across VE-cadherin and PECAM-1. *Curr Biol* (2013) **23**:1024–1030. doi:10.1016/j.cub.2013.04.049

28. Mohamadzadeh M, DeGrendele H, Arizpe H, Estess P, Siegelman M. Proinflammatory stimuli regulate endothelial hyaluronan expression and CD44/HA-dependent primary adhesion. *J Clin Invest* (1998) **101**:97–108. doi:10.1172/JCI1604

29. Livre:Poiseuille - Recherches sur les causes du mouvement du sang dans les vaisseaux capillaires, 1835.djvu - Wikisource. Available at: https://fr.wikisource.org/wiki/Livre:Poiseuille_-_Recherches_sur_les_causes_du_mouvement_du_sang_dans_les_vaisseaux_capillaires,_1835.djvu [Accessed September 17, 2019]

30. Callens N, Minetti C, Coupier G, Mader M-A, Dubois F, Misbah C, Podgorski T. Hydrodynamic lift of vesicles under shear flow in microgravity. *EPL* (2008) **83**:24002. doi:10.1209/0295-5075/83/24002

31. Saintyves B, Jules T, Salez T, Mahadevan L. Self-sustained lift and low friction via soft lubrication. *PNAS* (2016) **113**:5847–5849. doi:10.1073/pnas.1525462113

32. Urzay J, Llewellyn Smith SG, Glover BJ. The elastohydrodynamic force on a sphere near a soft wall. *Physics of Fluids* (2007) **19**:103106. doi:10.1063/1.2799148

33. Davies HS, Débarre D, El Amri N, Verdier C, Richter RP, Bureau L. Elastohydrodynamic Lift at a Soft Wall. *Phys Rev Lett* (2018) **120**:198001. doi:10.1103/PhysRevLett.120.198001

34. Wu MA, Tsvirkun D, Bureau L, Boccon-Gibod I, Inglebert M, Duperray A, Bouillet L, Misbah C, Cicardi M. Paroxysmal Permeability Disorders: Development of a Microfluidic Device to Assess Endothelial Barrier Function. *Front Med (Lausanne)* (2019) **6**:89. doi:10.3389/fmed.2019.00089

35. Radeva MY, Waschke J. Mind the gap: mechanisms regulating the endothelial barrier. *Acta Physiologica* (2018) **222**:e12860. doi:10.1111/apha.12860

36. Bravi L, Dejana E, Lampugnani MG. VE-cadherin at a glance. *Cell Tissue Res* (2014) **355**:515–522. doi:10.1007/s00441-014-1843-7

37. Mehta D, Malik AB. Signaling Mechanisms Regulating Endothelial Permeability. *Physiological Reviews* (2006) **86**:279–367. doi:10.1152/physrev.00012.2005

38. Wu MH, Ustinova E, Granger HJ. Integrin binding to fibronectin and vitronectin maintains the barrier function of isolated porcine coronary venules. *The Journal of Physiology* (2001) **532**:785–791. doi:10.1111/j.1469-7793.2001.0785e.x

39. Kanchanawong P, Shtengel G, Pasapera AM, Ramko EB, Davidson MW, Hess HF, Waterman CM. Nanoscale architecture of integrin-based cell adhesions. *Nature* (2010) **468**:580–584. doi:10.1038/nature09621

40. Montesano R. In vitro rapid organization of endothelial cells into capillary-like networks is promoted by collagen matrices. *The Journal of Cell Biology* (1983) **97**:1648–1652. doi:10.1083/jcb.97.5.1648

41. Wang X, T. Phan DT, Sobrino A, C. George S, W. Hughes CC, P. Lee A. Engineering anastomosis between living capillary networks and endothelial cell-lined microfluidic channels. *Lab on a Chip* (2016) **16**:282–290. doi:10.1039/C5LC01050K

42. Shao J, Wu L, Wu J, Zheng Y, Zhao H, Lou X, Jin Q, Zhao J. A microfluidic chip for permeability assays of endothelial monolayer. *Biomed Microdevices* (2010) **12**:81–88. doi:10.1007/s10544-009-9362-0

43. Zervantonakis IK, Hughes-Alford SK, Charest JL, Condeelis JS, Gertler FB, Kamm RD. Three-dimensional microfluidic model for tumor cell intravasation and endothelial barrier function. *PNAS* (2012) **109**:13515–13520. doi:10.1073/pnas.1210182109

44. Sato M, Sasaki N, Ato M, Hirakawa S, Sato K, Sato K. Microcirculation-on-a-Chip: A Microfluidic Platform for Assaying Blood- and Lymphatic-Vessel Permeability. *PLOS ONE* (2015) **10**:e0137301. doi:10.1371/journal.pone.0137301

45. Myers DR, Sakurai Y, Tran R, Ahn B, Hardy ET, Mannino R, Kita A, Tsai M, Lam WA. Endothelialized Microfluidics for Studying Microvascular Interactions in Hematologic Diseases. *Journal of Visualized Experiments : JoVE* (2012) doi:10.3791/3958

46. Tsvirkun D, Grichine A, Duperray A, Misbah C, Bureau L. Microvasculature on a chip: study of the Endothelial Surface Layer and the flow structure of Red Blood Cells. *Sci Rep* (2017) **7**: doi:10.1038/srep45036

47. Guerasimova A, Nyársik L, Girnus I, Steinfath M, Wruck W, Griffiths H, Herwig R, Wierling CK, O'Brien J, Eickhoff H, et al. Ireland Colorimetric Assay to Quantify Macromolecule Diffusion across Endothelial Monolayers. in

48. Yen W, Cai B, Yang J, Zhang L, Zeng M, Tarbell JM, Fu BM. Endothelial surface glycocalyx can regulate flow-induced nitric oxide production in microvessels in vivo. *PLoS ONE* (2015) **10**:e0117133. doi:10.1371/journal.pone.0117133

49. Chappell Daniel, Jacob Matthias, Paul Oliver, Rehm Markus, Welsch Ulrich, Stoeckelhuber Mechthild, Conzen Peter, Becker Bernhard F. The Glycocalyx of the Human Umbilical Vein Endothelial Cell. *Circulation Research* (2009) **104**:1313–1317. doi:10.1161/CIRCRESAHA.108.187831

50. Potter Daniel R., Damiano Edward R. The Hydrodynamically Relevant Endothelial Cell Glycocalyx Observed In Vivo Is Absent In Vitro. *Circulation Research* (2008) **102**:770–776. doi:10.1161/CIRCRESAHA.107.160226

51. Barker AL, Konopatskaya O, Neal CR, Macpherson JV, Whatmore JL, Winlove CP, Unwin PR, Shore AC. Observation and characterisation of the glycocalyx of viable human endothelial cells using confocal laser scanning microscopy. *Phys Chem Chem Phys* (2004) **6**:1006–1011. doi:10.1039/B312189E

52. Shi Z-D, Wang H, Tarbell JM. Heparan sulfate proteoglycans mediate interstitial flow mechanotransduction regulating MMP-13 expression and cell motility via FAK-ERK in 3D collagen. *PLoS ONE* (2011) **6**:e15956. doi:10.1371/journal.pone.0015956

53. Rezakhaniha R, Agianniotis A, Schrauwen JTC, Griffa A, Sage D, Bouten CVC, van de Vosse FN, Unser M, Stergiopulos N. Experimental investigation of collagen waviness and orientation in the arterial adventitia using confocal laser scanning microscopy. *Biomech Model Mechanobiol* (2012) **11**:461–473. doi:10.1007/s10237-011-0325-z

54. Hadi HA, Suwaidi JA. Endothelial dysfunction in diabetes mellitus. *Vasc Health Risk Manag* (2007) **3**:853–876.

55. Funk SD, Yurdagul A, Orr AW. Hyperglycemia and Endothelial Dysfunction in Atherosclerosis: Lessons from Type 1 Diabetes. *Int J Vasc Med* (2012) **2012**: doi:10.1155/2012/569654

56. van der Meer AD, Poot AA, Feijen J, Vermes I. Analyzing shear stress-induced alignment of actin filaments in endothelial cells with a microfluidic assay. *Biomicrofluidics* (2010) **4**:011103. doi:10.1063/1.3366720

57. Milovanova T, Chatterjee S, Hawkins BJ, Hong N, Sorokina EM, DeBolt K, Moore JS, Madesh M, Fisher AB. Caveolae are an essential component of the pathway for endothelial cell signaling associated with abrupt reduction of shear stress. *Biochimica et Biophysica Acta (BBA) - Molecular Cell Research* (2008) **1783**:1866–1875. doi:10.1016/j.bbamcr.2008.05.010

58. Fisher AB, Chien S, Barakat AI, Nerem RM. Endothelial cellular response to altered shear stress. *American Journal of Physiology-Lung Cellular and Molecular Physiology* (2001) **281**:L529–L533. doi:10.1152/ajplung.2001.281.3.L529

59. Manevich Y, Al-Mehdi A, Muzykantov V, Fisher AB. Oxidative burst and NO generation as initial response to ischemia in flow-adapted endothelial cells. *American Journal of Physiology-Heart and Circulatory Physiology* (2001) **280**:H2126–H2135. doi:10.1152/ajpheart.2001.280.5.H2126

60. Leemreis JR, Versteilen AMG, Sipkema P, Groeneveld ABJ, Musters RJP. Digital image analysis of cytoskeletal F-actin disintegration in renal microvascular endothelium following ischemia/reperfusion. *Cytometry Part A* (2006) **69A**:973–978. doi:10.1002/cyto.a.20269

61. Dmitriev RI, Papkovsky DB. Optical probes and techniques for O2 measurement in live cells and tissue. *Cellular and Molecular Life Sciences* (2012) **69**:2025–2039. doi:10.1007/s00018-011-0914-0

62. Zhao Y, Davis HW. Hydrogen peroxide-induced cytoskeletal rearrangement in cultured pulmonary endothelial cells. *Journal of Cellular Physiology* (1998) **174**:370–379. doi:10.1002/(SICI)1097-4652(199803)174:3<370::AID-JCP11>3.0.CO;2-D

63. Hikita T, Mirzapourshafiyi F, Barbacena P, Riddell M, Pasha A, Li M, Kawamura T, Brandes RP, Hirose T, Ohno S, et al. PAR-3 controls

endothelial planar polarity and vascular inflammation under laminar flow. *EMBO reports* (2018) **19**:e45253. doi:10.15252/embr.201745253

64. McCue S, Dajnowiec D, Xu F, Zhang M, Jackson MR, Langille BL. Shear Stress Regulates Forward and Reverse Planar Cell Polarity of Vascular Endothelium In Vivo and In Vitro. *Circulation Research* (2006) **98**:939–946. doi:10.1161/01.RES.0000216595.15868.55

65. Schalkwijk CG, Stehouwer CDA. Vascular complications in diabetes mellitus: the role of endothelial dysfunction. *Clin Sci (Lond)* (2005) **109**:143–159. doi:10.1042/CS20050025

66. Eelen Guy, de Zeeuw Pauline, Simons Michael, Carmeliet Peter. Endothelial Cell Metabolism in Normal and Diseased Vasculature. *Circulation Research* (2015) **116**:1231–1244. doi:10.1161/CIRCRESAHA.116.302855

67. Piconi L, Quagliaro L, Assaloni R, Ros RD, Maier A, Zuodar G, Ceriello A. Constant and intermittent high glucose enhances endothelial cell apoptosis through mitochondrial superoxide overproduction. *Diabetes/Metabolism Research and Reviews* (2006) **22**:198–203. doi:10.1002/dmrr.613

68. Singh A, Ramnath RD, Foster RR, Wylie EC, Fridén V, Dasgupta I, Haraldsson B, Welsh GI, Mathieson PW, Satchell SC. Reactive Oxygen Species Modulate the Barrier Function of the Human Glomerular Endothelial Glycocalyx. *PLOS ONE* (2013) **8**:e55852. doi:10.1371/journal.pone.0055852

69. Maier JAM, Cialdai F, Monici M, Morbidelli L. The Impact of Microgravity and Hypergravity on Endothelial Cells. *BioMed Research International* (2015) **2015**:1–13. doi:10.1155/2015/434803

English summary

The entire inner part of the vascular tree is covered by endothelial cells. From the larger diameter arteries to the smaller capillaries and vein, endothelial cells are the only layer common to all blood vessels. Endothelial cells are responsible for blood homeostasis, vascular tone regulation, permeability to liquid, protein and solute from blood and finally acting as a selective barrier for circulating cells. Since the early 80's, the ability of endothelial cells to sense their mechanical environment has been studied. The first observations were made on rabbit aorta microscopic observations and later confirmed in vitro with the first experiment including shear stress condition.

The study of endothelial cells and moreover endothelial function has been approached differently in the field of cardiovascular research depending on the main goal of the studies. The adaptive behavior (ie elongation of the cell body by formation of actin stress fibers oriented parallel to the flow direction) was described thanks to devices reproducing the mechanical stimulus associated to blood flow. Such biomimetic devices aim at reproducing environmental conditions as close as possible as the one experienced by a biological system in its native location, and appear to be fundamental for the study of cells that are strongly influenced by these stimuli. In paralell studies focusing on angiogenesis were conducted on endothelial cell behavior in 3D collagen matrix, concluding that microvascular endothelial cells were able to from tubular structure, with a properly orientated polarization of the cell body and a lumen while their culture was embedded in collagen gel. Thess observations were the first proof that endothelial cell can none solely sense mechanical environment on their luminal surface, but that the stiffness of their substrate was inducing a particular behavior, namely tube formation.

In this work we will focus on three main aspects of the endothelial function: (i) its ability to adapt to different mechanical stresses, with the impact of a reduced shear stress or impaired mechanosensor on endothelial cell phenotype; (ii) the influence of the modification of the concentration of one of the metabolite present in blood and fuel of the cell, the glucose, and the impact of an increase of its concentration on endothelial cells phenotype, and finally (iii) the ability of our system to assay endothelial permeability with perfusion of bradykinin, a molecule well known to induced vascular leakage.

Endothelial cells are able to probe the hydrodynamic friction on their surface due to blood flow thanks to a particular structure: the glycocalyx. The glycocalyx, or endothelial surface layer, is a dense polymer-rich coating located at the surface of the apical membrane, facing blood flow. This gel like matrix of polymer is composed of glycoprotein-anchored polysaccharides and proteoglycans. These proteoglycans have been identified as the main mechanosensor of the cells.

Indeed, heperan sulfate members Glypican-1 and Syndecan-1 are respectively responsible for nitric oxide production and actin stress fibers reorganization. As mentioned earlier, endothelial cell are able to respond to shear stress by producing vasodilator such as nitric oxide, and also to adapt to this mechanical condition by modifying their phenotype. The actual model proposed for endothelial cells early adaptation to shear stress is as follows: before exposition to shear stress, endothelial cells cultured in static condition present an actin cytoskeleton composed of three main structures: a cortical actin web (ACW) attached to the endothelial surface layer beneath the luminal plasma membrane via syndecan-1 intra-cellular domain; a dense peripheral actin band (DAPB) which transmits force to cell-cell junction and also link to ACW; actin stress fibers, anchored to the basal membrane on one side and to DAPB or luminal membrane on the other side. The transduction of mechanical signals can be summarized as follows: after exposure of endothelial cells to shear stress, the ACW transmits the force acting on the glycocalyx to cell-cell junctions and disrupts DAPB. This process results in the so-called atheroprotective phenotype, with a reorganization of the actin cytoskeleton in long and thick stress fibers oriented parallel to the flow direction, a reorganization of adhesion to substrate and cell-cell adhesion stabilization. The stabilization of cell-substrate and cell-cell junctions participates to maintainthe endothelium integrity. Indeed, proper adherence leads to controlled permeability. At the origin of many diseases, dis-regulation of endothelial barrier function can bring deadly events. In this work we focused on conditions grouped under the name of paroxysmal permeability disorder. These pathologies arise either from circulating or cellular factors that lead to an acute phase with a huge upload of plasma and proteins in tissues. This event can be lethal in case of laryngeal edema but are also characterized by a complete restauration of physiological permeability after the acute phase. The transport of liquid through the endothelial barrier in our case pass through cell-cell junctions. Endothelial junction's most studied complex is Ve-Cadherin, which form adherent junctions. This junctional complex is specific to endothelial cells and interacts with neighboring cells by binding extracellular domain of another cadherin. The cytoplasmic tails is linked to the actin cytoskeleton through a set of adaptor protein which participate in the stabilization of the junction. Ve-Cadherin knock-down in mouth is lethal due to immature vascular development and perturbation of the adhesion between cadherin leads to impaired barrier function. Tight junctions also play an important role in permeability with their main component Claudins. Tight junctions are also linked to the actin cytoskeleton and their level of expression in a particular zone of the endothelium is related to the permeability of the endothelium in this area.

In this thesis, we aimed at developing a system allowing for the microscopic observation of living or fixed endothelial cells cultured under constant shear stress, with a fine control of the level of shear and of the composition of the medium to which endothelial cells would be exposed while confined into microvessel-mimicking channels. To do so, we chose to use microfluidic tools, in order to design a network of channels allowing multiplexing the experiments in "micro vessel

condition“, with several identical channels (16 parallel channels) of the size of a capillary (30 µm) with a physiological level of shear stress (0.4 Pa). PDMS is casted on a positive photoresist (SU8) mold and cured. A glass coverslip is used to seal the microfluidic PDMS circuit. After coating with a protein from the extracellular matrix, the microfluidic network can be seeded with a suspension of endothelial cells. The endothelial cells are then left to grow under flow until they cover the four walls of the channels of the circuit. Medium supply is performed using a syringe pump connected to a set of tubing allowing the medium to flow from an inlet reservoir trough the microfluidic network to the syringe. Setting properly the medium flow rate generates an adequate shear stress inside the endothelialized microfluidic device. Human Umbilical Vascular Endothelial Cells (HUVEC) are cultured in endothelial cell growth medium supplemented by growth factor. After fixation cells are stain for F-actin, Nuclei and Glycocalyx. Reduction of shear stress was performed by decreasing the flow rate by fivefold, 150 mUI/mL solution of neuraminidase was use for enzymatic removal of the glycocalyx, 30mM glucose final concentration in endothelial cells growth medium was used to test the effect of hyperglycemia on endothelial cell phenotype, and finally permeability assay was done in biotinylated fibronectin coated channel in 3 conditions: (i) usual endothelial cells culture medium as a control, (ii) plasma from healthy volunteer, diluted 1:1 with medium for ECs culturing, (iii) bradykinin diluted in endothelial cells culture medium at a concentration of 25 µM. FITC-Avidin was then perfused for 5 min, and wall-bound Avidin was imaged after rinsing. Confocal fluorescence microscopy was performed on an inverted microscope. XYZ image stacks were obtained in raster mode using a Zeiss LSM710 module and a 40x/NA1.3 oil-immersion objective. The acquired image stacks were processed and analyzed using the Fiji open-source platform and its built-in plugins.

In order to compare phenotypic modifications of HUVEC in our different conditions, we describe HUVEC phenotype in basic control conditions first: (i) 2D static cultured of HUVEC, (ii) 3D culture under constant shear stress of 0.4 Pa. In control (i), cells form a cobblestone shaped monolayer with no particular orientation of the cell body. Actin staining reveals primarily a marked peripheral band and an enrichment in cortical grooves. Few stress fibers are also present in various length and thickness with no preferential orientation. In control (ii), cells display long and thick stress fibers, oriented parallel to the flow direction. The actin fibers are ventral fibers going underneath the nuclei and are grouped in bundle, forming thick structures that split or joined while they cross the cell length. The low fluorescence signal at the cell membrane shows that actin is sparsely present in the cortex. As we none solely intended to qualitatively described HUVEC phenotype, we used the ImageJ build-in plugin OrientationJ to quantify and measure actin stress fibers orientation. The processing computed structure tensor from intensity gradient, attributing a value of energy E and coherency C to each pixel. Using this two parameters we have been able to measure the relative amount of anisotropic structure within an image and to quantify the angular distribution of these structures.. Comparing 2D static condition and 3D shear condition we found: (i) An increased amount of anisotropic structure in shear adapted endothelial cells (ii) the

angular distribution is sharply peaked around 0° (corresponding to an angle parallel to the flow direction) for cell submitted to shear stress, indicating that the stress fibers orientation is driven by flow direction whereas 2D cultures show no particular preferred orientation of anisotropic structure, resulting in broad distribution of the histogram. Then, in order to probe the effect of reduced flow, as it happens in ischemia, or simulate a loss of mechanosensing as it happens during oxidative stress with glycocalyx shedding, we performed two different experiments: (i) a decreased flow rate for 1 to 6 hours and, (ii) channel perfusion with neuraminidase solution to degrade the endothelial surface layer. In (i), F-actin staining after 1 hours of shear reduction reveals a major disruption of the cytoskeleton compared to control condition. Indeed, most of the stress fibers are disassembled or reoriented. The remaining structure are thinner and their path is less rectilinear. Stress fibers display a more disorganized pattern. This trend is maintained and amplified in cells exposed for 6 hours to reduced shear stress. We also observe an important increase of background signal consistent with an important elevation of the signal at the cell membrane. Region with really high uniform staining appears. Finally, this relocation of the signal to the cell border shows that cell shape and orientation is also more randomized compared to control. In 3D observation of cells submitted to reduce shear stress we observe a slight increase in cell body thickness. To quantify this increase we measured the height of nuclei in both conditions. In addition to this, we notice that upon long exposure to reduce shear stress (6 hours or more) cells were detaching from the substrate. Quantitatively,we observe a reduction of anisotropic structure in reduce shear stress condition compared to shear adapted endothelial cells.. Moreover, when looking at the distribution of angles in the images, the larger value between 40 and 90° are more represented for cells submitted to reduce shear stress during 1 or 6 hours. The loss of stress fibers is accompanied by a disorientation of the actin cytoskeleton resulting in a broadening of the angular distribution. For (ii) degradation of the endothelial surface layer by neuraminidase does not affect the cytoskeleton organization induced by shear stress as the relative amount of anisotropic structure remain unchanged as well as the orientation histogram. The effective degradation of the glycocalyx was confirmed by microsopic observations, we observe a signal decrease of WGA-alexa488 staining which indicate the removal of some component of the glycocalyx, This suggest that degradation of only sialic acid residue do not pertube the mechnosensory machinery implicated in the organization of the actin cytoskeleton.

Hyperglycemia presents an increased cardiovascular risk and mortality such as atherosclerosis, obesity, hypertension, metabolic syndrome and heart failure. Some of the effect of hyperglycemia on endothelial cell are known but not so much importance have been given to its effect on the F-actin cytoskeleton phenotype of endothelial cell. Indeed most experiments are done on 2D static cultures where shear stress is totally absent. Here we proposed to look at the effect of an increased concentration of glucose in cell cultured medium on the phenotype of HUVEC cultured under constant shear stress of 0.4 Pa. Cell morphology is greatly impaired by the exposition to high glucose concentration. Indeed, the cell body is

no longer elongated as in control condition, cells adopt a more scared shape. 3D stacks also show that cell thickness is bigger. Cells are less stretched and more relaxed. F-actin cytoskeleton is also clearly affected by the exposure to high concentration of glucose. Even if stress fibers appear to be present as numerous as in the control we observe shorter and thicker stress fiber compared to control and their organization is different. Stress fibers are less oriented parallel to the flow direction. It also appears that some of the SF are no longer crossing the cell from side to side. On the other hand 3D stacks show that just as in control stress fiber appear to be ventral as they go underneath the nuclei. Interestingly there is a strong relocation of actin at the cell membrane. Indeed microscopy observation shows the presence of an increased signal of F-actin at the cell cortex compared to control. In order to confirm and quantify the change in orientation of actin stress fiber we proceed to the same processing done on images of control HUVEC. Comparing the relative frequency of orientation of stress fibers, the processing shows that in high glucose condition a lower amount of fibers are oriented between 0 and 16° and that this amount increases after 16°, meaning that less fibers are oriented in the flow direction. The distribution of angle is broaden compare to control.

Most techniques developed to assay permeability of endothelial cell under clinical condition lacks the mechanical environment which shear stress represents. We used our system combined with the use of the high affinity couple Biotin/Avidin to assay the barrier function of HUVEC in confined microchannel. As stated earlier, permeability was assayed in three different conditions: (i) control with medium, (ii) plasma from healthy volunteers and, (iii) Bradykinin infused channel. Doing so we observe that no major difference in permeability can be seen between the control and the 50%-plasma from healthy volunteer conditions. In the circuit exposed to 25µM solution of bradykinin the presence of fluorescent avidin linked to biotinylated fibronectin indicates a leak of the flowing solution through the endothelium.

In conclusion, we showed that our system is suitable for the study of endothelial function in vitro and that its biomimetic properties are verified by the presence of the atheroprotective phenotype observe both in vivo and in vitro. Concerning reduced flow experiments, we have been able to demonstrate that the exposition to a low shear stress for 1 to 6 hours results in a reorganization of the F-actin cytoskeleton. This observation suggests that the process of mechanosensing and adaptation is a reversible dynamic process. For later investigation, it would be interesting to look at markers of polarity before and after exposition to reduced shear stress to see if the polarity is modified. Enzymatic degradation of the endothelial surface layer did not show a significant difference on F-actin organization compared to control. This result could be explain by the fact that Neuraminidase is a sialidase, hydrolyzing only sialic acid residues in the glycocalyx. It therefore might not be sufficient to perturb the mechanosensing machinery of the cell, which is suspected to rely mainly on Heparane Sulfate, a component of the glycocalyx that is not degraded by Neuraminidase. Then, experiment on simulated hyperglycemia showed a marked reorganization of the F-actin cytoskeleton and a modification of cell shape. These results only allow us to

observe the loss of orientation of Actin stress fibers when cells are exposed to high glucose concentration. The mechanism behind this orientation could be affected either by a perturbation of the mechanosensory machine of the cell or by a loss of the polarity established during adaption to shears stress. Finally, we confirmed that our system is suitable for the study of a well-known permeability perturbation molecule as bradykinin. The increased level of permeability has been shown and measured and these results are promising concerning none solely the investigation of the effect of circulating factors but also the response of endothelial cells.

French summary

Les dispositifs biomimétiques visent à reproduire in vitro l'environnement physiologique auquel un système biologique est soumis in vivo. L'étude des cellules endothéliales et dans notre cas, la fonction endothéliale a été abordé différemment dans le domaine de la recherche cardiovasculaire selon l'objectif principal de ces études. Depuis le début des années 80, la capacité des cellules endothéliales à détecter leur environnement mécanique a été étudiée. Les premières observations ont été faites sur des observations microscopiques de l'aorte de lapin et confirmées plus tard in vitro avec la première expérience incluant la condition de contrainte de cisaillement. Le comportement adaptatif (c'est-à-dire l'allongement du corps cellulaire par formation de fibres de contrainte d'actine orientées parallèlement à la direction de l'écoulement) a été décrit grâce à un dispositif biomimétique reproduisant l'environnement mécanique tel que la contrainte de cisaillement. Entre-temps, en étudiant l'angiogenèse, des études ont été menées sur le comportement des cellules endothéliales dans une matrice de collagène 3D. En effet, les cellules endothéliales microvasculaires ont pu partir de la structure tubulaire, avec une polarisation correctement orientée du corps cellulaire et une lumière alors que leur culture était noyée dans du gel de collagène. Ces observations ont été la première preuve que les cellules endothéliales ne peuvent pas uniquement détecter l'environnement mécanique sur leur surface liminale mais que la rigidité de leur substrat induisait un comportement particulier, la formation tubulaire.

Les cellules endothéliales sont le principal acteur de la fonction endothéliale. Maintenant l'homéostasie sanguine, la fonction endothéliale est responsable de la régulation du tonus vasculaire, de la perméabilité aux liquides, aux protéines et aux solutés du sang et, enfin, agit comme une barrière sélective pour les cellules en circulation. Les cellules endothéliales vasculaires couvrent toute la partie interne du système vasculaire, des artères aux capillaires et veines, elles sont la seule couche commune à tous les vaisseaux sanguins. Pour ces raisons, l'endothélium est désormais considéré comme un organe et a une implication majeure dans la plupart, sinon la totalité, des maladies cardiovasculaires.

Dans ce travail, nous nous concentrerons sur trois aspects principaux de la fonction endothéliale: (i) sa capacité à s'adapter à différentes contraintes mécaniques, avec l'impact d'une réduction de la contrainte de cisaillement ou d'un mécanocapteur altéré sur le phénotype des cellules endothéliales; (ii) l'influence de la modification de la concentration de l'un des métabolites présents dans le sang et le carburant de la cellule, le glucose, et l'impact d'une augmentation de sa concentration sur le phénotype des cellules endothéliales et enfin; (iii) la capacité de notre système à doser la perméabilité endothéliale avec la perfusion de bradykinine, une molécule bien connue pour induire des fuites vasculaires.

Les cellules endothéliales sont capables de sonder le frottement du flux sanguin à leur surface grâce à une structure particulière, le glycocalyx. Le glycocalyx ou couche de surface endothéliale est une brosse en polymère dense et riche située à la surface de la membrane apicale, face au flux sanguin. Ce gel comme matrice de polymère est composé de polysaccharides ancrés aux glycoprotéines et de protéoglycanes. Ces protéoglycanes ont été identifiés comme le principal mécanocapteur de la cellule. En effet, les membres sulfate d'héperan Glypican-1 et Syndecan-1 sont respectivement responsables de la production d'oxyde nitrique et de la réorganisation des fibres de stress d'actine. Comme mentionné précédemment, les cellules endothéliales sont capables de répondre à la contrainte de cisaillement en produisant un vasodilatateur sous forme d'oxyde nitrique et également adaptées à cette condition mécanique en modifiant leur phénotype. Le modèle actuel proposé pour l'adaptation précoce des cellules endothéliales à la contrainte de cisaillement est le suivant: avant l'exposition à la contrainte de cisaillement, les cellules endothéliales cultivées en condition statique présentent un cytosquelette d'actine composé de trois structures principales: une toile d'actine corticale (ACW) attachée à la couche de surface endothéliale sous la membrane plasmique luminale via le domaine intracellulaire du syndecan-1; une bande d'actine périphérique dense (DAPB) qui transmet la force à la jonction cellule-cellule et se lie également à l'ACW; fibres de stress d'actine, ancrées à la membrane basale d'un côté et à la membrane DAPB ou luminale de l'autre côté. Rapidement, la transduction du signal mécanique peut être présentée comme suit: après exposition des cellules endothéliales à une contrainte de cisaillement, l'ACW transmet la force agissant sur le glycocalyx aux jonctions cellule-cellule et perturbe le DAPB. Ce processus aboutit au phénotype dit athérosoprotecteur avec une réorganisation du cytosquelette d'actine en fibres de stress longues et épaisses orientées parallèlement à la direction de l'écoulement, une réorganisation de l'adhésion au substrat et une stabilisation de l'adhésion cellule-cellule. La stabilisation de la jonction cellule-substrat et cellule-cellule participe au maintien de l'intégrité de l'endothélium. En effet, une bonne adhérence conduit à une perméabilité contrôlée. A l'origine de nombreuses maladies, la dérégulation de la fonction de barrière endothéliale peut entraîner des événements mortels. Dans ce travail, nous nous sommes concentrés sur les conditions regroupées sous le nom de trouble de perméabilité paroxystique. Ces pathologies découlent de facteurs circulants ou cellulaires qui conduisent à une phase aiguë avec un énorme chargement de plasma et de protéines dans les tissus. Cet événement peut être mortel en cas d'œdème laryngé mais se caractérise également par une restauration complète de la perméabilité physiologique après la phase aiguë. Le transport de liquide à travers la barrière endothéliale dans notre cas passe par des jonctions cellule-cellule. Le complexe le plus étudié de la jonction endothéliale est la ve-cadhérine, qui forme des jonctions adhérentes. Ce complexe jonctionnel est spécifique aux cellules endothéliales et interagit avec les cellules voisines en se liant au domaine extracellulaire d'une autre cadhérine. La queue cytoplasmique est liée au cytosquelette d'actine par un ensemble de protéines adaptatrices qui participent à la stabilisation de la jonction. La suppression de la ve-cadhérine dans la bouche est mortelle en raison du développement vasculaire immature et la

perturbation de l'adhésion entre la cadhérine entraîne une altération de la fonction de barrière. Les jonctions serrées jouent également un rôle important dans la perméabilité avec leur composant principal Claudins. Des jonctions serrées sont également liées au cytosquelette d'actine et leur niveau d'expression dans une zone particulière de l'endothélium est lié à la perméabilité de l'endothélium dans cette zone.

Nous visons à développer un système permettant l'observation microscopique de cellules endothéliales vivantes ou fixes cultivées sous une contrainte de cisaillement constante avec un contrôle fin du niveau de cisaillement, de la composition moyenne tandis que les cellules endothéliales seraient confinées telles qu'elles sont dans la microcirculation. Pour ce faire, nous décidons d'utiliser des outils microfluidiques, afin de concevoir un canal microfluidique permettant le multiplexage des expériences en «micro vaisseau condition», avec de nombreux canaux identiques (16 canaux parallèles) de la taille d'un capillaire (30 µm) avec un niveau physiologique de contrainte de cisaillement (0,4 Pa). Le PDMS est coulé sur un moule de résine photosensible positive (SU8) et durci. Une lamelle de verre est utilisée pour sceller le circuit microfluidique PDMS. Après revêtement avec une protéine de matrice extracellulaire, le canal microfluidique peut être ensemencé avec une suspension de cellules endothéliales. Les cellules endothéliales peuvent maintenant se développer et couvrir les quatre parois des canaux du circuit. L'approvisionnement en milieu est effectué à l'aide d'une pompe à seringue connectée à un ensemble de tubulures permettant au milieu de s'écouler d'un réservoir d'entrée à travers le réseau microfluidique vers la seringue. Un réglage correct du débit moyen génère une contrainte de cisaillement adéquate à l'intérieur du dispositif microfluidique endothélialisé. Les cellules endothéliales vasculaires ombilicales humaines (HUVEC) sont cultivées dans un milieu de croissance de cellules endothéliales complété par un facteur de croissance. Après la fixation, les cellules sont colorées pour la F-actine, les noyaux et le glycocalyx. La réduction de la contrainte de cisaillement a été réalisée en diminuant le débit par cinq, une solution de neuraminidase de 150 mUI / mL a été utilisée pour l'élimination enzymatique du glycocalyx, une concentration finale de glucose de 30 mM dans le milieu de croissance des cellules endothéliales a été utilisée pour tester l'effet de l'hyperglycémie sur les cellules endothéliales le test de phénotype et enfin de perméabilité a été effectué dans un canal revêtu de fibronectine biotinylée dans 3 conditions: (i) milieu de culture de cellules endothéliales habituel comme témoin, (ii) plasma de volontaire sain, dilué 1: 1 avec du milieu pour la culture des CE, (iii) bradykinine dilué dans du milieu de culture de cellules endothéliales à une concentration de 25 uM ensuite, du FITC-Avidine a été perfusé pendant 5 min. La microscopie à fluorescence confocale a été réalisée sur un microscope inversé. Les piles d'images XYZ ont été obtenues en mode raster en utilisant un module Zeiss LSM710 et un objectif à immersion dans l'huile 40x / NA1.3. Les piles d'images acquises ont été traitées et analysées à l'aide de la plate-forme open source des Fidji et de ses plug-ins intégrés.

Afin de comparer la modification phénotypique de HUVEC dans nos différentes conditions, nous avons d'abord décrit le phénotype HUVEC dans une condition de

contrôle de base: (i) Culture statique 2D de huvec, (ii) Culture 3D sous contrainte de cisaillement constante. (i) Les cellules présentent une monocouche en forme de pavé sans orientation particulière du corps cellulaire. La coloration à l'actine révèle principalement une bande périphérique marquée et un enrichissement en sillons corticaux. Peu de fibres de contrainte sont également présentées en différentes longueurs et épaisseurs sans orientation préférentielle. (ii) Les cellules présentent des fibres de contrainte longues et épaisses, orientées parallèlement à la direction de l'écoulement. Les fibres d'actine sont des fibres ventrales passant sous les noyaux et sont regroupées en faisceau, formant une structure épaisse qui se divise ou se joint pendant qu'elles traversent la longueur de la cellule. Le mauvais signal au niveau de la membrane cellulaire montre que l'actine est peu présente dans le cortex. Comme nous ne voulions pas uniquement décrire qualitativement le phénotype HUVEC, nous avons utilisé le plugin intégré ImageJ OrientationJ pour quantifier et mesurer l'orientation des fibres de stress d'actine. Le traitement calcule le tenseur de structure à partir du gradient d'intensité, attribuant une valeur d'énergie E et de cohérence C à chaque pixel correspondant respectivement à une région à structure orientée uniforme ou multiple et au niveau d'anisotropie dans cette région. Comme alternative à la fonction de seuillage intégrée du plugin, nous constatons que la procédure suivante fonctionne mieux en termes de résolution finale: à partir de l'image d'entrée, nous exécutons orientationJ pour obtenir les cartes d'orientation E, C et non filtrées. Nous seuillons ensuite les images E et C (aux mêmes niveaux que ceux utilisés dans la fonction intégrée du plugin) et les binarisons. En parallèle, nous binarisons l'image d'entrée en utilisant la méthode de Bernsen à seuil local implémentée dans ImageJ. Nous multiplions ensuite l'image binarisée E, C et Bernsen afin de créer un masque binaire que nous utilisons pour filtrer la carte d'orientation. L'orientation filtrée nous permet de construire un histogramme d'orientation au sein de l'image. En comparant la condition statique 2D et la condition de cisaillement 3D, nous avons constaté que: (i) en comparant la distribution de √EC de la condition statique et de l'écoulement, nous observons une plus grande population sur de grandes valeurs pour les cellules adaptées au cisaillement (√EC> 0,2) compatible avec la présence de structure anisotrope en tant que fibres de contrainte alors que la distribution de √EC est plus choisie autour d'une valeur plus petite pour la condition 2D (valeur √EC max autour de 0,08), et (ii) la distribution angulaire est fortement culminée autour de 0 ° (correspondant à un angle parallèle à la direction d'écoulement) pour la cellule soumise à une contrainte de cisaillement, indiquant que l'orientation des fibres de contrainte est entraînée par la direction de l'écoulement alors que la culture 2D ne montre aucune orientation préférée particulière de la structure anisotrope, résultant en une large distribution de l'histogramme. Ensuite, afin de tester réduire le débit comme cela se produit dans l'ischémie ou simuler une perte de mécanosensibilité comme cela se produit pendant le stress oxydatif avec l'excrétion de glycocalyx, nous avons effectué deux expériences différentes: (i) une diminution du débit pendant 1 à 6 heures et, (ii) canaliser la perfusion avec une solution de neuraminidase pour dégrader la couche superficielle endothéliale. Dans (i) la coloration de F-actine après 1 heure de réduction de cisaillement révèle une perturbation majeure du cytosquelette par rapport à la condition témoin. En

effet, la plupart des fibres de contraintes sont démontées ou réorientées. Les structures restantes sont plus minces et leur trajet est moins rectiligne. Les fibres de stress présentent un motif plus anarchique. Cette tendance est maintenue et amplifiée dans les cellules exposées pendant 6 heures pour réduire la contrainte de cisaillement. Nous observons également une augmentation importante du signal de fond compatible avec une élévation importante du signal au niveau de la membrane cellulaire. Une région avec une coloration uniforme très élevée apparaît. Enfin, cette relocalisation du signal à la frontière cellulaire montre que la forme et l'orientation des cellules sont également plus aléatoires que le contrôle. Dans l'observation 3D des cellules soumises pour réduire la contrainte de cisaillement, nous observons une légère augmentation de l'épaisseur du corps cellulaire. Pour quantifier cette augmentation, nous avons mesuré la hauteur des noyaux dans les deux conditions. En plus de cela, nous remarquons que lors d'une longue exposition pour réduire la contrainte de cisaillement (6 heures ou plus), les cellules se détachaient du substrat. Quantitativement, la contrainte de cisaillement réduite √ La distribution EC est plus peuplée sous 0,2 valeur, indiquant tout aussi purement la culture statique que la quantité de structure anisotrope est réduite par rapport aux cellules adaptées à 0,4 Pa. Encore plus, lorsque l'on regarde la distribution de l'angle dans les images, la plus grande valeur entre 40 et 90 ° est plus représentée pour cellule soumise pour réduire la contrainte de cisaillement pendant 1 ou 6 heures. La perte de fibres de stress s'accompagne d'une désorientation du cytosquelette d'actine entraînant un élargissement de la distribution angulaire. Pour (ii) la dégradation de la couche de surface endothéliale par la neuraminidase, entraînant une diminution du signal de la coloration WGA-alexa488 qui indique l'élimination de certains composants du glycocalyx, n'affecte pas l'organisation du cytosquelette induite par la contrainte de cisaillement. En effet, le nombre de structure anisotrope (valeurs √EC) et de distribution angulaire est très similaire au contrôle.

Long abstract

Endothelial cells are the cells lining the inner surface of every blood vessel. Acting as a selective barrier for circulating cells and molecules, endothelial cells are directly exposed to blood flow. Such flow generates viscous friction at their surface, which induces morphological changes and is involved in the maintaining of endothelial function. Endothelial cells are able to sense blood flow thanks to mechanosensors located at their surface. These mechanosensors have been identified recently, and have been shown to be part of a polymer coating covering the surface of the cells. This gel like matrix of polymers is called the endothelial surface layer, or glycocalyx, and is of major importance for the regulation of endothelial function. Grouped under the name of endothelial function are the passive or active response of endothelial cells that maintain vascular health. The glycocalyx mechanosensing properties allow the endothelium to regulated vascular tone, its composition allow the recruitment of immune cell in case of infection or injuries and finally its implication in permeability to fluid and small molecule has been recently brought to light. In physiological condition, the endothelium adopts a particular morphology called the atheroprotective phenotype, which is a sign of a proper endothelial function.

In this work, we focus on the phenotypic modification brought by perturbations of the environment of endothelial cells. To do so, we use biomimetic microfluidic devices allowing for the culture of confined endothelial cells submitted to constant hydrodynamic shear stress. Such devices allow for the observation of living or fixed endothelial cells by conventional confocal microscopy. The system is a circuit where the cell culture medium flows through a network of microchannel thanks to a syringe pump allowing an easy control of the biochemical composition of the fluid that perfuse the circuit. We find that under a physiological level of shear stress, cells display long actin stress fibers oriented parallel to the flow direction, a signature of the atheroprotective phenotype. We observe that a decrease in shear stress induces a reorganization of the actin cytoskeleton, with stress fibers being disassembled or randomly reoriented and actin being recruited at the cells' periphery. In a second set of experiments, we challenge shear-adapted endothelial cells with a diabete-mimicking high glucose concentration, and observe that the F-actin cytoskeleton loses its flow-oriented character. Finally our system was tested for the detection of endothelial permeability. We provide of proof-of-concept by challenging cells with bradykinin, known to induce vascular leakage, and show that we are indeed able to measure an increased permeability of the endothelium cultured under constant shear stress.

In conclusion, we have developed an in vitro model system suitable for the study of endothelial function and observation of phenotypic modification via microscopic observation. Our work thus brings insights into the cell response to a loss of mechanical stimulation, and to an increase in the concentration of a metabolite or a permeabilization factor. Such a biomimetic system opens routes for future studies of the endothelial function in which the combined action of mechanical and biochemical stimuli can be deciphered.

Short abstract

The endothelial function is responsible for maintaining vascular health and its dysregulation is at the origin of numerous vascular pathologies such as atherosclerosis or angioedemas. Indeed, endothelial cells are present on the internal surface of all blood vessels and are therefore in direct contact with blood flow. Blood flows generate frictional forces on the surface of endothelial cells which results in modification of their morphological characters but also their biochemical response. We have therefore developed a biomimetic system to reproduce the physiological mechanical environment of the endothelium. To do this we use a microfluidic system where the cells are cultivated in a confined way in micro-channels and in the presence of a continuous flow. This device allowed us to study the effect of mechanical and metabolic disturbances on the phenotype and the permeability of a model endothelium.

Résumé long

Les cellules endothéliales sont les cellules qui tapissent la surface interne de chaque vaisseau sanguin. Agissant comme une barrière sélective pour les cellules et molécules en circulation, les cellules endothéliales sont directement exposées au flux sanguin. Un tel écoulement génère des frictions à leur surface, ce qui induit des changements morphologiques et participe au maintien de la fonction endothéliale. Les cellules endothéliales sont capables de détecter les frictions du flux sanguin grâce à des mécanorécepteurs situés à leur surface. Ces mécanorécepteur ont été identifiés récemment et se sont révélés faire partie d'une couche de polymère recouvrant la surface des cellules. Cette matrice de polymères est appelée couche de surface endothéliale, ou glycocalyx, et est d'une importance majeure pour la régulation de la fonction endothéliale. Regroupées sous le nom de fonction endothéliale sont les réponses passives ou actives des cellules endothéliales qui maintiennent la santé vasculaire. Les propriétés de mécanosensibilité du glycocalyx permettent à l'endothélium de réguler la pression sanguine, sa composition permet le recrutement de cellules immunitaires en cas d'infection ou de blessure et enfin son implication dans la perméabilité au fluide et aux petites molécules a été récemment mise en évidence. En condition physiologique, l'endothélium adopte une morphologie particulière appelée le phénotype athéroprotecteur, qui est le signe d'une fonction endothéliale appropriée.

Dans ce travail, nous nous concentrons sur les modifications phénotypiques apportées par les perturbations de l'environnement des cellules endothéliales. Pour ce faire, nous utilisons des dispositifs microfluidiques biomimétiques permettant la culture de cellules endothéliales confinées soumises à une contrainte de cisaillement hydrodynamique constante. De tels dispositifs permettent l'observation de cellules endothéliales vivantes ou fixées par microscopie confocale. Le système est un circuit où le milieu de culture cellulaire circule à travers un réseau de microcanaux grâce à une pompe à seringue permettant un contrôle du débit ainsi que de la composition biochimique du fluide qui perfuse le circuit. Nous constatons que sous un niveau physiologique de contrainte de cisaillement, les cellules présentent de longues fibres de stress d'actine orientées parallèlement à la direction de l'écoulement, ce qui est caractéristique du phénotype athéroprotecteur. Nous observons qu'une diminution de la contrainte de cisaillement induit une réorganisation du cytosquelette d'actine, les fibres de stress sont dépolymérisées ou réorientées au hasard et l'actine est recrutée à la périphérie des cellules. Dans une deuxième série d'expériences, nous soumettons les cellules endothéliales adaptées au cisaillement à une concentration élevée de glucose imitant le diabète, et observons que le cytosquelette d'actine perd son caractère orienté. Enfin, notre système a été testé pour la détection de la perméabilité endothéliale. Nous fournissons une preuve de concept exposant les cellules à de la bradykinine, connue pour induire des fuites vasculaires, et montrons que nous sommes en effet capables de mesurer une perméabilité accrue de l'endothélium après exposition a cette molécule.

En conclusion, nous avons développé un système modèle in vitro adapté à l'étude de la fonction endothéliale et à l'observation des modifications phénotypiques via des observations microscopiques. Notre travail apporte ainsi des informations sur la réponse cellulaire à une perte de stimulation mécanique, à une augmentation de la concentration d'un métabolite et leur réponse en présence d'un facteur de perméabilisation. Un tel système biomimétique ouvre des voies pour de futures études de la fonction endothéliale dans lesquelles l'action combinée des stimuli mécaniques et biochimiques peut être déchiffrée.

Résumé court

La fonction endothéliale est responsable du maintien de la santé vasculaire et son dérèglement est à l'origine de nombreuse pathologie vasculaire comme l'athérosclérose ou les angioedèmes. En effet, les cellules endothéliales sont présentes sur la surface interne de tous les vaisseaux sanguins et sont donc en contact direct avec le flux sanguins. Les écoulements sanguins génèrent des forces de frictions à la surface des cellules endothéliales ce qui a pour conséquence la modification de leurs caractères morphologique mais aussi leur réponse biochimique. Nous avons donc développé un système biomimétique permettant de reproduire l'environnement mécanique physiologique de l'endothélium. Pour ce faire nous utilisons un système de microfuidique où les cellules sont cultivées de manière confinée dans des micro-canaux et en présence d'un écoulement continu. Ce dispositif nous a permis d'étudier l'effet de perturbations mécaniques et métaboliques sur le phénotype et la perméabilité d'un endothélium modèle.